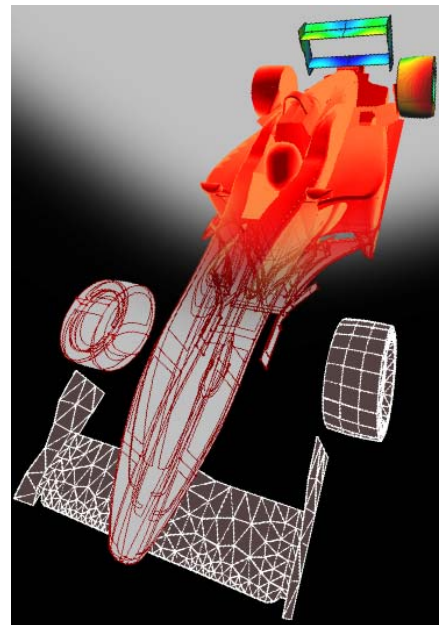


# GiD 2008

## 4<sup>th</sup> Conference on Advances and Applications of GiD

A. Coll, M. Pasenau, E. Escolano  
J. Suit and A. Melendo (Eds.)



**GiD 2008**  
**4<sup>th</sup> Conference on Advances  
and Applications of GiD**

A. Coll, M. Pasenau, E. Escolano  
J. Suit and A. Melendo (Eds.)

**Monograph CIMNE N<sup>o</sup>-110, May 2008**

INTERNATIONAL CENTER FOR NUMERICAL METHODS IN ENGINEERING  
Edificio C1, Campus Norte UPC  
Gran Capitán s/n  
08034 Barcelona, Spain  
[www.cimne.upc.es](http://www.cimne.upc.es)

First edition: May 2008

**GiD 2008. 4th Conference on Advances and Applications of GiD**  
Monografía CIMNE M110  
© The authors

ISBN: 978-84-96736-52-8

Depósito legal: B-24011-2008

## PREFACE

The extended use of simulation programs has leaned on the advances in user-friendly interfaces and in the capability to generate meshes for any generic complex geometry. More than ten years of development have made GiD grow to become one of the more popular pre and postprocessing systems at international level. The constant dialogue between the GiD development team and the users has guided the development of GiD to cover the pre-post needs of many disciplines in science and engineering. Following this philosophy, the biannual GiD Conference has become an important forum for discussion and interchange of experiences among the GiD community.

This book includes the contributions of the participants to the fourth edition of the GiD Conference held in the island of Ibiza from 8-9 May 2008. Sessions related to specific areas were complemented by Keynote Lectures on targeted research topics in the field of pre and postprocessing given by reputed international experts.

The following list gives an indication of the topics addressed in the conference:

- Interface with CAD data (IGES, VDA, DXF, etc.)
- CAD data repair
- Mesh generation
- Medical images treatment
- Remote Computing
- Interface of between GiD and commercial codes (LS-Dyna, Plaxis, etc)
- Visualization and animation of numerical results (simple and coloured streamlines, isosurfaces, vectors, combined results in several meshes, etc.)
- Examples of applications of GiD in science and engineering
  - GIS
  - Geotechnics
  - Multi-physics
  - CFD
  - Structural analysis
  - Electromagnetics
  - Physics
  - Chemistry
  - Bio-Engineering
  - Others

On behalf of all who have been involved in the organization of the GiD conference and in the edition of this book, we would like to thank all authors contributing to this publication. We also hope that the different practical cases selected in this book will help towards new developments and advances in the pre and post-processing field and in future versions of GiD .

Abel Coll  
Enrique Escolano  
CIMNE  
Co-Chairmen of GiD 2008



# Contents

## Keynote Lectures

<b>Possibilities and Limitations of the Finite Element Method for Geotechnical Applications</b> <i>R.B.J. Brinkgreve and W. Swolfs</i> .....	11
<b>CardioSense3D: Towards Patient-Specific Cardiac Simulation for Clinical Applications</b> <i>H. Delingette and M. Fernandez</i> .....	17

## Contributed Papers

<b>Integration of GID with tension structure computer analysis program using Ada95</b> <i>C. Almeida Bueno e Silva and A. R. Pulino Filho</i> .....	23
<b>Using GID to Design an Intravascular Support System</b> <i>M. Bordone, E. Soudab, M. Chiumenti and E. Oñate</i> .....	27
<b>PFEM applications in Fluid-structure Interaction Problems</b> <i>M.A. Celigueta, A. Larese and S. Latorre</i> .....	31
<b>GID-ATENA Interface - Advanced Simulation of Reinforced Concrete Structures</b> <i>Jan Cervenka and Jiri Niewald</i> .....	39
<b>CARPA, a Problemtyp for a Free Surface Flow Modelling Software</b> <i>G. Corestein and E. Bladé</i> .....	43
<b>Fluid-structure Interaction of Elastic Cylindrical Structures with Moderately High Turbulent Flow.</b> <i>C. Corte</i> .....	47
<b>Kratos a Framework for Multi-Disciplinary Code Development</b> <i>P. Dadvand</i> .....	51
<b>Non-linear Analysis of Masonry Walls using Digital Photography</b> <i>D. Di Capua and L. Alvarez</i> .....	55
<b>Development of a Dedicated Software Tool for the Global Thermomechanical Analysis of Plate-Fin Heat Exchangers</b> <i>J. DIB, F. Biltvyst, J.L. Batoz and I. Lewon</i> .....	59
<b>Accurate Simulation of Tailored-Welded-Blanks to Reduce the Process Design Time for the Sheet Pressing Industry</b> <i>A. Ferriz, O. Fruitos and A. Maymó Molina</i> .....	63
<b>Incremental Sheet Forming: A Nowadays Vision</b> <i>O. Fruitos Bickham, A. Maymó Molina and A. Ferriz Canals</i> .....	69

<b>Cooling Tank break Simulation with CARPA and GiD Software</b> <i>O.A. Fuentes, M.L. Arganis, E. Bladé, F. De Luna, J.E. Mendoza, J.A. Cruz, and M. Sanchez</i> .....	75
<b>An Interface for an Hp-Adaptative Finite Element Package using GiD</b> <i>D. García-Doñoro, L.E. García-Castillo and I. Gómez-Revuelto</i> .....	79
<b>Application of GiD to Generate the 3D finite Element Mesh for the Study of Marine Circulation in the Bay of Biscay</b> <i>A. German, M. Espino, J. Blasco, M. Maidana, E. Escolano and M. Pasenau</i> .....	83
<b>GiD LS-Dyna Graphical Interface</b> <i>S. González Horcas</i> .....	87
<b>The General Purpose Software XFINAS 3.0 for Analysis of Bridge</b> <i>Ki-Du Kim, S. Suthasupradit, P. Chobsilprakob and P. Norachan</i> .....	91
<b>Sphere Packing for Discrete Element Simulation on GiD</b> <i>C. Labra, E. Oñate and E. Escolano</i> .....	95
<b>Artificial Neural Networks for Optimal Airfoil Design</b> <i>R. Lopez, R. Flores, E. Escolano and E. Oñate</i> .....	99
<b>GiD Pre/Post Processing System as an Interface for Parallel Reservoir Simulator (PaRSi)</b> <i>M.T. Manzari, H. Naderan, R. Fatehi, S. Farnoush, M. Abedi and M. Fayyaz Bakhsh</i> .....	103
<b>Multiphysical Simulations Using NACS in Combination with GiD</b> <i>M. Meiler, H. Landes and M. Kaltenbacher</i> .....	107
<b>Simulation of Coupled Electromagnetic-Mechanical Sheet Forming</b> <i>R. Mendez, A. Ferriz and O. Frutos</i> .....	111
<b>Modeling the Structural and Acoustic Behavior of Sonar Transducer with ATILA code and GiD</b> <i>H. Mestouri, A. Loussert and G. Keryer</i> .....	117
<b>Numerical Topology Optimisation Using GiD</b> <i>J.A. Oliveira, J. Pinbo-da-Cruz, A. Andrade-Campos and F. Teixeira-Dias</i> .....	121
<b>Coupled THM Problems in Geotechnical Engineering Using CODE_BRIGHT-GiD</b> <i>S. Olivella, J. Vaunat, B. Garitte and N. Pinyol</i> .....	125
<b>An Automated Reconstruction of the Lungs for CFD Simulations</b> <i>J. Pennecot</i> .....	135
<b>A New System for Problem Types Creation</b> <i>M.R. Peyrau Rubio and R. Ribó Rodríguez</i> .....	139
<b>GID-PAK Interface</b> <i>D. Rakic, A. Nikolic, M. Zivkovic and R. Slavkovic</i> .....	143

<b>1D Numerical Model of Arteries in GiD</b>	
<i>E. Soudah and E. Oñate</i> .....	147
<b>Batch Controlled Pre-Processing for Shield Tunnelling Problems in GiD</b>	
<i>J. Stascheit and G. Meschke</i> .....	151





## **Keynote Lectures**



## POSSIBILITIES AND LIMITATIONS OF THE FINITE ELEMENT METHOD FOR GEOTECHNICAL APPLICATIONS

Ronald B.J. Brinkgreve<sup>\*</sup> and Wendy M. Swolfs<sup>†</sup>

<sup>\*</sup> Delft University of Technology, Faculty of Civil Engineering and Geo-sciences, Geo-engineering Section

Stevinweg 1, 2628 CN Delft, The Netherlands  
e-mail: r.b.j.brinkgreve@tudelft.nl, web page: <http://geo.citg.tudelft.nl>

<sup>†</sup> Plaxis bv

Delftechpark 53, 2628 XJ Delft, The Netherlands  
e-mail: w.swolfs@plaxis.nl, web page: <http://www.plaxis.nl>

**Key words:** Soil, geotechnical applications, modelling issues, meshing, interface elements

**Abstract.** *In this paper some modelling issues of geotechnical finite element applications are highlighted. Modelling professionals involved in the analysis of geotechnical projects ought to be familiar with the possibilities and limitations of the finite element method as well as the available soil constitutive models in order to make the right modelling decisions. Lack of knowledge may lead to severe damage or collapse of the geotechnical structure. The presentation is intended to create awareness about the subject, with the purpose to further improve the quality of finite element calculation results for geotechnical applications. In particular, the role of mesh coarseness and interface elements is highlighted. An example is elaborated using Plaxis-GiD to demonstrate some modelling aspects.*

### 1 INTRODUCTION

Deformation-based finite element calculations for geotechnical applications (deformation, bearing capacity and stability of excavations, tunnel projects, foundations, embankments, etc.) give special requirements to the finite element model being used. Because of the highly non-linear and time-dependent behaviour of soils, advanced constitutive relationships are needed in the finite element model, preferably with a separation between effective stress and pore pressure. This material non-linearity and time-dependency not only requires a robust step-wise solution procedure, but, since ordering and timing are important, the finite element model should also allow for a realistic simulation of the construction process.

When structures are involved, structural behaviour as well as soil-structure interaction needs to be taken into account. In particular, when bearing capacity of soil structures is to be analysed, the coarseness of the finite element mesh plays an important role. Unfortunately, the finite element method gives an upper bound (*unsafe*) solution for bearing capacity problems. Upon mesh refinement the bearing capacity reduces towards its theoretical value. Also interface elements play an important role, not only to properly model the soil-structure

interaction, but also to accurately calculate bearing capacities.

The next Chapter (2) describes an example which involves some issues that are typical for geotechnical applications or soil-structure interaction problems. The subsequent Chapter (3) elaborates on issues such as model boundaries, meshing, interface elements, construction stages, soil modelling and bearing capacity. The paper ends with some conclusions on the possibilities and limitations of the finite element method for geotechnical applications.

## 2 EXAMPLE: SUCTION CAISSON SUBJECTED TO LOADING

The example problem considers the determination of the bearing capacity of a suction caisson loaded by a point load at an angle of 30 degrees with the horizontal (see Figure 1)<sup>1</sup>. The caisson has a diameter of 5 meter and a penetration depth of 7.5 m. The load is attached to the caisson at a depth of 6 m.

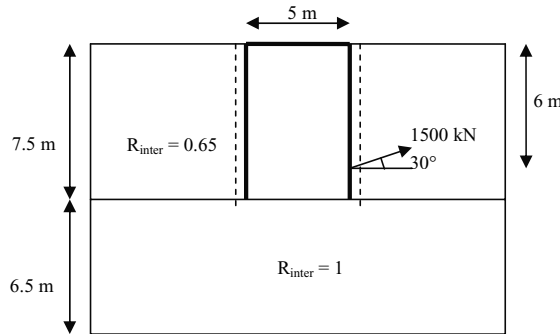


Figure 1: Geometry of the suction caisson

The geometry is extended 7.5 m around the caisson and 6.5 m below to avoid influence of the geometry boundaries. Interfaces are added around the caisson to model the soil-structure interaction. To avoid locking of the interfaces, they are extended 0.5 meter below the caisson bottom.

The soil has an effective unit weight of  $5.5 \text{ kN/m}^3$  and is modelled by means of the Tresca model with a Young's modulus of  $10 \text{ kN/m}^2$  at the surface increasing with  $125 \text{ kN/m}^2$  per meter depth, a Poisson's ratio of 0.45 and a cohesion (undrained shear strength) of  $0 \text{ kN/m}^2$  at the surface increasing with  $1.25 \text{ kN/m}^2$  per meter depth. Along the caisson the strength reduction factor of the interface ( $R_{\text{inter}}$ ) is set to 0.65. Below the caisson, this factor is set to 1.0 to neglect the reduction of the interface strength here.

The initial stresses are generated using the K0-procedure with a K0-value of 0.55 in both horizontal directions. The caisson will be installed in phase 1, where it is modelled by a non-porous linear-elastic material with an effective unit weight of  $7.75 \text{ kN/m}^3$ , a Young's modulus of  $10^5 \text{ kN/m}^2$  and a Poisson's ratio of 0.2. In phase 2 the load will be activated at a value of 1500 kN (1300 kN in horizontal direction and 750 kN in vertical direction). As the theoretical solution of this example gives a maximum force of  $1220 \text{ kN}^1$ , loading towards 1500 kN should give failure before reaching this value.

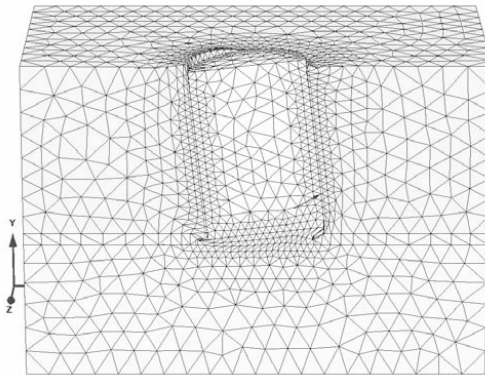


Figure 2: Deformed mesh of the suction caisson at failure

### 3 MODELLING ISSUES

#### 3.1 Model boundaries

In reality the sub-soil is virtually unlimited, but finite element models require model boundaries with appropriate boundary conditions. The larger the model, the more elements and thus more calculation time and computer memory is required, which means higher costs. On the other hand, boundaries should not influence the results. Symmetry boundaries with proper boundary conditions may be used to reduce significantly the calculation costs (i.e. the x-y plane in the example of Chapter 2). In order to accurately calculate *deformations*, model boundaries should generally be put further away than for stability or bearing capacity calculations. In dynamic calculations the boundaries should be set sufficiently far away such that possible reflections do not reach the domain of interest during the time interval of the analysis.

For problems involving unloading using a simple soil model that does not take into account the high stiffness at small strain levels, unrealistic heave will occur in ‘deep’ elements, where in reality hardly any heave or deformations take place. Therefore, it might be considered to place the bottom boundary not very deep below the excavation or retaining wall, but it is better to use a high small-strain stiffness in deeper layers.

From the example in Chapter 2 it can be seen that a fully developed failure mechanism fits nicely in the model (see Figure 2). However, the final stress state at the model boundaries is not equal to the initial stress state, and therefore it may be thought that there is some influence from the boundary conditions. As we are using a soil constitutive model with undrained shear strength, the shear strength does not depend on the stress state. So even if the stress state would be influenced by the boundary conditions, it will not affect the failure level.

#### 3.2 Meshing

In particular for stability and bearing capacity problems, the accuracy of the solution depends on the type and size of the elements. Upon global or local mesh refinement, the accuracy of results tends to improve, but the failure level is approached from the *unsafe* side (over-prediction). Particularly near loads, structures or other parts of the model where stress or strain concentrations are expected, local refinement is required. For geotechnical

applications, the use of higher-order elements is highly recommended to allow for at least a linear distribution of stress and strain within elements and to avoid locking. For 3D models, most accurate results are obtained using 20-node brick elements. The 10-node tetrahedral elements as used in the example are less accurate in calculating failure loads. Despite the local refinement around the anchor, the theoretical value (1220 kN) is exceeded by 8.8%.

### 3.3 Interface elements

Many geotechnical applications involve the interaction between soil and structures in or on the soil. Soil-structure interaction problems can be modelled using interface elements with limited shear strength and tension capacity. The elastic stiffness of interface elements is a numerical compromise to obtain on one hand small (negligible) elastic deformations (means: very high stiffness) and on the other hand a non-diverging iterative procedure (means: stiffness not too high). The shear strength in the interface can conveniently be related to the shear strength of the surrounding soil by using an interface strength reduction factor. The tension capacity is usually zero, which leads to gapping between a structure and the surrounding soil as soon as tensile stresses tend to occur.

It is recommended to extend interfaces below the bottom of a structure in the soil and at corners of massive structures in the soil in order to avoid locking and to enable a smooth stress distribution<sup>ii</sup>. For similar reasons, circular structures should be modelled with curved (iso-parametric) elements and corresponding curved interface elements to avoid locking and stress peaks.

In the example iso-parametric interface elements have been used around the caisson as well as extended interface elements at the bottom. Alternative models without extended interface elements and interface elements at the bottom showed a significantly higher failure load and peak stresses at the corners.

### 3.4 Soil modelling

In the example a rather simple linear elastic perfectly-plastic model with Tresca failure criterion has been used. The shear strength is increasing with depth. This 'undrained shear strength' approach is often used in bearing capacity (ultimate limit state) analysis on soft soil under undrained conditions, but one cannot expect accurate deformations (serviceability states) from such a simple model. If accurate deformations are to be calculated, the use of a more advanced model is recommended. Such a model ought to include stress-dependency of stiffness, high stiffness at small strains, plastic compaction in primary loading, plastic shearing in mobilising the material's shear strength and an effective strength formulation. In any case, when the material strength is modelled by means of effective strength properties, it is recommended to check the final stress state and to compare this with a known shear strength profile. Even advanced soil models may have difficulties predicting realistic shear strength using effective strength properties.

### 3.5 Calculations

Because of the non-linearity of soil behaviour, a geotechnical project needs to be modelled in sufficient detail, taking into account various stages of construction, since the order in which events happen matters. In addition to the calculation of deformations and forces under serviceability states, limit state criteria may need to be applied for all construction stages. Critical or decisive events may occur in intermediate stages and not necessarily the final

stage. This requires facilities in the finite element program for staged construction and safety analysis. The latter should preferably be done for geotechnical calculations using a strength reduction technique<sup>iii</sup> rather than increasing the load, except if the strength has been modelled as undrained shear strength, such as in the example problem. New methods are being developed to include partial factors for model parameters, actions (loads) and resistances according to Eurocode 7.

#### 4 CONCLUSIONS

In this contribution some issues related to finite element calculations for geotechnical applications are considered. On the basis of an example, the bearing capacity of a suction caisson, some particular issues are highlighted. This leads to some conclusions about the possibilities and limitations of the finite element method for geotechnical applications.

- The position of model boundaries should be chosen in accordance with the type of analysis and the type of soil model.
- Element type, size and local refinement, as well as extended and iso-parametric interface elements are essential to accurately predict bearing capacity in soil-structure interaction problems.
- Simple soil models with direct input of shear strength may be adequate to calculate bearing capacity (ultimate limit state), but more advanced models are required to accurately model deformations (serviceability states).
- Always compare the resulting stress state with a known shear strength profile.
- It may be necessary to apply limit state criteria to all construction stages and not only the final stage.

#### REFERENCES

- [i] Andersen K.H., Murff J.D., Randolph M.F., Clukey E.C., Erbrich C., Jostad H.P., Hansen B., Aubeny C., Sharma P., Supachawarote C. (2005). Suction anchors for deepwater applications. Proc. Int. Symp. On Frontiers in Offshore Geotechnics, ISFOG, Perth. Rotterdam: Balkema.
- [ii] Van Langen, H. (1991). Numerical analysis of soil-structure interaction. Dissertation. Delft University of Technology.
- [iii] Brinkgreve R.B.J., Bakker H.L. (1991). Non-linear finite element analysis of safety factors. Proc. 7th Int. Conf. on Comp. Methods and Advances in Geomechanics, Cairns, Australia, pp. 1117-1122.





## CARDIOSENSE3D: TOWARDS PATIENT-SPECIFIC CARDIAC SIMULATION FOR CLINICAL APPLICATIONS

H. Delingette<sup>\*</sup>, M. Fernandez<sup>†</sup>

<sup>\*</sup> Asclepios Team, Institut National de Recherche en Informatique et Automatique (INRIA)  
2004 Route des Lucioles, BP 93, Sophia-Antipolis, France  
e-mail: Herve.Delingette@inria.fr , web page: <http://www-sop.inria.fr/asclepios/>

<sup>†</sup> Reo Team, Institut National de Recherche en Informatique et Automatique (INRIA)  
Route de Voluceau, Rocquencourt, France  
Email: Miguel.Fernandez@inria.fr - Web page: <http://www-rocq.inria.fr/reo>

**Key words:** Cardiac Simulation, Electrophysiology, biomechanics

**Abstract.** *In this paper, we overview the objectives and achievements of the CardioSense3D project dedicated to the construction of an electro-mechanical model of the heart.*

### 1 CARDIOSENSE3D

CardioSense3D is a 4-year Large Initiative Action launched in 2005 and funded by the French national research center INRIA which focuses on the electromechanical modeling of the heart. The objectives of CardioSense3D are threefold:

To build a cardiac simulator, with identifiable parameters, that couples 4 different physiological phenomena: electrophysiology, mechanical contraction and relaxation, myocardium perfusion and cardiac metabolism

To build data assimilation software that can estimate patient specific parameters and state variables from given observations of the cardiac activity,

To build several application software based on this simulator and data assimilation techniques to solve clinical problems related to the diagnosis or therapy of cardiac pathologies in order to:

- • Significantly improve medical practice in terms of better prevention, diagnosis, quantitative follow-up, simulation and guidance of therapy,
- • support biomedical research in the preparation and evaluation of new diagnostic and therapeutic tools,
- • advance the fundamental knowledge of the integrative physiology of the heart.

CardioSense3D relies on the expertise of four INRIA research teams (resp. Asclepios, Reo, Macs, Sosso2) covering the fields of medical image analysis, computational structural and fluid dynamics, numerical analysis and control. But is also a collaborative framework that involves clinical centers such as the Guy's Hospital London, the Laboratory of Cardio-Energetics at the National Institutes of Health, the Hospital Henri Mondor (J. Garot), and other partners listed [here](#). Reaching those three objectives requires tackling the following challenges:

- The introduction of models and related numerical procedures to represent some important physiological phenomena still not considered, in particular: cardiac metabolism, perfusion and tissue remodeling. The extended models must remain

identifiable with the available data and computationally tractable. This sets the limits of the otherwise endless quest for model fidelity and simulation accuracy.

- The formulation of effective data assimilation methodologies associated with those models that can estimate patient-specific indicators from actual measurements of the cardiac activity. Major shortcomings of existing methods include robustness and computational cost (the "curse of dimensionality").
- The adaptation and optimization of the cardiac simulator (including both direct and inverse approaches) to some targeted clinical applications.

For each application, specific problems connected with clinical science will be considered.

### 3 SOME CARDIOSENSE3D RESEARCH ACTIVITIES

We illustrate below some of recent research advances performed within CardioSense3D.

#### Statistical Analysis of Diffusion Tensor Imaging of canine hearts. In Figure 1 and 2,

We show in Figure 1 some recent results<sup>6</sup> concerning the statistical analysis of Diffusion Tensor Imaging (DTI) of nine canine hearts. Diffusion imaging helps to reveal the fine structure of the myocardium such as the fiber orientation and possibly the location and orientation of laminar sheets. This structural information is crucial for modeling both the mechanical and electrophysiological function of the heart.

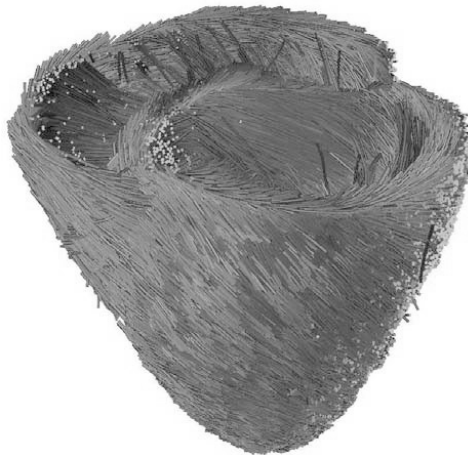


Figure 1 : Fiber tracking performed on an average Canine heart build from nine canine images.

#### Electro-physiology Modeling

Several electrophysiological models have been proposed within CardioSense3D, including front propagation techniques<sup>10</sup> phenomenological models<sup>7</sup> and a 8-variable cardiac cell model

describing the dynamics of calcium<sup>6</sup>. Model-based ECG processing for identification of restitution curves have also been proposed<sup>3</sup>

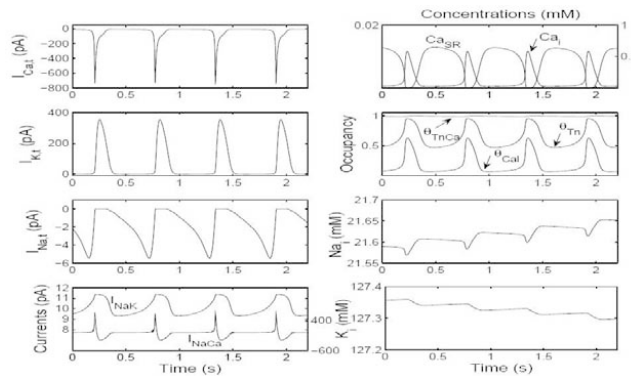


Figure 2 : Computed spontaneous action potential and ionic currents (left) and intracellular Ca++ dynamics (from (Djabella and Sorine 2006a)).

### Electro-mechanical model of the heart

The coupling between electrophysiology and mechanics<sup>1</sup> is governed by a chemically-controlled constitutive law which is consistent with general thermodynamics and with the behavior of myosin molecular motors. The biomechanical model is based on a Hill-Maxwell rheological scheme<sup>4</sup> pressure boundary conditions being controlled by valve and Winkessel models<sup>9</sup> Figure 4 shows the biventricular model at end diastole and end systole.

### Coupling Models with Observations

The objective of estimating model parameters from observations is a key aspect of CardioSense3D. Preliminary results have been obtained on this front, by globally integrating the electromechanical heart models with clinical datasets<sup>13,8</sup> (3D endocardial mapping with tagged, SSFP and late enhancement MR images), by estimating apparent electrical conductivities from electrophysiological mappings<sup>5</sup> and by estimating regional contractilities<sup>12,9</sup> from motion information.

### REFERENCES

- [1] Bestel, J., F. Clément, and M. Sorine (2001). A biomechanical model of muscle contraction. In W. Niessen and M. Viergever (Eds.), *Medical Image Computing and Computer-Assisted intervention (MICCAI'01)*, Volume 2208 of *Lecture Notes in Computer Science (LNCS)*, pp.1159–1161. Springer.
- [2] Djabella, K. and M. Sorine (2006, July 31-August 4). A reduced differential model for cardiac action potentials. In *SIAM Conference on the Life Sciences*, Raleigh, USA.
- [3] Illanes Manriquez, A., Q. Zhang, C. Medigue, Y. Papelier, and M. Sorine (2006). Electrocardiogram-based restitution curve. In *Computers in cardiology*, Valencia, Spain.
- [4] Krejci, P., J. Sainte-Marie, M. Sorine, and J. Urquiza (2006, September). Solutions to muscle fiber equations and their long time behaviour. *Nonlinear Analysis: RealWorld Applications* 7(4).
- [5] Moreau-Vill'eger, V., H. Delingette, M. Sermesant, H. Ashikaga, O. Faris, E. McVeigh, and N. Ayache (2006, August). Building maps of local apparent conductivity of the epicardium with a 2D electrophysiological model of the heart. *IEEE Transactions on Biomedical Engineering* 53(8), 1457–1466.

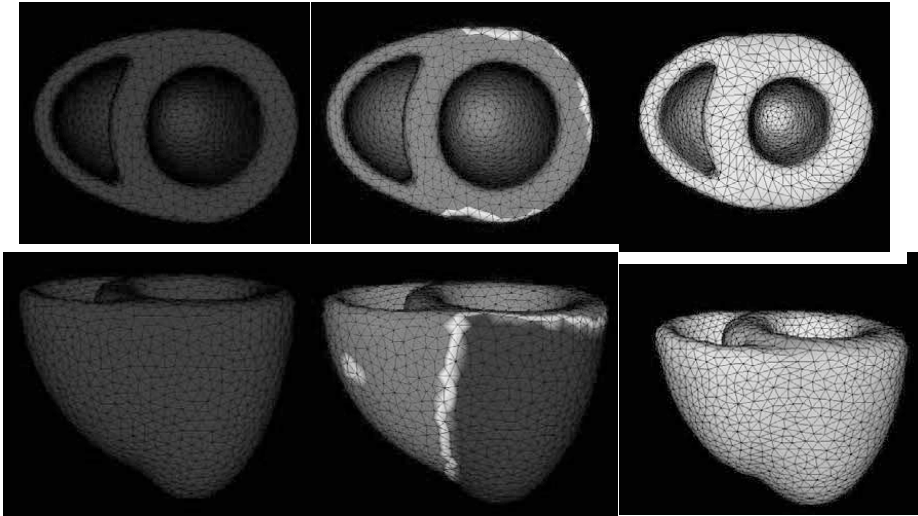


Figure 3: Short axis (top row) and long axis (bottom row) views of an electromechanical heart model during end diastole (left column), ventricular depolarization (middle column) and end systole (right column).

- [6] Peyrat, J.-M., M. Sermesant, H. Delingette, X. Pennec, C. Xu, E. McVeigh, and N. Ayache (2006, 2-4 October). Towards a statistical atlas of cardiac fiber structure. In Proc. of MICCAI' 06, Part I, Number 4190 in LNCS, pp. 297–304.
- [7] Pop, M., M. Sermesant, Y. Coudi'ere, J. Graham, M. Bronskill, A. Dick, and G. Wright (2006). A theoretical model of ventricular reentry and its radiofrequency ablation therapy. In 3rd IEEE 4 International Symposium on Biomedical Imaging: Macro to Nano (ISBI'06), pp. 33–36.
- [8] Rhode, K., M. Sermesant, D. Brogan, S. Hegde, J. Hipwell, P. Lambiase, E. Rosenthal, C. Bucknall, S. Qureshi, J. Gill, R. Razavi, and D. Hill (2005). A system for real-time XMR guided cardiovascular intervention. *IEEE Transactions on Medical Imaging* 24(11), 1428–1440.
- [9] Sainte-Marie, J., D. Chapelle, R. Cimrman, and M. Sorine (2006). Modeling and estimation of the cardiac electromechanical activity. *Computers & Structures* 84, 1743–1759.
- [10] Sermesant, M., Y. Coudi'ere, V. Moreau-Vill'eger, K. Rhode, D. Hill, and R. Ravazi (2005). A fast-marching approach to cardiac electrophysiology simulation for XMR interventional imaging. In Proceedings of MICCAI'05, Volume 3750 of LNCS, Palm Springs, ,pp. 607–615. Springer Verlag.
- [11] Sermesant, M., H. Delingette, and N. Ayache (2006). An electromechanical model of the heart for image analysis and simulation. *IEEE Transactions in Medical Imaging* 25(5), 612–625.
- [12] Sermesant, M., P. Moireau, O. Camara, J. Sainte- Marie, R. Andriantsimiavona, R. Cimrman, D. Hill, D. Chapelle, and R. Razavi (2006). Cardiac function estimation from MRI using a heart model and data assimilation: Advances and difficulties. *Medical Image Analysis* 10(4), 642–656.
- [13] Sermesant, M., K. Rhode, G. Sanchez-Ortiz, O. Camara, R. Andriantsimiavona, S. Hegde, D. Rueckert, P. Lambiase, C. Bucknall, E. Rosenthal, H. Delingette, D. Hill, N. Ayache, and R. Razavi (2005). Simulation of cardiac pathologies using an electromechanical biventricular model and XMR interventional imaging. *Medical Image Analysis* 9(5), 467–480.

## **Contributed Papers**



## INTEGRATION OF GID WITH A TENSION STRUCTURE COMPUTER ANALYSIS PROGRAM USING ADA95

Cristina A. B. e Silva<sup>\*</sup> and Athail R. Pulino Filho<sup>†</sup>

<sup>\*</sup> Civil and Environmental Engineering Department  
Universidade de Brasília  
Campus Universitário Darcy Ribeiro, 70910-900 Brasília-DF, Brasil  
e-mail: crisabs@gmail.com, web page: <http://www.unb.br/ft/enc/estruturas>

<sup>†</sup> Civil and Environmental Engineering Department  
Universidade de Brasília  
Campus Universitário Darcy Ribeiro, 70910-900 Brasília-DF, Brasil  
e-mail: arpulino@gmail.com, web page: <http://www.unb.br/ft/enc/estruturas>

**Key words:** Tension structure, Membrane structure, Non linear analysis

**Abstract.** *The use of structures built with metallic masts, high resistance cables and synthetic fabric for different purposes has had a quite significant growth. The research goal was the integration of Membrane, Lights and GiD programs for preliminary geometry and tension analysis of the Community Center roof at the Universidade de Brasília because although the program Lights solves problems faced by other systems in structures analysis with finite displacements, it doesn't have pre and post processing methods. GiD was a program made for this purpose, using systems developed by the user. The programs Membrane, Lights and GiD were integrated using Ada95, making it possible to exchange files and results among these programs, besides the graphic visualization in GiD of the tensions and displacements calculated. A manual was created with an example step by step which includes all these integration possibilities. The obtained results with static wind load and pre tensioning show how important it is to know the parameters that define the membrane mechanical characteristics to be used and how complex is the analysis of this type of structure. To evaluate properly the effects of the wind, it is necessary to make wind tunnel tests. The results analysis of the Community Center was not very accurate due to lack of information about the materials used in the construction and a detailed project.*



## 1 INTRODUCTION

The use of structures built with metallic masts, high resistance cables and synthetic fabric, called tensioned fabric structures, had a reasonable growth in the last decade of the 20<sup>th</sup> century. Constructions for different purposes were built with this technology. This structural type has important advantages, such as: it allows large spans, has low self weight, it can be easily produced, transported and assembled.

A tension structure project is usually divided in three parts: shape finding, cutting pattern and structural analysis. The membrane final shape is the result of architectural design and structural studies considering the following loads depending on the case: pre stressing, wind, snow, self weight and accidental loads.

To have a lasting and stable tension structure, the membrane must be always prestressed, guaranteeing an anticlastic surface. To be able to make a good project, the tension-deformation relation of the material has to be tested if it is not already known.

## 2 GOAL

The research goal was the integration of Membrane, Lights and GiD programs for preliminary geometry and tension analysis of the Community Center roof at the Universidade de Brasília because although the program Lights solves problems faced by other systems in structural analysis with finite displacements, it doesn't have pre and post processing methods. GiD was a program made for this purpose, using systems developed by the user<sup>iii</sup>.

## 3 INTEGRATION OF PROGRAMS USING ADA95 AND RESULTS

Membrane, Lights and GiD were integrated through the development of smaller programs called GiDLights, GiDMembrane and MembraneLights and the adaptation of the program Lights into LightsGiD using Ada95<sup>iii</sup>, making it possible to exchange files and results among these programs.

Lights<sup>iv</sup> is a program that calculates and allows the analysis of tension structures using finite element method, including the membrane, cables and frame elements. The stable equilibrium configuration of the structure is calculated by minimizing the total potential energy with Quasi-Newton method<sup>v</sup>.

LightsGiD is a version of Lights with procedures developed in this research that calculate, organize and create files with necessary data for graphic visualization of tensions and displacements results in GiD.

With the basic geometry data of the structure that is going to be studied, it is possible to make the contour drawing in GiD pre process mode or to import the drawing from another program. Then inside GiD a three node triangle finite element mesh is generated and exported.

If only the initial shape is desired, with GiDMembrane program the input file for Membrane is created. After running Membrane, the results can be seen in GiD post process mode.

When a satisfying shape is found, with MembraneLights program it is possible to create one of the input files for LightsGiD, which can load the structure with different combinations.

LightsGiD may also include cable and frame elements, and not only membrane, in the analysis according to the needs of the project. The results from this program may be seen in GiD post process mode.

Another possibility is to use the program GiDLights to make one of the input files for LightsGiD right after generating the mesh in GiD.

If only part of the mesh is generated at first and then mirrored (Fig. 1), it is recommended to use GiD version 8.0 or the latest one available because these newer versions maintain the normal vector of a mirrored mesh in the same direction of the original mesh. The older versions reverse the direction of the normal vector when a mesh is mirrored, causing problems when loading the structure.

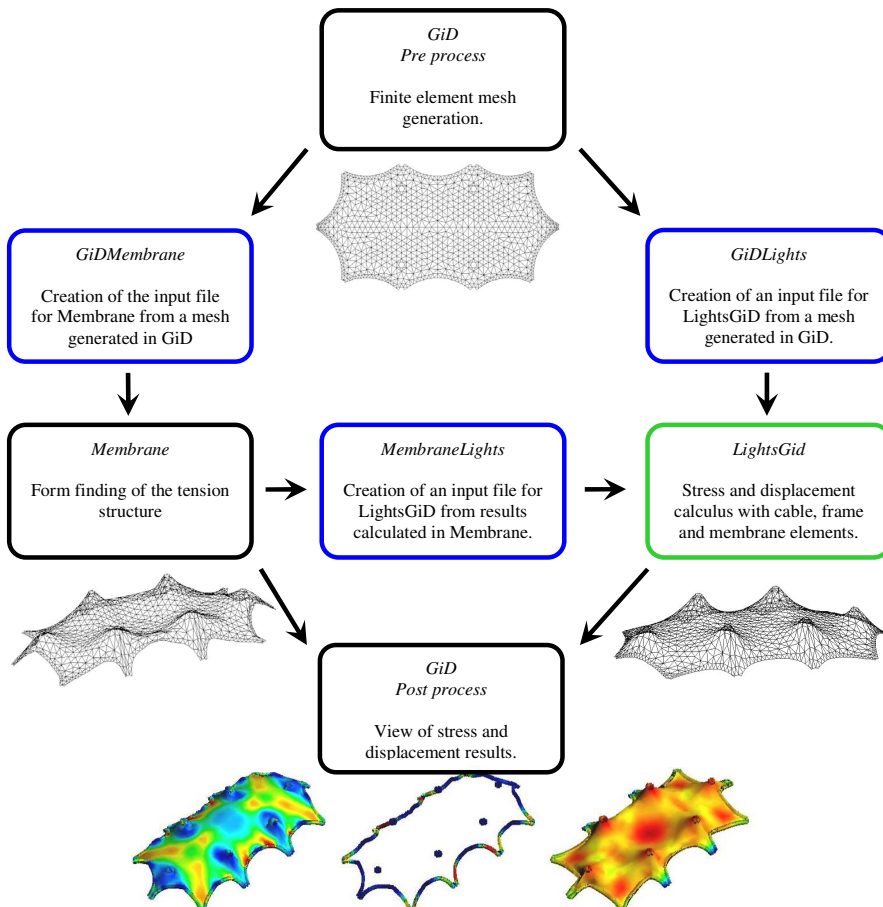


Figure 1: Scheme of the developed (blue) and modified (green) programs with examples of results<sup>vi</sup>.

This routine with all the programs was tested with simple examples of tension structures, steel towers with cables and with a tension structure built for events at the Universidade de Brasília called Athos Bulcão Community Center. The graphics shown in figure 1 are from the analysis of this structure in Brasília.

During the studies of this specific case, loads were distributed on all membrane elements to simulate a static wind load of  $75 \text{ kgf/m}^2$  in each direction. After that, the cables were stressed to search for a configuration without compressed membrane elements.

A manual was created to make it easier to use these programs with an example step by step which includes all these integration possibilities. The master thesis<sup>vi</sup> presented with this work also includes a CD with examples and source codes of the programs.

#### 4 CONCLUSIONS

The obtained results with static wind load and pre tensioning showed how important it is to know the parameters that define the mechanical characteristics of the membrane to be used and how complex is the analysis of this type of structure. To evaluate properly wind effects it is necessary to make wind tunnel tests.

The results analysis of Athos Bulcão Community Center tension structure was not very accurate due to lack of information about the materials used in the construction and a detailed project.

#### ACKNOWLEDGMENT

We would like to thank FINATEC – Fundação de Empreendimentos Científicos e Tecnológicos for the financial help during the development and presentation of this article.

#### REFERENCES

- [i] R. Ribó et al. *GiD The Personal Pre and Postprocessor: Reference Manual*, Barcelona, Version 8. Available at: <<http://www.gidhome.com>>. Access: 17 jul. 2006. ISBN 84-95999-95-1 (2006).
- [ii] R. Ribó et al. *GiD The Personal Pre and Postprocessor: User Manual*, Barcelona, Version 8. Available at: <<http://www.gidhome.com>>. Access: 17 jul. 2006. ISBN 84-95999-94-3 (2006).
- [iii] J. Skansholm. *Ada 95: From the Beginning*, Essex: Addison Wesley Longman ISBN 0-201-40376-5 (1997).
- [iv] V.F. Arcaro. *Lights User's Manual*, Campinas. Available at: <<http://www.arcaro.org/tension>>. Access: 15 set. 2006.
- [v] V.F. Arcaro. *A Simple Procedure for Shape Finding and Analysis of Fabric Structures*, Campinas. Available at: <<http://www.arcaro.org/tension>>. Access: 15 set. 2006.
- [vi] C.A.B. Silva. *Modelo computacional para análise da tensoestrutura de cobertura do Centro Comunitário da Universidade de Brasília*, Master Thesis in Structures and Civil Construction, Departamento de Engenharia Civil e Ambiental, Universidade de Brasília. (2006).

## USING GiD TO DESIGN AN INTRAVASCULAR SUPPORT SYSTEM

Maurizio Bordone<sup>\*</sup>, Eduardo Soudah<sup>\*</sup>, Eugenio Oñate<sup>\*</sup>, Michele Chiumenti<sup>\*</sup>

<sup>\*</sup> International Center for Numerical Methods in Engineering (CIMNE)  
Universidad Politécnica de Cataluña  
Campus Norte UPC, 08034 Barcelona, Spain  
E-mail: gidconf@cimne.upc.edu, web page: <http://www.cimne.com/>

**Key words:** GiD, cardiovascular diseases, intravascular supports, auto-expandible

**Abstract.** *Vascular diseases are very common, nowadays, especially as people age, due to bad eating habits and physical inactivity, among other causes. This fact is very important because this problem trends to grow up quickly, especially in industrialized countries. New kinds of surgical techniques use to detect and treat vascular diseases, every day, micro-invasive approaches, like endo-surgery, endoscopy and catheterism. Medical solutions like stent applications, substitutions of cardiac valvulas use today these innovative techniques. Due to this fact the study of the materials used in these devices becomes an important matter. GiD gives the possibility to design and study through different problems type's devices that can be used to solve problems like these. The object of this work is to model and analyze with GiD and with the thermo-mechanical computational code COMET an intravascular metallic support that can be compressed until the right dimension is reached, so it can be inserted via-catheter in situ. The decompression of the device is of primary importance because every plastic deformation can interests the final disposition of the support and it could change its properties and the capacity to perform properly. This investigation will focus in the study of the forces implied and the effects on the device material. Also the different behaviour of various bio-materials like Steel, Titanium and Nitinol are studied. This study can help to find the best configuration for this kind of devices.*

### 1 INTRODUCTION

Cardiovascular diseases (CVD) are the first cause of death in European people. CVD provokes 4,35 millions of deaths in the 52 states of European Region. WHO estimates more than 1,9 millions of deaths in EU, and affirm that CVD plays a big rule in reduction of quality life and like cause of physical handicaps, especially in older people; this fact is very important considering that the world population trend to get older generation by generation.

Modern surgery looks for minimal invasive solutions like the mini-invasive technique of surgery. This technique consists to reach internal cavity without cut or open the patients

minimizing post-operative risks, in this group are included endoscopy, arthroscopy and other more.

Mini-invasive surgery finds also applications in the applications of cardiovascular stents, probe, valves replacements, using catheters and travelling trough arteries like femoral, coronary or aortic vessel. *GiD* results very utile to design and reproduce the movements of these devices

## 2 METHODS

Target of the study will be the design of a new indo-vessel support and a comparison of this new hypothetical device with a commercialized support. Studying with FEM<sup>i</sup> the existent devices it is possible to have some guide-lines that will be followed to design new devices. The design of the support wants to follow some fundamental directive: the simplicity of the structure, the employ of hyper-elastic material (Nitinol in these tests), the repetition of a single sample that will be repeated to construct the complete geometry. Four different geometries will be compared in the capacity of flexibility and resistance at radial stress, finally radial force of every devices will be compared with the radial force of the *Edward Sapien THV valve support*.

### 2.1 Geometry

The first requirement for a support is the possibility to couple the support with the vessel, so a pseudo-cylindrical geometry is required. Implementing a *macro* that transform a 3D-planar mesh in a 3D-cylindrical one, is possible to design a single sample in Cartesian coordinates, and work assigning the properties of the material, conditions and meshing the geometry and finally transform the mesh in the desired configuration.

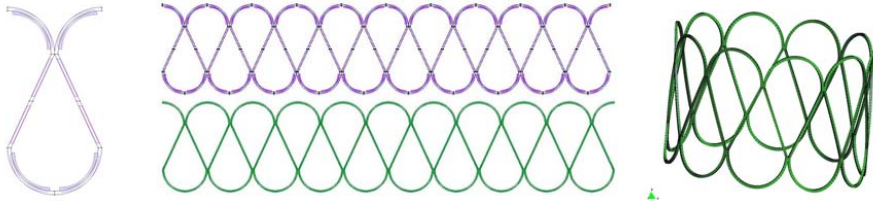


Figure 1: Design of the support

*Comet*<sup>ii</sup> will be the *problem type* used to solve the mechanical problem studied. The four geometries propose different characteristics, model N1 is a simple snake-curl blade, model N2 takes the N1 geometry but presents two samples more and a curvature in upper and lower extremity to enjoy a better radial force and improve the coupling capacity of the device. Model N3 and N4 have similar geometries to N1 and N2 but present more compacted samples, able to reach upper level of radial force. N4 presents less linear parts and bigger common strong parts respect N3.

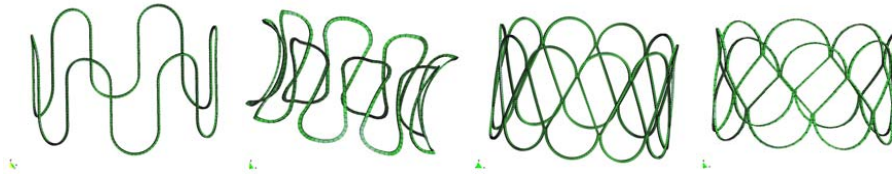


Figure 2: N1, N2, N3 and N4 in the final configurations of work.

## 2.1 Conditions

The testes performed focus to study the behaviour of the different models in compression, to value the capacity to reach a diameter of only 5 mm, so that have a compression of 500%. The tests study the possibility to reach this dimension without present plastic deformation on the material, for this reason Nitinol<sup>iii</sup> will be selected. Secondly will be effectuated a comparison between these 4 prototypes and a commercial device, actually on sale. The comparison shows the resistance to an external pressure that simulates the body vessel compression, because the real action of the body is unknown. For first test a prescribed displacement is used to compress the supports, the tension and stresses are studied and compared to value the best geometry in compression. Second test is performed with a surface load that provokes a compressive pressure in all the external surfaces of the device

## 3 RESULTS

### 3.1 Compression Study

First test studies the maximal stress provoked in the devices. Every single model reaches the desired final configuration.

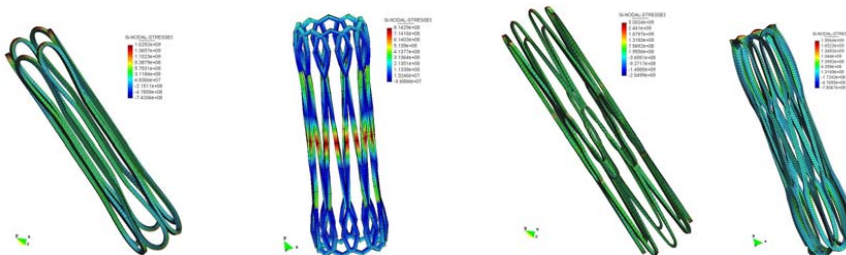


Figure 3: N1, N2, N3 and N4 in the compressed configurations.

GiD Permits to study precisely the zones of maxim tension and stresses, allowing to define the regions that overpass elastic regime, identical results are been obtained studying only half part of the body. GiD post-processor can mirror the geometry in result configuration and visualize the entire structure, this option permit to save time and to reduce computational costs, this operation was possible with another macro, inserted in GiD that transform linear coordinates in cylindrical ones but with only 180 degrees of rotation . Videos of simulations was been registered to show clearly the movements and the displacement of the different devices.

### 3.1 Radial Forces Study

The comparison of the different models in work-configuration is performed by the study of the device deformation under external superficial pressure. Using graph tools of GiD, deformation / pressure graphics was exported and elaborated to obtain other interesting data in the points of interest for every studied geometry.

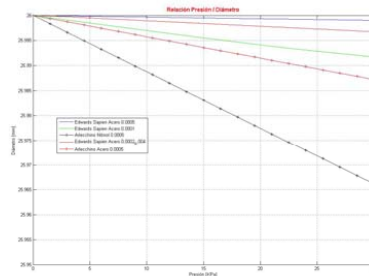


Figure 4: Relation between pressure and diameter reduction in some of studied devices.

## 4 DISCUSSION

The precision of registered and exported data permits to study exhaustively the devices characteristics, and allows raising the quality of the geometry that can performs all the required technical characteristics. Almost every corrections were been effectuated trough GiD wizard enjoying simplicity and rapidity data modifications the others one was done directly in calculation files created by GiD pre-processor. The possibility of work with calculation files permits to export GiD outputs and use them with other software, raising the portability of GiD technology.

## 5 CONCLUSIONS

All goals imposed at the beginning of the study was been reached trough GiD pre and post processor. The results were used to give the bases of future probable development of a real vascular support. The development of geometrical transformation macro, allows constructing hard geometry in a simpler way and saving time to calculate the tests.

## REFERENCES

- [i]O.C. Zienkiewicz and R.L. Taylor, *The finite element method*, McGraw Hill, Vol. I., 1989, Vol. II, (1991).
- [ii]M. Cervera, C. Agelet de Saracibar and M. Chiumenti, *COMET Coupled Mechanical and Thermal Analysis*, CIMNE 2002
- [iii]F.Auricchio, L. Faravelli, G. Magonette and V. Torra, *Shape Memory Alloys. Advances in Modelling and Applications*, CIMNE aReries of Handbooks on Theory and Engineering Applications of Computational Methods

## PFEM APPLICATIONS IN FLUID-STRUCTURE INTERACTION PROBLEMS

M.A. Celigueta, A. Larese and S. Latorre

International Center for Numerical Methods in Engineering (CIMNE)  
Campus Norte UPC, Edifici C1, Gran Capitan, 08034, Barcelona  
e-mail: [maceli@cimne.upc.edu](mailto:maceli@cimne.upc.edu), [antoldt@cimne.upc.edu](mailto:antoldt@cimne.upc.edu)  
[latorre@cimne.upc.edu](mailto:latorre@cimne.upc.edu)  
web page: <http://www.cimne.com/pfem>

**Key words:** PFEM, Fluid Dynamics, FSI

**Abstract.** *In the current paper the Particle Finite Element Method (PFEM), an innovative numerical method for solving a wide spectrum of problems involving the interaction of fluid and structures, is briefly presented. Many examples of the use of the PFEM with GiD support are shown. GiD framework provides a useful pre and post processor for the specific features of the method. Its advantages and shortcomings are pointed out in the present work.*

### 1 INTRODUCTION

Nowadays there is an increasing interest in the development of robust and efficient numerical methods for the analysis of engineering problems involving the interaction of fluids and structures accounting for large motions of the fluid free surface and the existence of fully or partially submerged bodies.

Examples of this kind are common in ship hydrodynamics, off-shore and harbor structures, ocean engineering, modeling of tsunamis, spillways in dams, free surface channel flows, liquid containers, stirring reactors, mould filling processes, etc.

The analysis of fluid-structure interaction (FSI) problems using the finite element method (FEM) with either the Eulerian formulation or the Arbitrary Lagrangian Eulerian (ALE) formulation encounters a number of serious problems. Among these we list the treatment of the convective terms and the incompressibility constraint in the fluid equations, the modeling and tracking of the free surface in the fluid, the transfer of information between the fluid and solid domains via the contact interfaces, the modeling of wave splashing, the possibility to deal with large rigid body motions of the structure within the fluid domain, the efficient updating of the finite element meshes for both the structure and the fluid, etc.

Most of these problems disappear if a Lagrangian description is used to formulate the governing equations of both the solid and the fluid domain. In the Lagrangian formulation the motion of the individual particles are followed and, consequently, nodes in a finite



element mesh can be viewed as moving particles. The motion of the mesh discretizing the total domain (including both the fluid and solid parts) is also followed during the transient solution.

The Particle Finite Element Method (PFEM) is a particular class of Lagrangian formulation aiming to solve problems involving the interaction between fluids and solids in a unified manner [4].

Being developed in CIMNE during the major part of its life, PFEM's natural evolution was linked to GiD, and even to GiD's evolution.

PFEM features and some examples of its applications to civil engineering problems are presented in the following sections. GiD powerful tools for the pre and post process of the analyzed cases are shown and a list of its weak points is also made to allow a continuous improvement of its possibilities.

## 2 AN OVERVIEW OF PFEM

The PFEM is the natural evolution of recent work of the authors for the solution of FSI problems using Lagrangian finite element and meshless methods [6], [3], [4] and [7].

In the PFEM approach, both the fluid and the solid domains are modeled using an updated Lagrangian formulation [1]. The finite element method (FEM) is used to solve the continuum equations in both domains. Hence a mesh discretizing these domains must be generated, in order to solve the governing equations for both the fluid and solid problems in the standard FEM fashion.

The mesh nodes in the fluid domain are treated as particles which can freely move and even separate from the main fluid domain representing, for instance, the effect of water drops. A finite element mesh connects the nodes defining the discretized domain where the governing equations are solved in the standard FEM fashion.

Adaptive mesh refinement techniques can be used to improve the solution in zones where large motions of the fluid or the structure occur [7]. The Lagrangian formulation allows us to track the motion of each single fluid particle (a node). This is useful to model the separation of water particles from the main fluid domain and to follow their subsequent motion as individual particles with an initial velocity and subject to gravity forces.

PFEM involves the following steps (schematically presented in fig. 1):

1. Discretize the fluid and solid domains with a finite element mesh. In our work we use an innovative mesh generation scheme based on the extended Delaunay tessellation [3], [4] and [7].
2. Identify the external boundaries for both the fluid and solid domains. This is an essential step as some boundaries (such as the free surface in fluids) may be severely distorted during the solution process including separation and re-entering of nodes. The Alpha Shape method [2] is used for the boundary definition.
3. Solve the coupled Lagrangian equations of motion for the fluid and the solid domains. Compute the relevant state variables in both domains at each time step: velocities,

pressure and viscous stresses in the fluid and displacements, stresses and strains in the solid.

4. Move the mesh nodes to a new position in terms of the time increment size. This step is typically a consequence of the solution process of step 3.
5. Generate a new mesh if needed. The mesh regeneration process can take place after a prescribed number of time steps or when the actual mesh has suffered severe distortions due to the Lagrangian motion.
6. Go back to step 2 and repeat the solution process for the next time step.

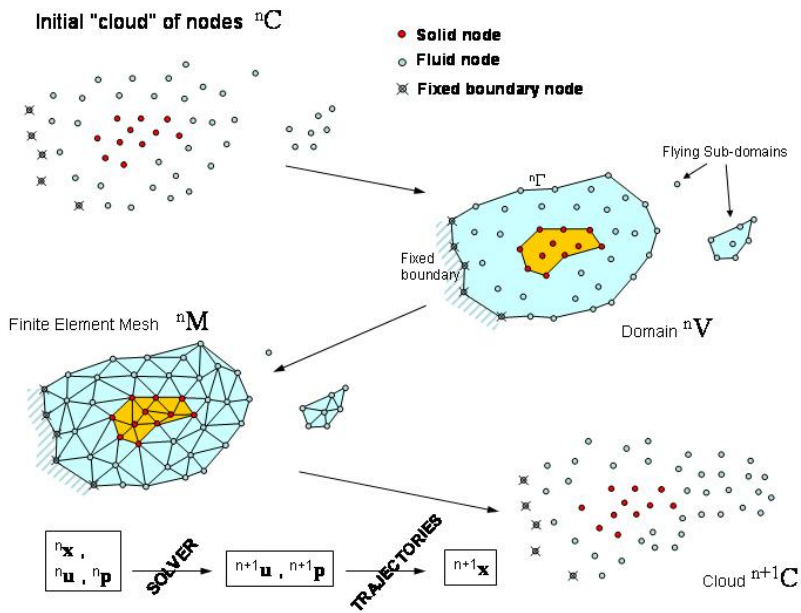


Figure 1: Sequence of steps to update a "cloud" of nodes from time  $n$  ( $t = t_n$ ) to time  $n+1$  ( $t = t_n + \Delta t$ ).

### 3 PFEM AND GiD. ADVANTAGES AND SHORTCOMINGS

From its early beginning the development of PFEM has been strictly connected to that one of GiD. Not only has it been linked to its use, but to its evolution as well, since every new feature in GiD was rapidly introduced in the pre and post-process of PFEM and its users have always been asking for new capabilities of GiD.

### 3.1 Pre-process

A simple problemtype that allows a graphical interface directly inside GiD is in continuous development in order to ease the introduction of data by the users, and it features the possibility to work with layers that separate different solid and fluid objects. The type of output results can be selected at will. At this level, no tcl-tk code has been necessary for the problemtype, only GiD language for problemtypes, which is quite understandable thanks to the very well suited tutorials.

The PFEM needs, first of all, a cloud of nodes to work with. The users get an initial geometry and mesh from GiD, using unstructured sized meshes and different layers organization, and the problemtype only takes the cloud of nodes and their properties for the PFEM, which creates a new triangulation with that information.

One of the worst drawbacks is that GiD is not a real CAD tool, but only a pre-processor for this type of work. So, sometimes the use of external powerful CAD programs becomes necessary, especially when complex geometries have to be generated.

However, the import module for external formats is quite useful and robust in these situations (fig. 2)

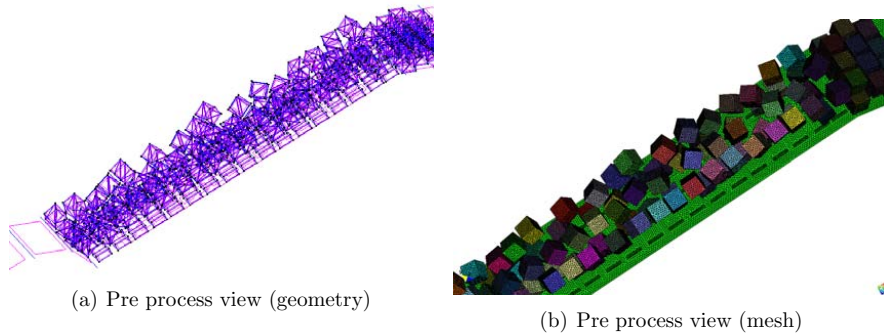


Figure 2: Complex geometry of multibodies imported from an external CAD tool

### 3.2 Post-process

The post-process is the only way to show the power of the PFEM. From the beginning, GiD has allowed PFEM users to customize the results they obtained. Since the PFEM re-meshes the domain at every time step, there are a lot of mesh files.

The feature *open several results* has made possible the creation of spectacular animations, which have been very useful when comparing numerical results with experimental tests like it is shown in fig. 3 where the sloshing phenomenon is studied [5] and the different results can be easily and directly compared. However, the dependence of this feature on the RAM space makes it very demanding in terms of hardware, taking into account that nowadays the PFEM is already able to run very large scale problems (millions of finite elements).

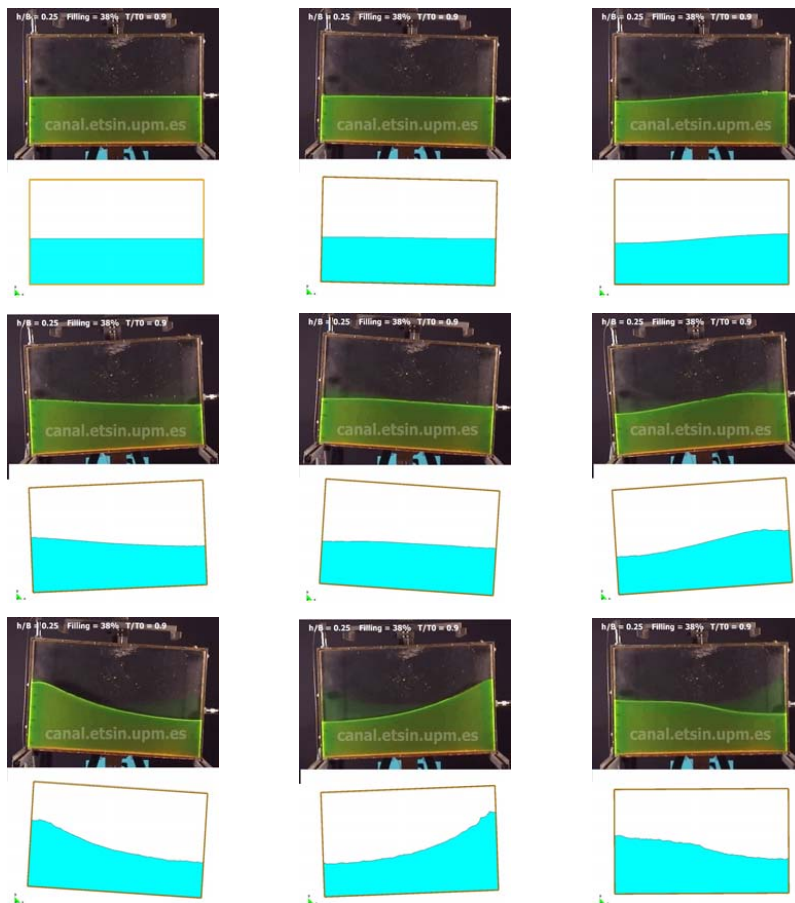


Figure 3: Comparison between PFEM and experimental results, in a sloshing analyzed phenomenon

For instance, the simulation of a multicellular box dock, pushed and carried by a heavy fluid (fig. 4), needed the creation of animations piece by piece, because each time step output files were about 200 MB (fig. 5). That was because the thickness of the problem was much smaller than the horizontal dimensions, but it could not be neglected to get a 2D model, so finally the mesh was as big as 3 million elements.

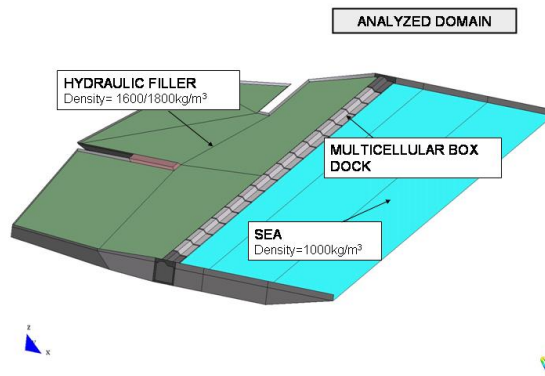


Figure 4: Domain of analysis of the 3 million elements model of a multicellular box dock between two fluids with different densities.

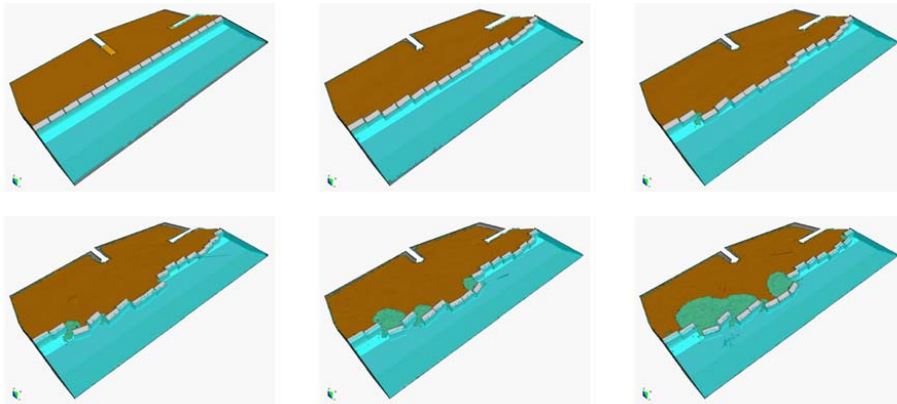


Figure 5: Evolution of the movement of the boxes because of the different density of the two fluids at the different sides

## 4 CONCLUSIONS

After 5 years of joint development the GiD-PFEM combination has proven to be a successful venture. The parallel evolution of both programs has been a synergic process which allowed all the parties involved to exploit their potential to a high level.

Nevertheless some issues remain which must be correctly addressed in order to fully realize the capabilities of this innovative tool suite. As already pointed out in the paper, high RAM consumption level in postprocess hampers users' productivity and limits their rate of progress.

However, all issues taken into account, the outlook for the future is extremely promising and we expect great improvements in robustness, computational cost and user-friendliness in the near term.

## REFERENCES

- [1] J. Donea and A. Huerta. *Finite Elements Methods for Flow Problems*. Wiley, 2003.
- [2] H. Edelsbruner and Mücke. E.P. Three dimensional alpha shape. *ACM Transaction on Graphics*, (1994).
- [3] S.R. Idelsohn, E. Oñate, and F. Del Pin. The particle finite element method: a powerful tool to solve incompressible flows with free-surfaces and breaking waves. *International Journal for Numerical Methods in Engineering.*, 61:61, 2004.
- [4] S.R. Idelsohn, E. Oñate, F. Del Pin, and N. Calvo. Fluid-structure interaction using the particle finite element method. *Computer Methods in Applied Mechanics and Engineering*, 195:2100–2123, 2006.
- [5] A. Larese, R. Rossi, E. Oñate, and S.R. Idelsohn. Validation of the particle finite element method (pfem) for simulation of free surface flows. *Accepted by: Engineering Computations*, 2008.
- [6] E. Oñate, J. García, S.R. Idelsohn, and F. Del Pin. Finite calculus formulations for finite element analysis of incompressible flows. eulerian, ale and lagrangian approaches. *Computer Methods in Applied Mechanics and Engineering*, 195:3001–3037, 2006.
- [7] E. Oñate, S.R. Idelsohn, F. Del Pin, and R. Aubry. The particle finite element method. an overview. *International Journal of Computational Methods*, 1:267–307, 2004.



## GID-ATENA INTERFACE – ADVANCED SIMULATION OF REINFORCED CONCRETE STRUCTURES

Jan Cervenka<sup>\*</sup>, Jiri Niewald<sup>\*</sup>

<sup>\*</sup> Cervenka Consulting  
Predvoje 22, 162 00 Praha 6  
e-mail: [cervenka@cervenka.cz](mailto:cervenka@cervenka.cz), web page: <http://www.cervenka.cz>

**Key words:** Nonlinear Analysis, Reinforced Concrete, Fracture Mechanics, Thermal Analysis, Creep Analysis, Dynamic Analysis

**Abstract.** *This paper describes the implementation and features of the GID interface to program ATENA. The interface supports several analysis types available in ATENA such as: static, creep, transport and dynamic. Special attention is devoted to the reinforcement modelling and implementation in the GID-ATENA interface.*

### 1 INTRODUCTION

ATENA<sup>1</sup> software is a finite element analysis system for advanced simulation of real behavior of reinforced concrete structures. It includes many unique features specific to the reinforced concrete analysis such as: robust and tested material models for concrete<sup>ii</sup>, reinforcement, steel and soil structure interaction. The system supports advanced analysis of statics, dynamics, transport as well as creep problems or extreme loading conditions such as for instance the structural damage and degradation due to fire.

The GID interface (Figure 1) for the ATENA software supports all analysis types available in ATENA, i.e. static, transport, creep and dynamics. Special treatment was necessary to facilitate the reinforcement modeling, which is an essential part of software targeted for the simulation of reinforced concrete structures. ATENA supports several methods of reinforcement modeling. The most comprehensive way of reinforcement modeling is based on the so-called embedded element approach (Figure 2). This approach is not directly supported by the GID pre-processing environment and special method had to be developed to facilitate a user-friendly as well as realistic reinforcement definition. The other supported methods are smeared reinforcement, layered reinforcement in shell elements or reinforcement fibers in beam elements.

The reinforcement modeling in GID-ATENA interface is schematically depicted in Figure 3. In the embedded reinforcement approach, the reinforcement crossing a mesh with three-dimensional elements is subdivided into truss elements, such that each truss element is defined by the intersection of the reinforcement bar with the individual solid elements, as it is



shown in Figure 2. The displacements of the nodes of these reinforcement trusses are then constrained to the deformation of the surrounding solid element. This subdivision of the reinforcement bars into the truss elements is not supported by GiD, and it is automatically handled by ATENA software at the beginning of the analysis.

The whole process is shown in Figure 3. The reinforcement is modeled as a line or poly-line, which in general case might be a curved entity. After the mesh generation, all one-dimensional entities that are not connected to any surface or region are automatically subdivided into 1D finite elements. These elements are then passed into ATENA software to describe the reinforcement geometry.

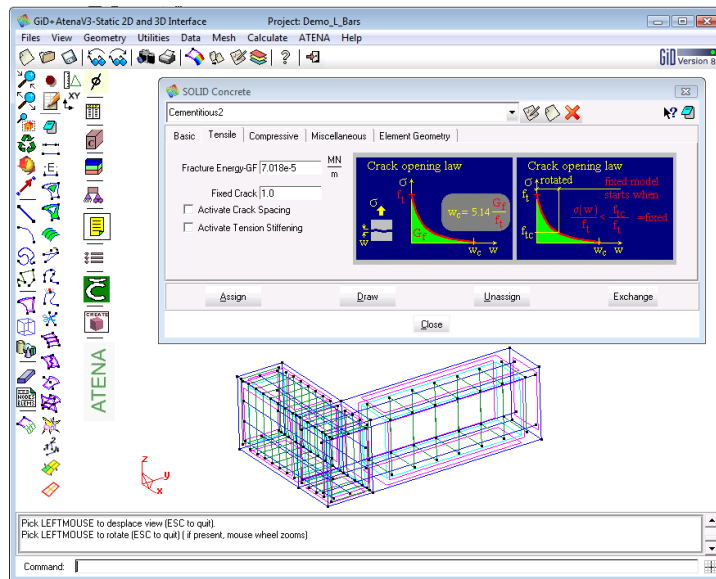


Figure 1: GiD-ATENA Interface – Reinforced Concrete

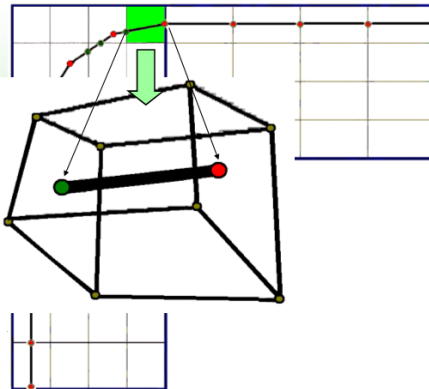


Figure 2: Modelling Reinforcement – Embedded Element Approach

Based on this information, ATENA determines the intersections with the basic three-dimensional solid model, and new truss elements and corresponding nodes are added to the structural numerical model. The newly created nodes are constrained to the existing nodes of the solid elements using the appropriate weight coefficients<sup>iii</sup>.

The presented approach has been successfully applied for many practical engineering problems. As an example of application, a nonlinear analysis of pre-stressed nuclear containment is selected. Figure 4 shows the resulting temperature distribution for an accident scenario from ATENA transport analysis. Figure 5 depicts the three-dimensional model created in GiD of the containment including the internal steel liner. The failure crack pattern and stresses in the complex arrangement of pre-stressing tendons is described in Figure 6.

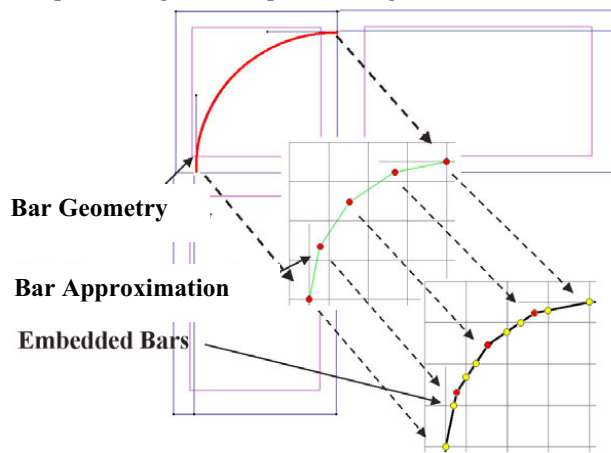


Figure 3: Modelling Reinforcement – Embedded Element Approach

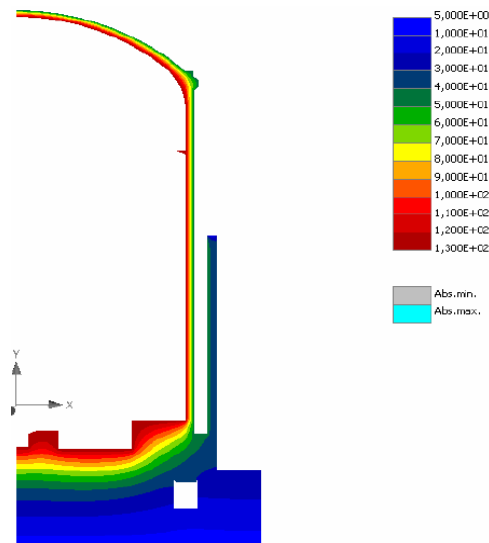


Figure 4: Thermal Analysis of Temperature Distribution at a Nuclear Containment during an Accident

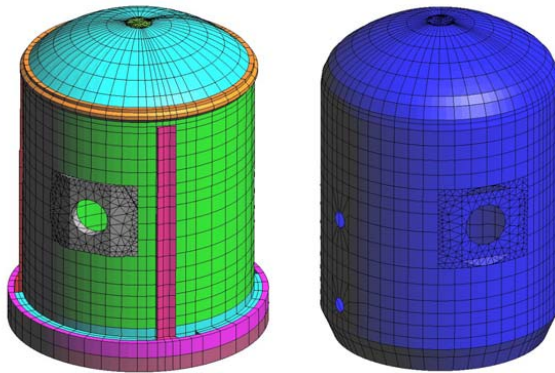


Figure 5: Numerical Model of Pre-stressed Containment (a) containment (b) steel liner

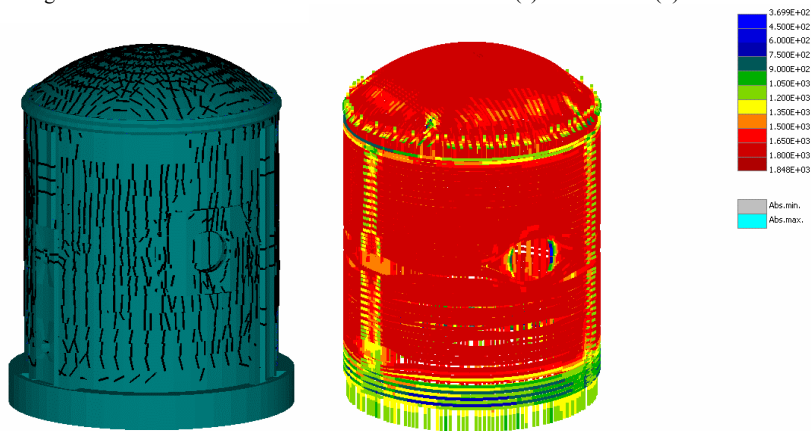


Figure 6: Crack Pattern at Failure and Yielding of Prestressing Tendons

## 2 CONCLUSIONS

The authors acknowledge the financial support of GACR project 103/07/1660 for the development of the transport interface and the European project I-SSB NMP2-CT-2006-026661 for the dynamic interface.

## REFERENCES

- [i] Červenka Consulting, (2007) *ATENA program documentation*, Part 1-8, [www.cervenka.cz](http://www.cervenka.cz)
- [ii] Červenka, J., and Papanikolaou, V.K. (2008) “Three dimensional combined fracture-plastic material for concrete”, *International Journal of Plasticity*, in press, doi:10.1016/j.ijplas.2008.01.004
- iii Jendele L., Cervenka J., (2007), On the Solution of Multi-Point Constraints - Application to FE Analysis of Reinforced Concrete Structures, submitted to *Computers and Structures*

## CARPA, A PROBLEMTYPE FOR A FREE SURFACE FLOW MODELLING SOFTWARE

Corestein, G. <sup>\*</sup>, Bladé, E. <sup>†</sup>

<sup>\*</sup> International Center for Numerical Methods in Engineering (CIMNE)  
Universidad Politécnica de Cataluña  
Campus Norte UPC, 08034 Barcelona, Spain  
Email: geocores@cimne.upc.edu

<sup>†</sup> Flumen Research Group.  
Universitat Politècnica de Catalunya  
Jordi Girona 1-3, D-1 08034 Barcelona, Spain  
Email: ernest.blade@upc.edu - Web page: <http://www.flumen.upc.edu>

**Key words:** GID Customization, DTM importation, 1D-2D hydrodynamic simulation

**Abstract.** *CARPA is the natural evolution of previous problemtype Ramflood created for the Ramflood EU Project (5<sup>th</sup> Framework Programme). From the initial capabilities of the software, new features have been included, both in the hydrodynamic simulation module and in the problemtype interface, both in the pre-process and post-process. Some of the new developments include new and re-organized menus to assign new properties related with hydrological processes, bedload sediment transport and parameters associated with the problem data as a resume option or the possibility of selecting the list of results to be visualized. These improvements, based in the experience acquired after using the system to solve various real engineering problems, have increased the robustness and efficiency of the whole system.*

### 1 INTRODUCTION

The first problemtype for CARPA simulation code (named *Ramflood*) was developed as part of the Ramflood EU Project. The number of different applications, the interest shown by various potential end users, and the natural evolution of the software has lead to create a new problemtype called now CARPA. CARPA has been proven to be a tool of practical interest to solve fluvial dynamics, hydraulic and hydrological engineering problem.

### 2 ABOUT THE SIMULATION CODE

Flood propagation on natural channels is done by numerically solving the Saint Venant equations. This can be done either with a one dimensional or two dimensional approximations, the first one with less computational and information cost, the second one with more precise results when the real flow pattern does not correspond with a 1D domain. CARPA<sup>[1]</sup> uses a 1D-2D integrated finite volume high resolution numerical scheme.

The numerical is explicit and uses a domain discretization in finite volumes, which means that the results are averages within one volume (reach in 1D, mesh element in 2D) and not at sections or mesh nodes. More precisely WAF (Weight Averaged Flux) scheme is used TVD (Total Variation Diminishing) extension, which is a shock capturing explicit finite volume scheme for hyperbolic conservation laws. WAF TVD scheme can also be understood as a high resolution extension of Godunov Method with Roe Approximate Riemman Solver. This kind of modern finite volume schemes show important advantages when compared with the classic finite differences or finite element schemes that are used by most commercial packages used for one end two dimensional free surface flow modeling.

Thus, the main simulation code can be used to predict the values of hydrodynamic variables (mainly water depths and velocities) from a set of initial conditions (including that of dry domain), boundary conditions, roughness or land use properties and wind action. More recent enhances include the possibility of taking into account the precipitation as a water source and also abstractions as infiltration or evaporation, allowing for the possibility of using CARPA also as a hydrological (rainfall-runoff) model.

Apart from the hydrodynamic- hydrological model, CARPA includes a set of simple bedload sediment transport formulations (Mayer-Peter and Müller equation and Einstein-Brown equation) to evaluate bedload solid discharge and predict morphodynamic variations (erosion and sedimentation) on a granular substrate.

### 3 ABOUT THE PROBLEMTYPE

Thanks to the problemtype, CARPA is fully integrated in GiD. Using GiD it is possible to import geometry, define which areas are going to be studied in 2D and which in 1D, build the computational meshes, assign initial conditions, roughness, boundary conditions, hydrological and sediment transport parameters, run the simulations and visualize the results both numerically and graphically.

#### 3.1 Preprocess

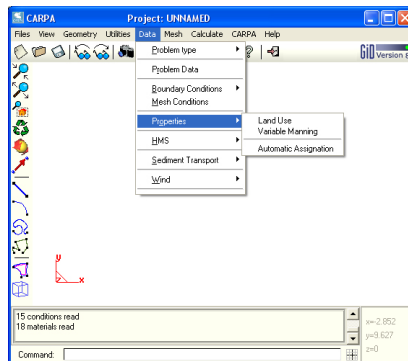


Figure 1: Screen capture of CARPA environment. Detail on menu.

The preprocess of this problemtype includes in the standard menu Data, submenus for assigning all the information required to run a simulation. Submenus are Problem Data,

Boundary Conditions, Mesh Conditions, Properties, HMS, Sediment Transport and Wind. Some of these submenus have particular interest like for example, *Problem Data* where the user can select time parameters for the simulation or the type of results to be printed for postprocess; *Properties*, where the user can assign the roughness coefficient in two different ways, using the standard material window of GiD or using the automatic assignation tool that was specifically developed for CARPA<sup>[2]</sup>.

Moreover, another menu was built-in to group the submenus related the specific tools created for the software. There are two groups of tools, the first is prepared to deal with DTM creation and importation<sup>[2]</sup>, and the second correspond to 1D geometrical creation and management<sup>[3]</sup>.

### 3.2 Postprocess

The results that are directly generated by CARPA are: depth and the two velocity components. However, in the post-process other results can be presented from those according with the selection done in preprocess options. CARPA problemtype also includes the possibility to present the results not in terms of hydraulic variables but in terms of hazard according to the Catalan Water Agency Criteria. This criterion classifies the flood in one point as a high hazard, moderate hazard or low hazard according to the value of depth, velocity and specific discharge.

## 4 APPLICATIONS

The software has been applied to solve question in a wide range of projects. As an example we presented following some representative images of studies done by CARPA.

The study of Tietar River in the south of Spain, involve the analysis of a stretch of about 53 km. Considering this dimension and other parameters was decide to apply an study 1D-2D and a important number of cross section was created from the original detailed geometry using the specific capabilities<sup>[3]</sup> that the program includes. Figure 2 shows two details of this 1D geometry visualized on top of a rendered image of the whole topography mesh.

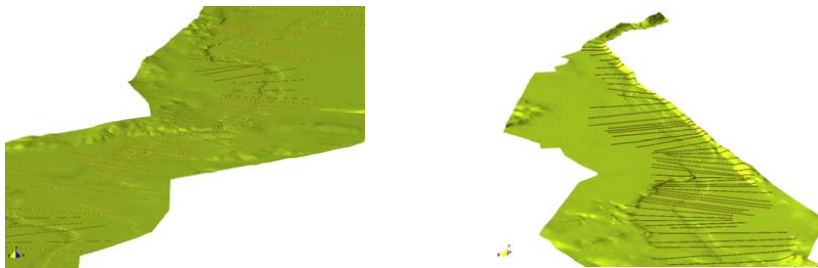


Figure 2: Tietar River, example of 1D cross sections.

Another interesting application is the case of a study of flood risks in Andorra. See Figure 3. In this case the analysis corresponds to an urban area, with the complexity that this type of topography implies. The capacity of the embanked main channel is not enough to contain the design flood, and the water spreads into the city along the streets. The geometry used for the

simulation is a Triangular Irregular Network obtained from a 0.5m x 0.5m grid which, in its turn, is the result of a LIDAR (Laser Scanner) flight. The simulation mesh corresponds with the TIN geometry (structured mesh with one element per TIN triangle).

The last application corresponds to the EU founded project RAMWASS; the study site is a section of River Elbe in Germany (approximated length 5.5 km, Elbe-km 512.5-518). The River carries important quantities of sediment and remarkable amount of these sediments are contaminated so is crucial to determine qualitatively and quantitatively the erosion and sedimentation process (Figure 4).

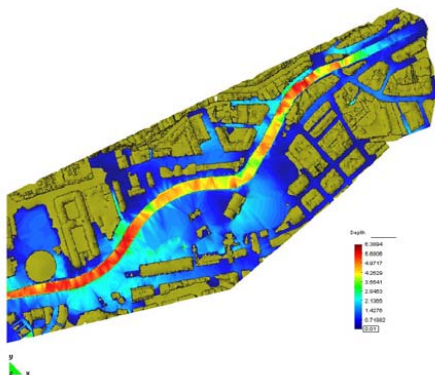


Figure 3: Andorra LaVella; water depths for a flood of 833 m<sup>3</sup>/s at the centre of the city.

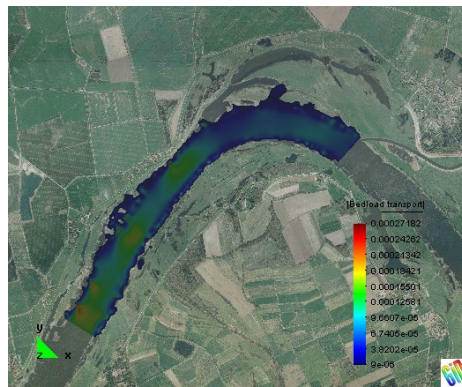


Figure 4: Elbe River; solid discharge during a flood event. Project webpage [www.cimne.com/ramwass](http://www.cimne.com/ramwass)

## 5 CONCLUSIONS

- A new software that fully integrates GiD and CARPA was developed and registered.
- The capabilities of GiD have shown to be one of the key factors in the success of this idea.
- There have been a good acceptance of the software between the community of users and potencial users of this kind of tools. CARPA is presently used by government environmental administrations, research groups and consultancy companies.

## REFERENCES

- [1] Bladé, E., Gómez-Valentín, M. *Modelación del flujo en lámina libre sobre cauces naturales. Análisis integrado en una y dos dimensiones*. Monograph CIMNE N°97 Barcelona (2006).
- [2] Corestein, G., Bladé, E. & all, *New GiD Interface for RAMFlood-DSS Project Hydraulic Simulation Code*, 2<sup>nd</sup> Conference on Advances and Application of GiD (2004).
- [3] Corestein, G., Bladé, E. & all, *1d cross sectionS from a 2d mesh, a feature for a hydraulic simulation tool*, 2nd Conference on Advances and Application of GiD (2004).
- [4] GiD Team, *GiD On-line Manual*, [www.gidhome.com/support](http://www.gidhome.com/support).

## FLUID-STRUCTURE INTERACTION OF ELASTIC CYLINDRICAL STRUCTURES WITH MODERATELY HIGH TURBULENT FLOW

Carsten Corte

International Center for Numerical Methods in Engineering (CIMNE)  
Universidad Politécnica de Cataluña  
Campus Norte UPC, 08034 Barcelona, Spain  
e-mail: corte@cimne.upc.edu , web page: <http://www.cimne.com>

**Key words:** Finite calculus approach (FIC), fluid-structure interaction, slender structures

**Abstract.** *Slender flexible structures can be exposed to excitation by surrounding fluid flow. Long-term excitation can therefore lead to material fatigue and eventually to complete failure of the structure. Numerical simulation to model fluid-structure interaction is an innovative approach to assess the dynamics of slender structures. Applying the finite calculus approach (FIC) to solve the Navier-Stokes equations numerically and a standard finite element approach (FEM) to solve the structural equation of motion, a coupling scheme to solve the coupled problem is presented. To account for the subsequent mesh deformation of the fluid domain mesh, an arbitrary Lagrangean-Eulerian method (ALE) is used. With the coupled approach fluid flow around an elastic thin-wall cylindrical structure is modelled, using an implicit stabilization in case of moderately high Reynolds number flow.*

*The GiD pre- and postprocessing software is applied to set up a joint finite element model for combined computation of fluid-structure interaction using the Tdyn code and the Ramseries code of Compass Ingeniería y Sistemas.*

### 1 INTRODUCTION

The finite calculus approach (FIC) to solve the Navier-Stokes equations has been presented by Oñate, García et al.<sup>i,ii,iii,iv,v</sup> with application to a variety of engineering problems. An approach for the stabilization of the convective parts of the governing equations has been proposed by García et al.<sup>vi</sup>. Standard methods for the time integration for the numerical solution of the structural equation of motion are based on the Newmark scheme<sup>vii</sup>. Simulation of fluid-structure interaction can be obtained by coupling above methods by mutual data interchange between the fluid and the structural solver scheme.

### 2 GOVERNING EQUATIONS

#### 2.1 Fluid flow equations

Viscous flow is modelled by the Navier-Stokes equations. To obtain a numerical solution,



the finite calculus approach (FIC) is applied.

## 2.2 Structural equation of motion

The dynamic motion of a structure can be modelled by the structural equation of motion. To evaluate the transient motion of an elastic structure, a standard finite element discretization is applied in combination with a Newmark family time integration scheme.

## 2.3 Coupling scheme, ALE formulation

To couple the fluid and the structural solution of the respective governing equations, a coupling scheme to interchange data at the common fluid-structure interface is applied. Further, to consider a moving fluid domain due to the deformation of the structure at the fluid-structure interface, an arbitrary Lagrangean-Eulerian approach (ALE) is used. The coupled scheme is split into eight subsequent steps:

1. Solve the fluid equations in the current deformed fluid domain for pressure and velocity at time step  $t_n$  iteratively, thereby considering the current mesh movement velocity of each node in the fluid domain.
2. Determine the current fluid stress vector at each fluid node on the fluid-structure interface at time step  $t_n$ .
3. Interpolate the fluid stress vector from the fluid nodes on the fluid-structure interface onto the structural nodes on the fluid-structure interface. For non-matching meshes for the fluid and the structure on the fluid-structure interface, linear interpolation of the fluid stress vector within a fluid element is performed to obtain an interpolated value of the fluid stress vector at the location of the considered structural node.
4. Compute the structural displacement due to the nodewise applied fluid stress vector onto each structural node on the fluid-structure interface at time step  $t_n$ .
5. Interpolate the structural displacement increment (the difference between nodal structural displacement at time step  $t_n$  and at time step  $t_{n-1}$ ) from the structural nodes on the fluid-structure interface onto the fluid nodes on the fluid-structure interface. For non-matching meshes for the fluid and the structure on the fluid-structure interface, linear interpolation of the structural displacement increment within a structural element is performed to obtain an interpolated value of the structural displacement increment at the location of the considered fluid node.
6. Compute the fluid domain mesh deformation due to structural boundary deformation of the fluid-structure interface at time step  $t_n$ . Therefore, the following concept is applied: As boundary condition for the fluid domain mesh deformation, the deformation increment on the fluid-structure interface of the fluid domain mesh (FSI boundary) is given by the interpolated structural displacement increments. On another part of the boundary of the fluid domain mesh, a zero displacement boundary condition for the fluid domain mesh movement is imposed (fixed boundary). On the rest of the boundary of the fluid domain mesh, fluid nodes are left to move according to the fluid domain mesh deformation procedure. The fluid domain mesh deformation procedure is illustrated separately in the paragraph below.
7. Update the current fluid mesh velocity nodewise by dividing the nodewise fluid mesh deformation increment by the current time step increment.
8. Increment time index  $n \leftarrow n+1$  and go to step 1.

The deformation of the fluid nodes between the FSI boundary and the fixed boundary of the fluid domain mesh is determined by an interpolation procedure. For the interpolation procedure, a binary tree approach is applied. In the binary tree, the fluid nodes are ordered in different layers. The top layer consists of the nodes that belong to the FSI boundary of the fluid domain mesh. The next layer consists of fluid nodes that are adjacent to the FSI boundary nodes. This setup of the binary tree is performed until all fluid nodes are positioned in the binary tree. The deformation increment for a fluid node in a certain layer is preliminarily obtained by the average mesh deformation increment of all nodes in the layer above that are connected to the considered node by the binary tree. This procedure gives a preliminary deformation increment for each fluid node. Subsequently, a nodewise specific scaling factor with value between zero and one is applied to the preliminary deformation increment of each fluid node. The scaling factor depends on the distance of the considered fluid node to the FSI boundary of the fluid domain mesh. For fluid nodes on the FSI boundary, the scaling factor is one; for fluid nodes on the fixed boundary, the scaling factor is zero. For fluid nodes between the FSI boundary and the fixed boundary, the scaling factor is determined by a nonlinear function, depending on the distance of the considered fluid node from the FSI boundary. The nodally determined scaling factor is applied to the nodewise preliminary deformation increment to obtain the mesh deformation increment of each fluid node. The obtained nodal mesh deformation increment is further smoothed over the fluid domain mesh, regarding the fluid element size (element volume) distribution over the fluid domain. Finally, the mesh deformation increment is added nodewise to the fluid mesh node coordinates.

### 3 COMPUTATIONAL EXAMPLE

The coupled approach has been applied to model the structural response of a thin-wall elastic cylinder due to surrounding fluid flow of Reynolds number 10000. Geometric data of the cylinder was height 8 m, diameter 2 m and wall thickness 0.01 m. The cylinder was fixed at the bottom and free at its top. The cylinder had isotropic material properties of modulus of elasticity  $E = 2.1e8 \text{ N/m}^2$ , density  $\rho = 7860 \text{ kg/m}^3$  and Poisson's ratio  $\nu = 0.3$ . The fluid material properties were density  $\rho_F = 1 \text{ kg/m}^3$  and viscosity  $\nu_F = 0.0002 \text{ kg/(m.s)}$ . The inflow velocity was constant with 1 m/s in longitudinal flow direction.

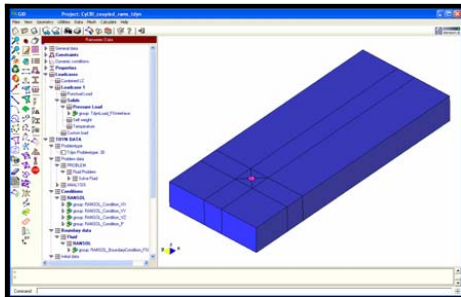


Figure 1: User interface for FSI cylinder model

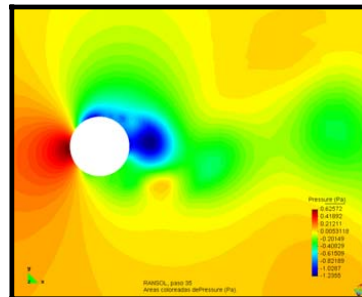


Figure 3: Pressure distribution

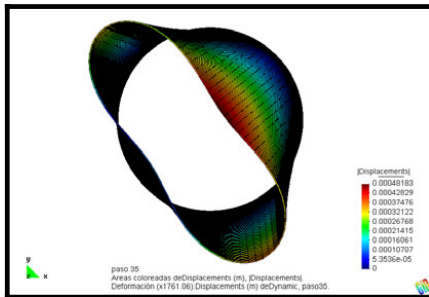


Figure 2: Deformed cylinder excited by fluid flow

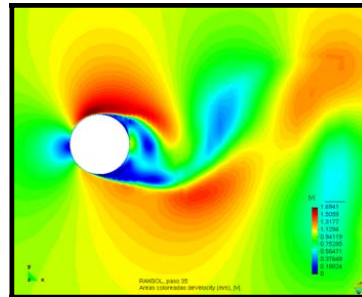


Figure 4: Velocity distribution

In figure 3 and 4 the pressure and velocity distribution around the cylinder are shown. Vortex evolution in the rear of the cylinder can clearly be identified. The vortex shedding frequency corresponds well with the Strouhal number of 0.2 at the considered Reynolds number. Figure 2 shows the deformed cylindrical structure as response to fluid flow excitation. It is clearly shown that the thin-wall cylinder does not behave as a beam-like structure. There is clear ovaling of the cylinder shell, which is in well accordance with the eigenforms of the considered structure.

#### 4 CONCLUSIONS

The presented coupling scheme to simulate fluid-structure interaction between the finite calculus approach (FIC) solution of the Navier-Stokes equations and a standard finite element solution of the structural equation of motion shows adequate results for the case of moderately high Reynolds number flow around a thin-wall elastic cylindrical structure. The structural response corresponds to the fluid flow excitation pattern. Moderately large structural deformations at the fluid-structure interface can be handled by the mesh deformation scheme for the fluid domain mesh.

#### REFERENCES

- [i] E. Oñate, *Derivation of stabilized equations for advective-diffusive transport and fluid flow problems*, Comp. Meth. Appl. Mech. Eng. 151, 233-267 (1998).
- [ii] E. Oñate, J. García, S. R. Idelsohn, *Ship Hydrodynamics*, Chapter 18 in Encyclopedia of Computational Mechanics, Vol. 3, Edts. E. Stein, R. de Borst, T. J. R. Hughes (2004).
- [iii] E. Oñate, J. García, S. R. Idelsohn, F. Del Pin, *Finite calculus formulations for the finite element analysis of incompressible flows. Eulerian, ALE and Lagrangian approaches*, Comp. Meth. Appl. Mech. Eng. 195, 3001-3037 (2006).
- [iv] E. Oñate, A. Valls, J. García, *Computation of turbulent flows using a finite calculus-finite element formulation*, Int. J. Num. Meth. Eng. 54, 609-637 (2007).
- [v] E. Oñate, A. Valls, J. García, *Modeling incompressible flows at low and high Reynolds numbers via a finite calculus-finite element approach*, Comp. Phys. 224, 332-351 (2007).
- [vi] J. García, A. Valls, E. Oñate, *Perspectives of the finite calculus-finite element method for the numerical modelling of turbulence in naval problems*.
- [vii] N. Newmark, *A method of computation for structural dynamics*, J. Eng. Mech. Div. ASCE, 85, 67-94 (1959).

## KRATOS A FRAMEWORK FOR MULTI-DISCIPLINARY CODE DEVELOPMENT

Pooyan Dadvand<sup>\*</sup>, Kratos Team

<sup>\*</sup> International Center for Numerical Methods in Engineering (CIMNE)  
Universidad Politécnica de Cataluña  
Campus Norte UPC, 08034 Barcelona, Spain  
e-mail: pooyan@cimne.upc.edu , web page: <http://www.cimne.com/>

**Key words:** Multi-disciplinary, Object-Oriented framework, FEM, Numerical Analysis

**Abstract.** *The world of computing simulation has experienced great progresses in recent years and requires more exigent multidisciplinary challenges to satisfy the new upcoming demands. Kratos, the framework created in this work, provides several tools for easy implementation of finite element applications and also provides a common platform for natural interaction of its applications in different ways. An innovative variable base interface, very efficient and flexible data structure, Python interface and different data are key features of this multi-disciplinary framework.*

### 1 INTRODUCTION

One of the relevant topics in the finite element method nowadays is the combination of different analysis (thermal, fluid dynamic, structural) with optimization methods, and adaptive meshing in one package with just one user interface and the possibility to extend the implemented solution to new types of problems, as an approach to a multi-disciplinary simulation environment. This was the origin of the Kratos as a framework which hides many difficulties in multi-disciplinary codes from applications developers and provides a standard interface for its applications which guarantees their interaction.

## 2 KRATOS, A MULTI-DISCIPLINARY FRAMEWORK

Kratos helps developers in implementing applications for different fields of analysis by providing input-output, data structures, solvers, basic tools, and standard algorithms. The applications implemented in this framework can be used for solving multi-disciplinary problems using any master and slave strategies or even by solving simultaneously. At this moment several solvers (incompressible fluid, structural, thermal, and electromagnetic) are implemented in Kratos. Combinations of these applications are also used to solve different multi-disciplinary problems, especially fluid-structure interaction and thermal-structural problems.

This framework provides a high level of flexibility and generality which is required for dealing with multi-disciplinary problems. Developers in different areas can configure Kratos for their needs without altering the standard interface used to communicate with other fields in coupled analysis. Also its python interface gives extra flexibility in handling nonstandard algorithms.

Several reusable components are provided to help developers allowing easier and faster implementation of their applications. Data structure, IO, linear solvers, geometries and different strategies are examples of these reusable components.

Kratos is also very extensible at different levels of implementation. Each application can add its variables, degrees of freedom, Properties, Elements, Conditions, and solution algorithms to Kratos. The object-oriented structure and appropriate patterns used in its design make these extensions easy while reducing the need for modifications. The extensibility is also validated at all levels by implementing different applications varying from standard finite element applications to optimization procedures using Kratos and its applications.

Last but not least, the performance of Kratos is comparable even to single purpose programs and different benchmarks show this in practice. This makes Kratos a practical tool for solving industrial multi-disciplinary problem.

## 3 USERS

Kratos is defined to be used by three groups of users at different levels:

- **Finite Element Developers** Kratos is defined to be used by finite element developers to implement a multi-disciplinary formulation easily. These developers, or users from Kratos point of view, are considered to be more expert in FEM, from the physical and mathematical points of view, than C++ programming. For this reason, Kratos provides their requirements without involving them in advanced programming concepts.
- **Application Developers** Kratos can be used as a finite element engine for other applications. This ability favors other teams of developers to work with Kratos. These users are less interested in finite element programming and their programming knowledge may vary from very expert to higher than basic. They may use not only Kratos itself but also any other applications provided by finite element developers, or other application developers. Developers of optimization programs or engineering design tools are the typical users of this kind.

- **Package Users** Engineers and designers are other users of Kratos. They can use the complete package of Kratos and its applications to model and solve their problem without getting involved in internal programming of this package. For these users Kratos provide a flexible external interface to enable them use different features of Kratos without changing its implementation. The interface to GiD provides an easy but effective way to deal with these users.

#### 4 GENERAL STRUCTURE

An object-oriented structure has been designed to maximize the reusability and extensibility of the code. This structure is based on finite element methodology and many objects are designed to represent the basic FEM concepts. In this way the structure becomes easily understandable for developers with a finite element method background.

Kratos uses a multi-layer approach in its design which reduces the dependency between different parts of program. It helps in maintenance of the code and also helps developers in understanding the code. These layers are defined in a way such as each user has to work in the smallest number of layers as possible. In this way the amount of code that each user has to be familiar with is minimized and the chance of conflict between users of different categories is reduced. The implementation difficulties needed for each layer is also tuned for the knowledge of users working in it. For example the finite element layer uses only basic to average features of C++ programming but the main developer layer use advanced language features in order to provide desired performance.

#### 5 VARIABLE BASE INTERFACE

Kratos uses a new variable base interface. All information about a concept or variable to be passed through this interface is encapsulated in the Variable class. The information about components of a variable also is encapsulated in the VariableComponent class which gives an additional flexibility to this interface. This interface is used at different levels of abstraction and proved to be very clear, flexible, and extensible.

Variable provides the type of data statically and objects can use it to configure their operations for a given type of data via template implementation. This type information also prevents the use of variables in procedures that cannot handle their type of data. Each variable has a unique key which can be used as the reference key in data structures. The name of variable as a string helps routines like IO to read and write them without requiring additional parameters. Finally it provides a zero value which can be used for initializing data independent of its type in generic algorithms. Beside this information, variable provides different methods for raw memory manipulations. These methods are excellent tools for low level generic programming, especially for writing heterogeneous containers.

#### 6 DATA STRUCTURE

New heterogeneous containers have been implemented in order to hold different types of

data without any modifications. The `DataValueContainer` can be used to store variables of any type without even explicitly defining the list of them. This container is very flexible but uses a search mechanism to retrieve given variable's data. The `VariablesListContainer` only stores the variables defined in its variables list which can be have any type but its advantage is its fast indirection mechanism for finding the variables data. In Kratos these two containers are used alternatively in places where performance or flexibility is more important. Being able to store even the list of neighbor Nodes or Elements shows their flexibility in practice.

An entity base data structure has been developed in Kratos. This approach gives more freedom in partitioning the domain or in creating and removing Nodes and Elements, for example in adaptive meshing. Several levels of abstraction are provided to help users in grouping model and data information in different ways. In Kratos the Model contains the whole model, divided to different ModelParts. Each model part can have different Meshes which hold a complete set of entities in Kratos. These objects are effectively used for separating domain information or sending a single part to some process.

## 7 FINITE ELEMENT IMPLEMENTATION

The Element and Condition classes are designed as the extension points of Kratos. Their generic interfaces provide all information necessary for calculating their local components and also are flexible enough for handling new arguments in the future.

Several processes and strategies have been developed to handle standard procedures in finite element programming. These components increase the reusability of the code and decrease the effort needed to implement new finite element application using Kratos.

## 8 INPUT-OUTPUT

A flexible and extensible IO module for finite element programs has been developed. It can handle new concepts. Any application built with Kratos can use IO for reading and writing its own concepts without making any change to it. This IO is multi-format. It can support new formats just by adding a new IO derived class and without changing any other part of IO.

Kratos uses Python as its script language. This flexible interpreter with its object-oriented high level language can be used to implement and execute new algorithms using Kratos. In this way the implementation and maintenance cost of a new sophisticated interpreter is eliminated.

More information about Kratos can be found in Kratos webpage<sup>i</sup>, Kratos developers webpage<sup>ii</sup> and Kratos wiki<sup>iii</sup>.

## REFERENCES

---

[i] Kratos Webpage, <http://www.cimne.com/kratos/>

[ii] Kratos' developers webpage , <http://kratos.cimne.upc.es/trac/>

[iii] Kratos Wiki, [http://kratos.cimne.upc.es/kratoswiki/index.php/Main\\_Page](http://kratos.cimne.upc.es/kratoswiki/index.php/Main_Page)

## NON-LINEAR ANALYSIS OF MASONRY WALLS USING DIGITAL PHOTOGRAPHY

Daniel Di Capua, Laura Alvarez Castells

Departamento de Resistencia de Materiales y Estructuras en la Ingeniería  
Escola Universitària d'Enginyeria Tècnica Industrial de Barcelona (EUNETIB)  
UPC

C. Comte d'Urgell, 187. 08036 Barcelona  
e-mail: dicapua@cimne.upc, laura.alvarezcastells@gmail.com

**Key words:** Masonry walls analysis, digital photography, non linear analysis.

**Abstract.** A methodology to analyse masonry structures using digital photography is presented. The idea is to employ with a digital photography of a masonry wall and then use techniques of images processing to obtain a finite element mesh. Then using software of non-linear analysis of structures, within the GiD environment, a complete study of the mechanical behaviour of the material can be performed.

### 1 INTRODUCTION

The objective of this study is to analyze any type of masonry wall, as can be: masonry bricks wall, masonry stones wall with regular and irregular forms. The only condition is that the different geometries can be distinguished with a naked eye. Starting with a digital photography, the geometry of the wall can be obtained. With this geometry an structural non-linear analysis of the masonry behaviour under different loads using of finite element method software can be performed. With a non-linear structural analysis, the behaviour of the wall under several boundary conditions and the evolution of the damage parameter to traction and compression can be studied. The evolution of these damage parameters represents the cracking of the wall. The information obtained from this analysis is very valuable, as can be used to predict the behaviour of the walls and to find the cause of their break.

### 2 DIGITAL PHOTOGRAPHY

In the analysis of images by computer is available a wide range of items ranging from light sources to illuminate the objects necessary to classify them responsible for the algorithms. By applying different techniques of image preprocessing and morphological changes can lead to extract the features that lead to the stages of interpretation and appreciation geometries.



One of the most useful information of the image are the edges that delimit the objects, as they define the limits between them and the background and between the objects together, edge detectors are aimed at the location of the points on there is a variation of intensity.

For the extraction of geometries from photographs always follow the same process:

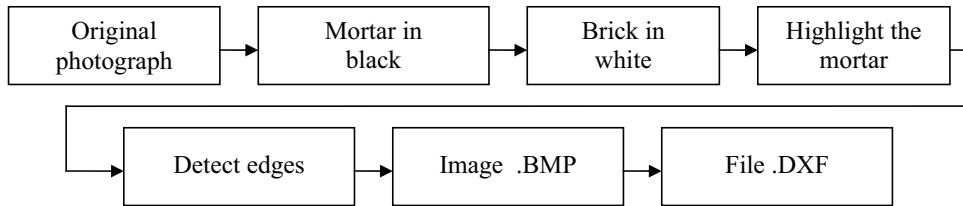


Fig 1. Flow chart.

Based on the entire picture select mortar and turn to black, then invert the selection in this case will be selected bricks or stones from the wall and paint these in white. The next step is to highlight the mortar, use the filter dilate (expand and enhances the dark areas). Currently photography has become in black and white and with the edges of the bricks well defined. Finally save the image format. Bmp, and pass directly the format .Bmp to .Dxf. In this moment we can introduce geometry in the analysis program.

### 3 CONSTITUTIVE EQUATION

The non-linear model of damage to traction and compression use the following equation:

$$\sigma = (1 - d^-) \bar{\sigma}^- + (1 - d^+) \bar{\sigma}^+ \quad (1)$$

This is a variable which range between “zero” while material is elastic and “one” when material reaches. The damage parameter indicates the status of damage at each point and represents the cracking of the wall.

In his view can be seen where the wall breaks, and where the crack moves.

### 4 APPLICATIONS

#### a-) Process for obtain the geometries

Starting from the original photograph of a wall, we get the different geometries that define the bricks or stones that make up it.

Irregular wall:

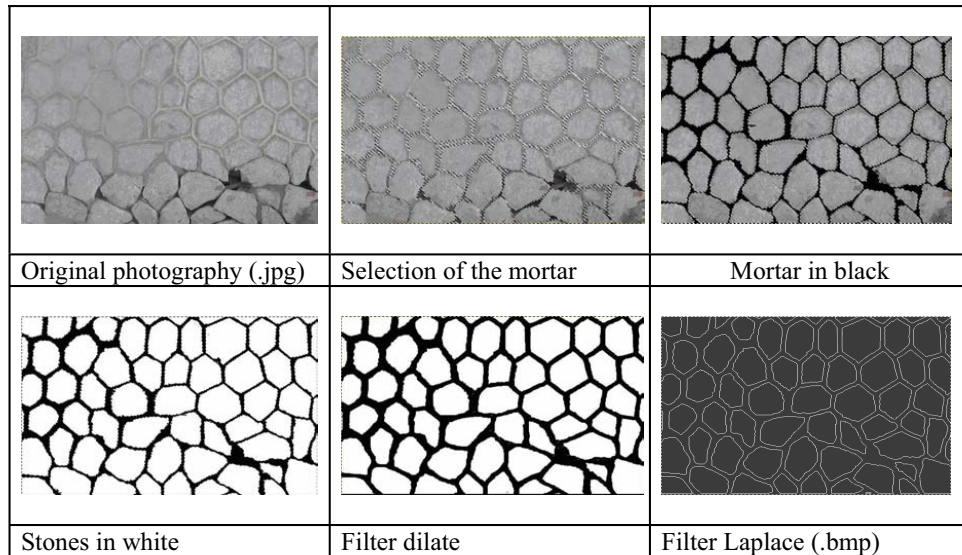


Fig 2. Obtaining the geometry.

b-) Non-linear analysis

For the analyses always follow the same steps: Introduce the data, calculation and finally display the results.

- Data input:

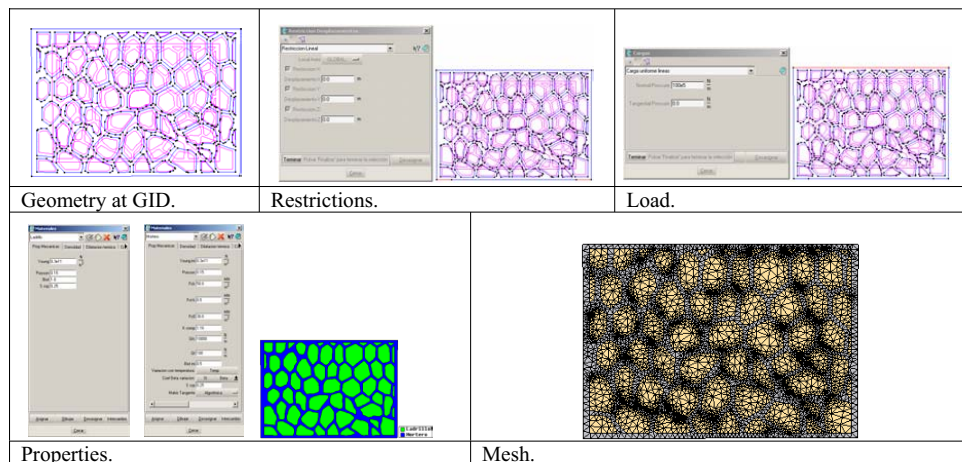


Fig 3. Introduction of data.

- Display the results:

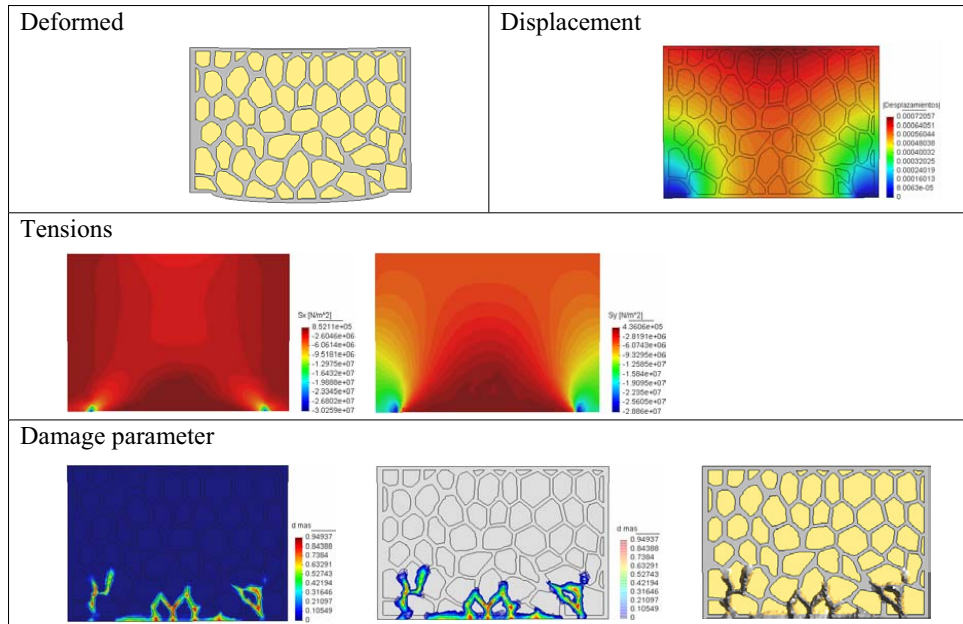


Fig 4. Display the results.

## 5 REFERENCES

Arturo de la Escalera Hueso. 2001. Visión por computador, Fundamentos y métodos. Ed. Prentice Hall.

Rui Faria<sup>1</sup>; Javier Oliver<sup>2</sup>; and Miguel Cervera<sup>3</sup>. Modeling Material Failure in Concrete Structures under Cyclic Actions. JOURNAL OF STRUCTURAL ENGINEERING © ASCE / DECEMBER 2004 / 1997

## DEVELOPMENT OF A DEDICATED SOFTWARE TOOL FOR THE GLOBAL THERMOMECHANICAL ANALYSIS OF PLATE-FIN HEAT EXCHANGERS

\*Johan Dib<sup>1</sup>, François Bilteryst<sup>2</sup>, Jean-Louis Batoz<sup>3</sup> and Ivan Lewon<sup>1</sup>

<sup>1</sup> Fives Cryo,  
 R&D department  
 25 bis rue du fort  
 F-88194 Golbey Cedex  
[johan.dib@fivesgroup.com](mailto:johan.dib@fivesgroup.com)  
<http://www.fivesgroup.com>

<sup>2</sup> GIP-InSIC,  
 Laboratoire LEMTA  
 27, rue d'Hellieule  
 F-88100 St-Dié-des-Vosges  
[francois.bilteryst@insic.fr](mailto:francois.bilteryst@insic.fr)  
[www.insic.fr](http://www.insic.fr)

<sup>3</sup> UTC, Départ<sup>l</sup>. GSU,  
 Centre P. Guillaumat  
 Rue du Docteur Schweitzer  
 F-60200 Compiègne  
[batoz@utc.fr](mailto:batoz@utc.fr)  
[www.utc.fr](http://www.utc.fr)

**Key words:** Plate-fin heat exchanger, homogenization, finite element, dedicated software tool

**Abstract.** *In this paper we describe the work [2] of developing a software tool based on the linear thermo-mechanical FE modeling of the heat exchanger using homogenization techniques.*

### 1 INTRODUCTION

Fives Cryo, implanted in Golbey (Vosges, France), is one of the major manufacturers of heat exchangers for gas processing industries. The company is continuously developing its know-how in design, manufacture, insulation, installation and maintenance of brazed aluminium plate fin heat exchangers (figure 1). In the last 40 years, a large variety of cryogenic processes have used this type of heat exchangers which provides excellent heat exchanges and mechanical characteristics at low temperatures. Brazed aluminium plate-fin heat exchangers are used in : process plants to separate feed gas into its constituents like applications in cryogenic separation and air liquefaction, natural gas processing and liquefaction, petrochemicals production and gas treatment, and large refrigeration systems...

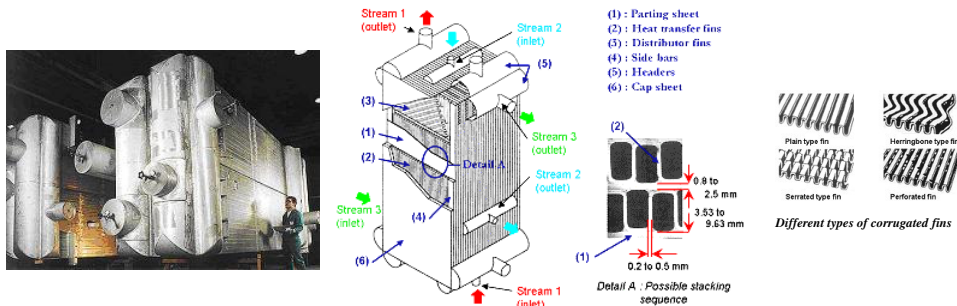


**Figure 1:** A typical multi-stream brazed aluminum plate-fin heat exchanger and its general description

A general description of a multi-stream brazed aluminum plate-fin heat exchanger is presented in reference [1] and figure 1. This type of heat-exchangers is mainly based on the stacking of different layers. Each layer is made by corrugated fins (corrugated aluminum sheets) disposed between two parting sheets (flat plates) and closed by side bars. Openings in side bars assure fluid inlets and outlets. Layers are designed according to specific conditions of operating pressures, temperatures and fluids characteristics, that can be different from one layer to another.

## 2 GLOBAL MODELING OF THE HEAT EXCHANGER

Since a complete FEM model would lead to several billions of structural elements (solid), we propose a 3D FEM model based on layer by layer homogenization techniques to obtain the equivalent (effective) stress-strain relations and thermal load vectors of the corrugated fins brazed with the parting sheets [2]. So a methodology for modeling the heat exchanger constituted by stacking of sheets and different brazed fins with different orientations, pressure and temperature loading is adopted (figure 2). Since the stacking sequence is considered as aleatory, we seek to determine a characteristic range of the effective behavior limited by a “rigid” and a “soft” medium behavior which are respectively determined by a partially periodic mechanical approach (PPMH) and a partially periodic kinematical approach (PPKH). These techniques are based on classical Hill-Mandel [3] methods where periodicity and fins orientation in each layer are taken into consideration. Other classical techniques can be applied to the identical layer stacking (e.g. asymptotic method [4]) where periodicity is considered in all directions.

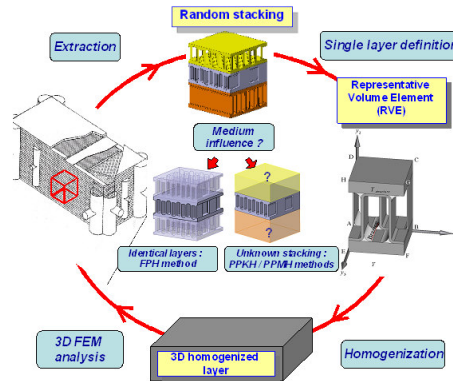
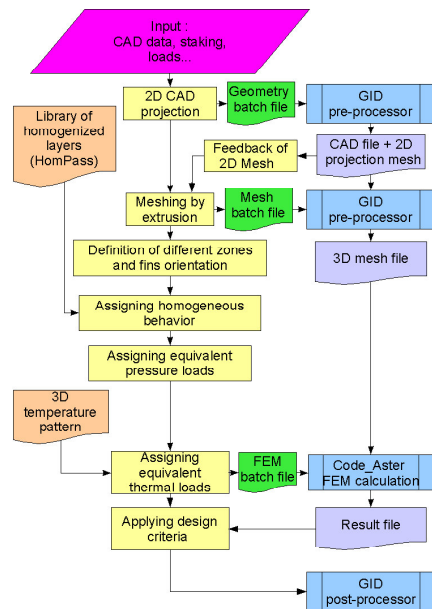


Figure 2: General homogenization approach for individual layer.

So in order to facilitate the layer-by-layer homogenization of the heat exchanger, a homogenization tool (HomPass) is then developed. That enables us to establish a library of elements having equivalent behaviors to each layer of brazed fins and sheets. This library can also include the elementary equivalent loadings in pressure and temperature. That contributes also to the development of the final software tool (SiTEME) dedicated to the global thermo-mechanical study of the heat exchanger.

## 3 DEDICATED SOFTWARE TOOLS

The main structure of HomPass and SiTEME (figure 3) is based on the interfacing between external modules through batch files : we use GiD<sup>®</sup> [5] as pre-post processor, and Code\_Aster<sup>®</sup> [6] for FEM calculations. Therefore, these software tools manage automatically industrial applications and ensure the connections with the specialized FEM modules. This gives also the advantage of updating continually external modules in order to optimize modeling performance. Beside, precise methods related to the global modeling and design are programmed inside these codes so that user can easily use them with other dedicated tools (e.g. thermal design software that generates 3D temperature pattern of the heat exchanger).



**Figure 3:** Architecture of SiTEME software tool

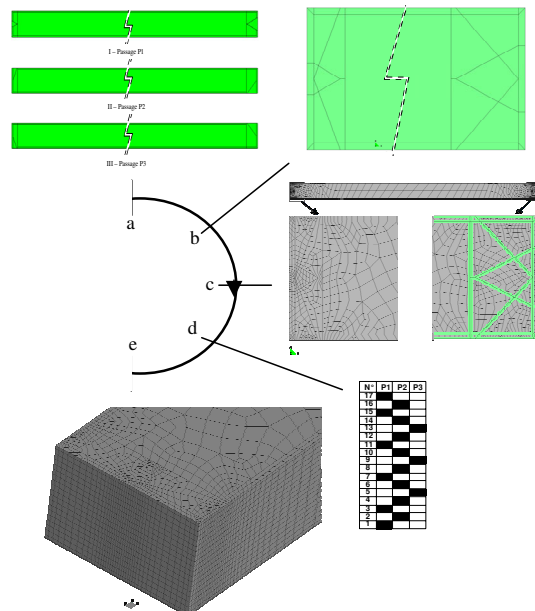


**Figure 4:** Pre-processing of the Heat exchanger (a- CAD of three different layers, b- 2D projection of layers, c- 2D mesh, d- staking of layers, e- 3D extruded mesh of the heat exchanger core)

Figure 3 illustrates the structure of the final software tool ‘SiTEME’ that is dedicated to the study of the thermo-mechanical behavior of the heat exchangers. This program can be divided into four parts :

- Heat exchanger input data : SiTEME is interfaced with other tools to recover automatically CAD data, staking of layers, pressure and temperature loads.
- Heat exchanger pre-processing where meshes are carried out as follows (figure 4) : First, all layers are projected on the same plane. Then, the projected surfaces are intersected and meshed. After that, the 2D mesh is extruded in respect of the layer stacking and with reason of one element by extruded layer. This will lead to the 3D mesh of the heat exchanger core where nodes are carefully connected whatever the arrangement of layers stacking is.
- Heat exchanger calculation : depending on the location of the elements in the 3D mesh, proper equivalent behaviors (pre-calculated by HomPass) are assigned with respect of the fins orientation. Then, from 3D temperature pattern and inside layer’s pressure, the equivalent thermal and pressure loads are assigned at their turn. This will lead to constitute the FEM batch file commands. This file and the 3D mesh are needed by Code\_Aster to launch FEM calculations.
- Heat exchanger design : FEM results are post-processed and viewed by GiD so that the appropriate design criteria can be easily applied.

## 4 FEM RESULTS

Heat exchanger global modeling can generate big size FEM problems (about 4 Million

degrees of freedom). Indeed it depends on the number of different circuits (can reach about 17 circuits), the staking size (up to 150 layers) and the number of headers taking in charge inlets and outlets of the different cryogenic fluids. However, in order to test the functionality of SiTEME, first results relating to a small heat exchanger model are presented in figure 5. We choose the heat exchanger's core presented in figure 4 on which we associate meshed head nozzles on welded joint interfaces. With a low pressure load of 1.3 MPa, results can be validated at different steps of SiTEME programming. They show also no significant stresses on the cap sheets and a maximum displacement order of 0.15 mm. However, displacements on the end (distributor) zone are more important than those at the center zone. This is due to the more rigid fins type used in that central transfer zone.

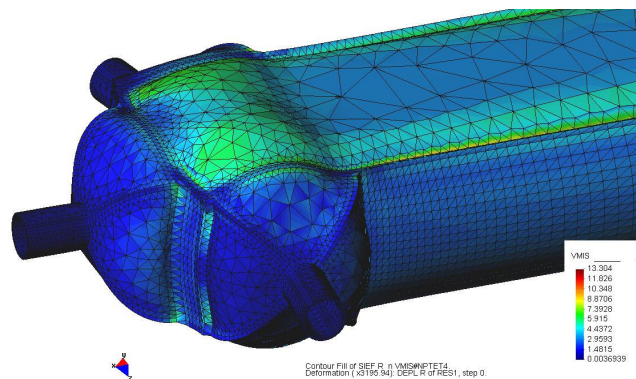


Figure 5: Global Von Mises stress (MPa) of heat exchanger under pressure load.

## 5 CONCLUSION

A dedicated software tool 'SiTEME' has been developed to study the thermo-mechanical behavior of the heat exchangers. This tool integrates homogenization techniques in order to replace geometrical heterogeneities of brazed fins and sheets and thus reducing considerably model size. This allows us, using external specialized modules like GiD and Code\_Aster, to run FEM calculation on the heat exchanger with its welded headers.

Despite of that, global modeling can reach quickly big FEM problems (about 4 Million degrees of freedom). So attention must be paid to optimise 3D mesh while increasing the quality of elements and reducing the processing time.

## REFERENCES

- [1] **ALPEMA**, *The standards of the brazed aluminium plate-fin heat exchanger manufacturer's association*, Second Edition, 2000, (<https://www.alpema.org>)
- [2] **J. Dib**, *Contribution à l'élaboration d'un logiciel métier par éléments finis pour l'analyse thermomécanique globale d'échangeurs de chaleur à plaques et ondes*, Thèse doctorat, Institut National Polytechnique de Lorraine, 2007.
- [3] **R. Hill**, "Theory of mechanical properties of fiber-strengthened material: I- Elastic behavior", J. Mech. Phys. Solids, Vol. **12**, pp. 199-212, 1964.
- [4] **F. Léné and D. Leguillon**, *Homogenized constitutive law for a partially cohesive material*, Int. J. Solids Structures, Vol. **18** (5), pp. 443-458, 1982.
- [5] **GiD**, *pre and post processor*, <http://gid.cimne.upc.es>, 2006.
- [6] **Code\_Aster**, *FEM calculator*, EDF R&D, <http://www.code-aster.org>, 2006.

## ACCURATE SIMULATION OF TAILORED-WELDED-BLANKS TO REDUCE THE PROCESS DESIGN TIME FOR THE SHEET PRESSING INDUSTRY

A. Ferriz, O. Frutos, A. Maymó

International Center for Numerical Methods in Engineering (CIMNE)  
Campus Norte UPC, 08034 Barcelona, Spain  
e-mail: metalform@cimne.upc.edu

**Key words:** Tailored Welded blank, HAZ, LDH drawing test, keystone test tube, Stampack.

**Abstract.** The forming of Tailored-Welded-Blanks (TWB) is a technology used to optimise weight, resistance and raw material consume in pieces obtained by forming processes. The welded sheets must have different thicknesses. This document explains basically the FEM simulation of two different tests adapted to TWB and oriented to guide the experimental search of failure limit conditions. Limit Dome height (LDH) test and the tensile test with non standard test tube will be described. In both tests a previous determination of Weld Line (WL) depth, Heat Affected Zone (HAZ) limits and base material is necessary.

### 1 INTRODUCTION

TWB technology is used when high performance is required without increase the weight and raw material consume.

The thickness distribution depends on structural solicitations. The weld method and its parameters (velocity, power, fingerprint, etc.) depend on material type. To establish failure criteria (in WL, HAZ and base material), the simulations by Finite Element Method (FEM) have been used at the same time with experimental tests.

The LDH test (see figures 1 and 2) was designed to obtain the Forming Limit Curves (FLC) [i]. By FLC the non failure conditions during conventional deep drawing processes are established. LDH test consists in the action of spherical punch with lineal movement normal to blank clamped by a blankholder with draw beads. The maximum stroke of the punch without failure and principal strains are the data to define the FLC.

The standard tensile test [ii] can not determinate the material properties in the HAZ (the failure localize in base thinner material always). In this article, the test tubes with keystone shapes are proposed. These special shapes are able to concentrate the strains in the WL or HAZ of thinner material. This behaviour is caused by effect of thick material that introduce a higher relative rigid restriction

The simulations of these tests allow a previous evaluation of the weld, HAZ and base



material behaviours. They guide the posterior experimental search of failure criteria (similar to generic FLC's but restricted to HAZ and WL).

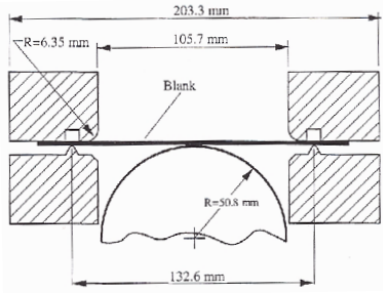


Fig. 1: Geometric initial configuration LDH test

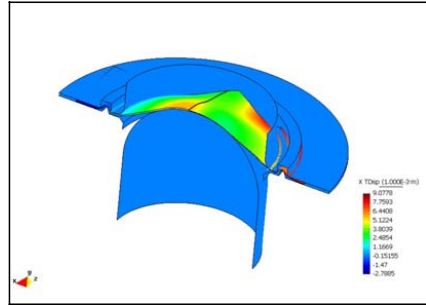


Figure 2: Virtual TWB piece during LDH test

This study is doing in the context of SIM-TWB project with economical support of EEC (financed by EC, contract n° COOP-CT-2006-032657).

## 2 DETERMINATION OF HAZ EXTENT

The HAZ limits determination is previous to forming mechanical simulation. A coupled thermo mechanical simulation is necessary to define the depth of the weld line and the width of the HAZ in function of thermal material properties and welding parameters.

By this way is possible to determinate the extent of the WL and the HAZ. The temperature in WL must be higher than the fusion temperature of the material. It will depend on the heat flux of and the speed of the weld laser. In figure 3 a graphic of temperature vs. distance (in perpendicular direction to WL) is shown.

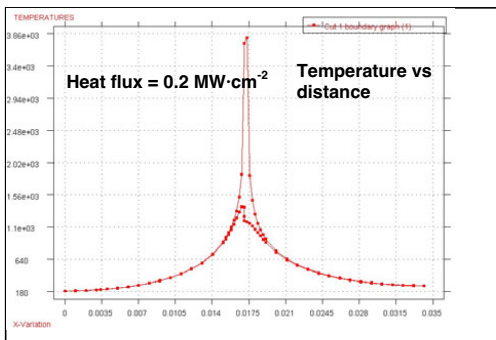


Figure 3: Temperature of one section of the welded blanks

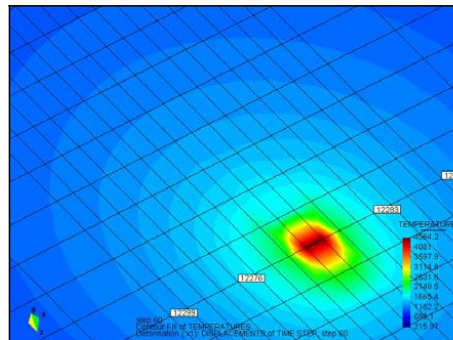


Figure 4: GiD platform postprocess of weld simulation

To define the graphical menus for management of thermo mechanical properties, kinematics and boundary conditions the GiD platform is being used.

### 3 MATERIAL DEFINITION

For the FEM simulations Basic Shell Triangle (BST) finite element [iii] is used. These simulations have been done with mild steel DC04 and aluminium alloy 5657H24 [iv] [v]. Both have been characterized with the exponential parameters of Nadai-Ludwick:

$$\sigma_{\text{TRUE}} = \text{CONSO} * (D + \varepsilon_{\text{pl}})^{\text{CONSN}} \quad (1)$$

Where:

$\sigma_{\text{true}}$ : true or real stress    $\varepsilon_{\text{pl}}$ : logarithmic effective plastic strain

CONSO, D, CONSN: Nadai-Ludwick coefficients

#### 3.1 Hardness definition

The different hardness degree of each welded blanks could be verified in a laboratory in function of the Vickers micro-hardness with load of 2N (HV0.2) all over perpendicular to WL direction. A proportional relation between yield stress and micro-hardness is normally accepted (2). In the case of Aluminium alloy 5657H24 it was experimentally validated in the context of SIM-TWB project in collaboration with the Science of materials Department of UPC (see figure 5).

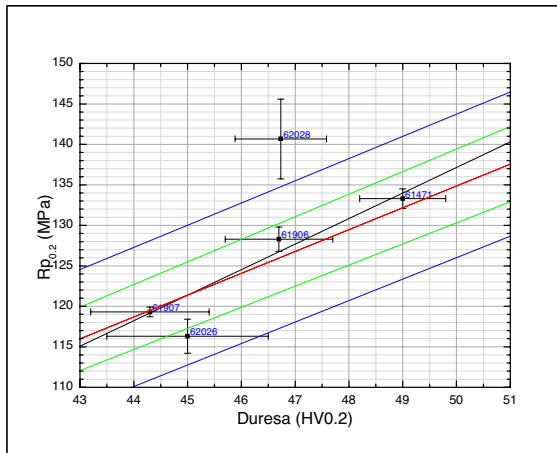


Figure 5: Vickers hardness proportionality (COVIT courtesy)

$$\sigma_Y^{\text{weld}} = \sigma_Y^{\text{sheet}} \frac{\mu\text{HV}^{\text{weld}}}{\mu\text{HV}^{\text{sheet}}} \quad (2)$$

Through the graphs of the figures 3 and 5 and the expression 2 different zones in WL and HAZ of the TWB can be defined to simulate de forming processes. Differentiated Nadai-Ludwick parameters and thickness materials, in these zones, were defined. For the forming process simulations explained in this paper the aluminium alloy 5657H24 was used.

#### 3.2 Zones definition

The GiD platform was used to define the graphical menus for the management of sheet mechanical properties. Through these menus the welded sheets properties are assigned by

zones. In this case, there are five zones:

- Base material (not heat affected) of 0,7 mm thickness.
- HAZ of 0,7 mm thickness and 2 mm thick.
- WL of 0,95 mm thickness and 0.25mm thick.
- HAZ of 1,2 mm thickness and 2 mm thick.
- Base material (not heat affected) of 1,2 mm thickness.

In the figure 6 the interface menu to define the sheet zones is shown.

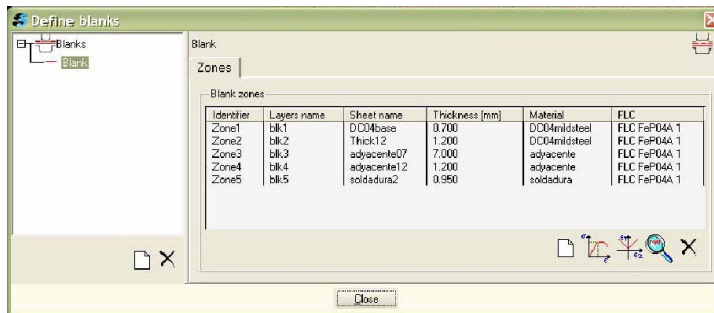


Figure 6: Interface menu of zones definition

#### 4 SIMULATION RESULTS

The simulations of 11° keystone tensile test and LDH test have detected that the WL becomes critical. The failure condition is established when necking condition (local increase of rate strain) is present. It means that the major and minor strains E11 and E22 are upper than FLC for the configuration of TWB under analysis (configuration of materials, thickness and welding parameters).

In figures 7 and 8 the failure conditions for keystone tensile test and for LDH test for configuration described in section 3, aluminium alloy 5657H24 and laser CO2 welding method are shown.

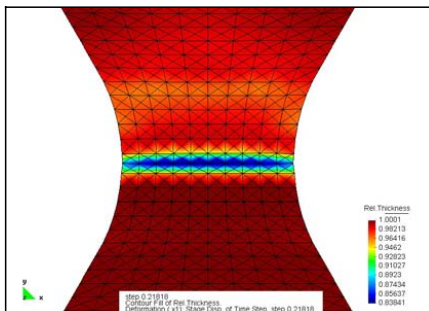


Figure 7: Thickness relation in a tensile test for aluminium alloy 5657H24

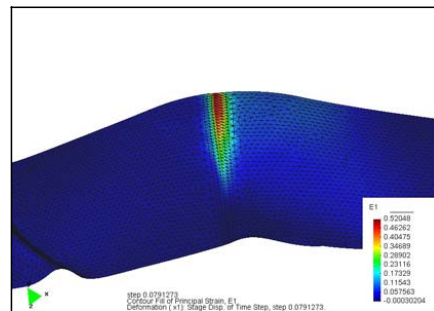


Figure 8: Main strain E11 of LDH test for aluminium alloy 5657H24.

## 5 CONCLUSIONS

- Keystone test tubes shapes are able to localize the necking zone in HAZ of TWB configurations. A point of FLC for HAZ is found.
- The methodology to determinate the HAZ extent (including WL depth) has been defined. This is based in solid thermo-mechanical simulation.
- The failure condition for simulated and experimental industrial forming processes will be oriented by the knowledge achieved by the previous simulations and experimental tests described.

## REFERENCES

- [i] Numisheet'96, Benchmark definition, part II, Edited by J.Lee, G. Kinzel and R.Wagoner, Ohio State University, 1996.
- [ii] Norm EN-UNE 10 002-1, Metallic materials; tensile testing; part 1: method of test, Ed. in Spain by EANOR, 2003
- [iii] Cendoya, P., Nuevos elementos finites para el análisis dinámico elasto-plástico no lineal de estructuras, laminares, Tesis doctoral UPC, Barcelona, 1996.
- [iv] UNE-EN 573-3, Aluminium and alloys. Chemical composition and shape of products, Ed. in Spain by EANOR, 2004.
- [v] Norm EN-UNE 485-2, Aluminium and aluminium alloys. Part 2: Mechanical properties, Ed. in Spain by EANOR, 1995.



## INCREMENTAL SHEET FORMING: A NOWADAYS VISION

**O. Frutos, A. Maymó, A. Ferriz**

International Center for Numerical Methods in Engineering (CIMNE)  
Campus Norte UPC, 08034 Barcelona, Spain  
e-mail: metalform@cimne.upc.edu

**Key words:** Incremental sheet forming, ISO format, Numerical methods, CAM trajectory, Results visualization, Springback.

**Abstract.** *The incremental sheet forming (ISF) is a rapid prototyping forming technique that has a high efficiency, quick and low cost process. In this paper, fundamental characteristics of real and simulated execution (numerical simulation -CAE- from CAD geometries and CAM trajectories) are described. The integration degree, results correspondence, treatment in GID platform and development lines are analyzed.*

### 1 INTRODUCTION

The ISF process consists in a sheet metal forming by means of a spherical punch placed on the head of conventional drilling tool machine controlled by 3 axes CNC or specific designed machine for ISF processes. The final shape will be determined by the trajectory (defined in CAM) and the die-support if would be necessary.

With ISF is possible to obtain complicated geometrical pieces that with a traditional method would have prohibitive price for only one piece or short series.

The main advantages of this kind of processes are:

- Process can be done with die less depending of the shapes. Sometimes, support surface is needed. This support could be made of wood, resin, aluminium, steel, etc.
- In most cases a special tool machine is not needed. Pieces can be formed with a three axis drilling machine controlled by CNC with accessories (clamped blankholder) to subject the sheet. The 3D trajectory is defined by commercial CAM programs.
- Cost, wearing and fracture of the tools are low. If more than one tool were needed, to define final radius for example, only differs in its diameter.
- The dimensional accuracy, surface finish and reproducibility are function of the

trajectory and friction conditions control.

However, there are also some disadvantages:

- The fabrication process is unitary. One tool machine creates one piece at the same time.
- The production is limited to short series.

## 2 REAL PROCESS DESCRIPTION

In this paper a real process execution, done in RWST-IBF institute [i], is described. This piece (see figs. 1 and 2) has been done with a carbide (Widia<sup>®</sup>) spherical punch of  $\text{Ø}10\text{mm}$ . The sheet is sustained by a support with rounded edges that prevent the sheet movement (see figure 3). The sheet fixation is supported with a blankholder that clamps the sheet.

Pieces of aluminium 1050 and mild steel DC04 have been done.

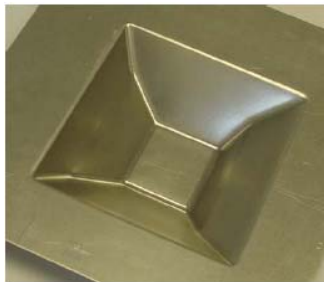


Figure 1: Real piece (Courtesy of RWTH-IBF)

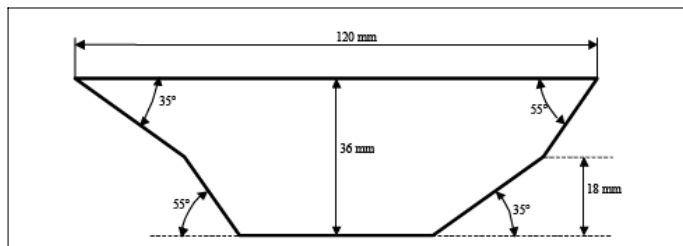


Figure 2: Lateral view and dimensions (Courtesy of RWTH-IBF)

## 3 COMPUTER SIMULATION PROCESS

For the virtual simulation is using the software oriented to sheet metal forming based in STAMPAK<sup>®</sup>. This development is doing in the FLEXFORM project context (financed by EC, Collective Research Proposal n° 030273). The specific and friendly user interface is based in GiD platform.

The movement of the virtual spherical punch and the sheet fixation is done at the same way that in the real process. Interface allows the user to transfer from CAM environment the trajectory in ISO format. Specific dialogue menus have been developed with TCL-TK programming language. The numerical treatment of ISO information, to generate the velocity

vs. time trajectory description, is done with a specific algorithm implemented in C++ [ii]. It is integrated in interface too. In the figure 4 is shown the tool trajectory.

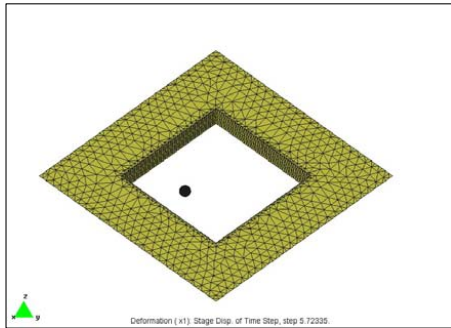


Figure 3: Mesh of support and spherical tool

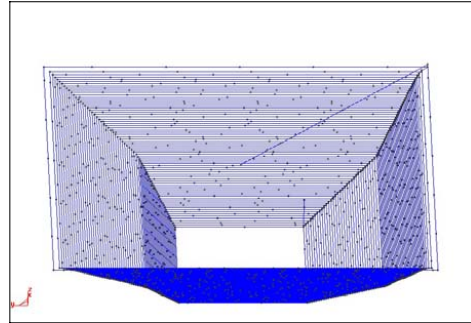


Figure 4: Trajectory generated in CAM and processed in the FEM program

The main process difficulty lies in the treatment of the contact forces, between the tool and the sheet. The high velocities and accelerations produced in the contact zone and its surrounding area are also principal objects of study.

### 3 EXPERIMENTAL AND SIMULATED RESULTS COMPARISON

To evaluate the software capacity, in development, to reproduce the ISF processes the next aspects are measured:

- Trajectory reproduction: the correspondence between real trajectory and simulated trajectory is high. The absolute error is below 0.01mm.
- Reproduction of the strains in the sheet: In the figure 5 the main strain at the end of the process for aluminium 1050 is shown.

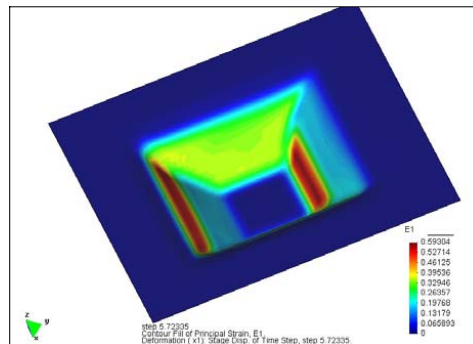


Figure 5: Major strain (at the end of the process for aluminium 1050)



The simulation results have been compared with experimental results and simulated results obtained with LS-Dyna® [i]. Figure 6 shows the comparison.

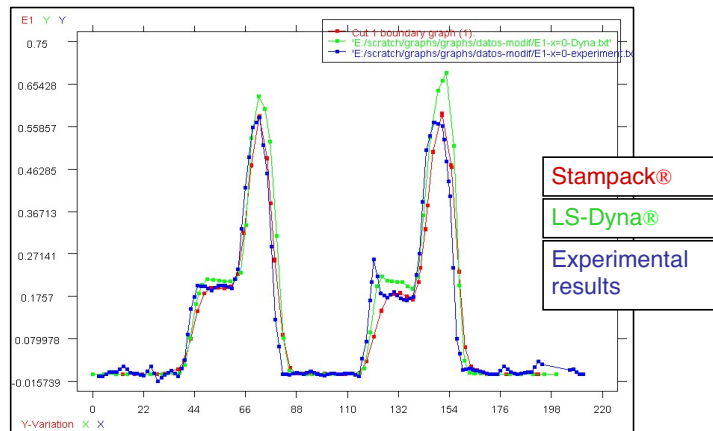


Figure 6: Experimental and simulated major strain comparison

Numerical simulations of cut and springback have been done too. The visualization of numerical results is shown in figures 7 and 8.

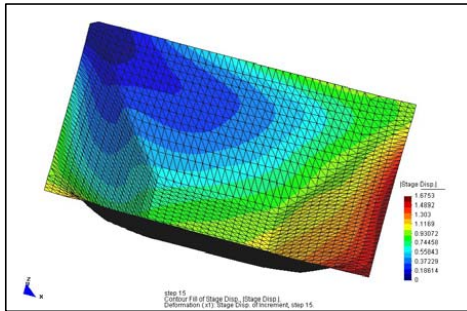


Figure 7: Cut of the remaining sheet

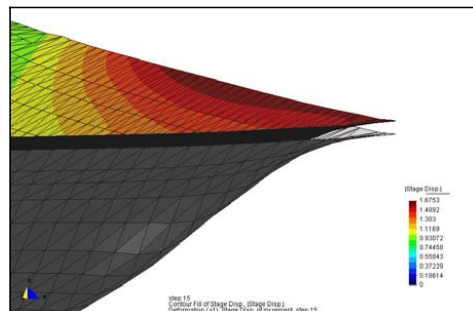


Figure 8: Springback after the end of the process

To do the springback some points have to be fixed. In the case of the figure above three points of the corner were fixed and the rest of the sheet was free.

## 12 CONCLUSIONS

- The discrepancy between the trajectory defined in CAM and the trajectory obtained by CAE simulation (error < 0.01 mm) is compatible with the industrial requirements.
- The discrepancy between experimental results and the simulations obtained in terms of main strains and stresses are inferior to 2%.
- With the specific user friendly interface, based in GiD platform, complete and complex processes of ISF can be simulated.

## REFERENCES

- [i] RWTH-IBF, Deliverable1-5\_FLEXFORM project, Parameters for the FEM-simulation, May 2007.
- [ii] Márquez, J., et. al, Estudio de procesos de deformación incremental de chapa, Informe técnico CIMNE IT s/n, Barcelona, Junio 2007.
- [iii] CIMNE, Activities progress report M1-M12, FLEXFORM project, Barcelona, Oct 2007



## COOLING TANK BREAK SIMULATION WITH CARPA AND GID SOFTWARE GID 2008

F Fuentes<sup>\*</sup>, O. A., Arganis, M.L.<sup>\*</sup>, Bladé, E.<sup>†</sup>, De Luna, F.<sup>\*</sup>, Cruz, J.A.<sup>\*</sup>, Mendoza, J.  
E.<sup>\*</sup>, Sánchez, M.<sup>†</sup>.

<sup>\*</sup> Instituto de Ingeniería UNAM, Circuito Escolar s/n Edificio 5 04510 Coyoacán, D. F.  
e-mail: ofm@pumas.iingen.unam.mx, MArganisJ@iingen.unam.mx, fluc@pumas.iingen.unam.mx

<sup>†</sup> E.T.S. d'Eginyers de Camins Canals I Ports, Campus Nord-UPC Jordi Girona 1-3 D1 E-8034  
Barcelona, España.  
e-mail: ernest.blade@upc.edu, marti.sanchez@upc.edu

**Key words:** Wall break, CARPA, finite volume, GiD, finite differences, flood plans

**Abstract.** A wall break simulation of a cooling tank in a thermoelectric plant was performed using two methods: The CARPA software (finite volume) in GiD environment and a 2D program (finite differences). The software CARPA applied with the GiD pre and post processor showed to be a powerful tool in animating the flood plans, with purposes related to interpretation of results in civil protection in a temporal and spatial way as well as to define the possible affected zones due to phenomena such as walls break.

### 1 INTRODUCTION

When a dike of a reservoir breaks or fails, a great water volume is released in very little time and travels downstream with high speed which can cause human lost and severe human damages. To estimate the flooded zones and their depths, as well as stream speeds has several important applications, because this allows to know the effects over the existing downstream population, buildings, agricultural and industrial areas; or even to formulate mitigation damages measures. In order to obtain the outflow hydrograph due to the failure, it is important to performance laboratory test; for simulating the downstream effects of such hydrograph, mathematic models are needed and they must be capable to represent as much as possible the physical phenomena.

Aureli and Mignosa<sup>1</sup> did a laboratory model of a dike to analyze the breach's shape and the 2D flux behavior in water surface downstream of the dike; afterwards they simulated the experimental conditions, by using the Mc Cormack shock capturing explicit predictor-corrector numerical scheme, with a second order accuracy in time and space, which solves the Channel 2D flux equations and includes a softer term for numerical oscillations presented typically in second order finite differences for shocks and Froude's numbers near to one.

Finally the made comparisons between measured and calculated area, concluding the viability of the Mc Cormack scheme in a dike break or a dam break analysis. There are several studies related with mathematical models which attempt to represent the physical phenomena of a flood wave. <sup>ii,iii,iv</sup>

In this study the eventual cooling tank break of Jose Lopez Portillo, Río Escondido, Coah, México, Thermoelectric Plant was analyzed. Such plant has four units of 300MW using charcoal as fuel; the cooling system is open type and required a tank construction with a surface of about 300 ha ( $3 \times 10^6 \text{ m}^2$ ). The tank was built over the natural ground using dikes with a length of about 13 km ( $13 \times 10^3 \text{ m}$ ), with a height up 10 m; the restock water is pumped using an aqueduct with a length of 30 km ( $30 \times 10^3 \text{ m}$ ), since Bravo river.

## 2 METHODOLOGY AND APPLICATION

### 2.1 Simulation models

#### CARPA model in GiD environment

The finite volume numerical algorithm used by the CARPA program is based in the WAF TDV scheme that can be interpreted as an extension of the systems of equations associated to the scheme developed by Lax-Wendroff, or otherwise as an accurate second-order extension of roe's scheme; it is based on the method of Godunov together with the so-called approximate Riemann solver by Roe <sup>v</sup>. Within the GiD environment the problemtype known as CARPA is selected to be able to import or to create a digital ground model; after such model is developed the boundary (or contour) conditions are established to carry out an analysis either in one or two dimensions or in a combination of both. Initial conditions are assigned as well as data to the mesh specifying if it is a one or two dimensional problem; roughness coefficients are also specified indicating the type of material and the coefficient  $n$  of Manning (more than one coefficient can be assigned depending on the land usage). Data are provided for calculation purposes and the calculation proceeds (execution of the CARPA program).

#### 2D Model II UNAM in finite differences

The 2D Model II UNAM uses central and forward finite differences to get a numerical scheme of solution for the system formed by continuity and momentum conservation equations, in 2D, with initial and boundary conditions. The model obtains the velocity components in two directions and the water surface elevation by considering and inflow to any cell in the grid, expressed as an unitary flow.

### 2.2 Breach outflow hydrograph experimental determination

The analyzed cooling tank is composed by several dikes: outer, central and deflecting, built mostly with clay, a sand center filter as protection against eventual dike's filtrations or cracks, and a rock wall. In Figure 1 a plant view and its elevation -volume curve is presented. A water body is located to the North of the tank, which is considered helpful to regulate the flood produced by an eventual dike break. To estimate the shape of the outflow hydrograph there were made lab models getting experimental results (Figure 2) and later, with dynamic similitude ( $Le=64$ ) the prototype hydrograph shape was obtained (Figure 3), such hydrograph

was used to feed the simulation models.

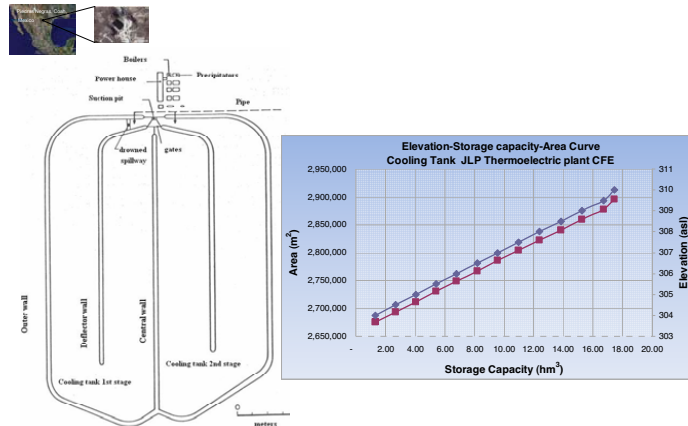


Figure 1: Cooling tank general plant and elevation volume curve

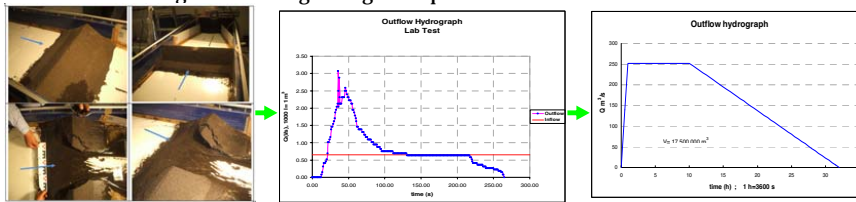


Figure 2: breach outflow hydrograph experimental determination

### 2.3 Input data to simulation models

In Table 1 representative input data applied in simulation models are reported.

Concept	CARPA-GiD	2D II UNAM
Mesh	Tin triangles 8253 elements	Grid 100x100
Method	Finite volumes	Finite differences
Dt (s)	1.0	1.5
time calculation (s)	1,360 (11.5 h)	6,240 (11.5 h)
n manning	0.032	0.040
Language	Fortran, TCL/TK	Visual Basic

Table 1: Input data

## 3 RESULTS

### 3.1 Depth maps

In figure 3 a results comparison is presented, for the instant 11.5 hours (an hour and a half after the break peak hydrograph), time at which the flood attenuation begins. a direct map is

obtained with GiD in which a depth graphic scale is shown, apart from the possibility of running animations, whereas with 2d program some additional work with another software must be done to get less detailed maps.

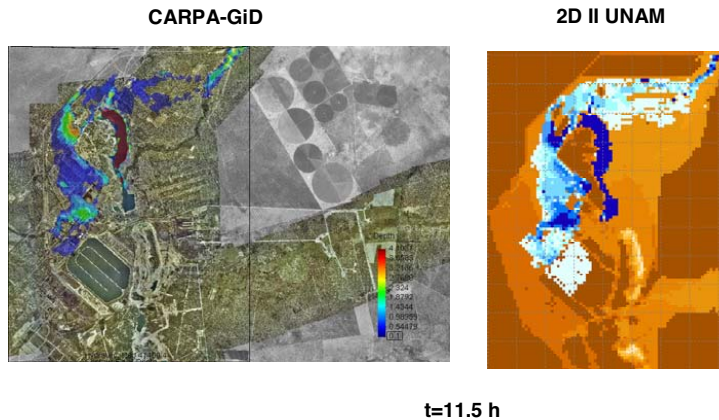


Figure 3: Depth maps comparison  $t=11.5$  h

#### 4 CONCLUSIONS

The application of CARPA program in GiD environment and a 2D model in Visual Basic was compared. GiD allowed to get more detailed maps of the possible affected zones by a dike break of a cooling tank. Furthermore, with GiD animations of the analyzed phenomena can be performed.

#### REFERENCES

- [i] Aureli, F. and Mignosa, P. "Comparison Between Experimental and Numerical Results of 2D Flows due to Levee-Breaking". XXIX IAHR Congress Proceedings, Beijing, China, 16-21 (2001).
- [ii] Fennema, R.J. and Chaudhry M.H. Explicit Numerical Schemes for Unsteady Free-Surface Flows with Shocks. *Wat. Resour. Res.*, 22 No.13, 1923-1939. (1986).
- [iii] Brufra, P. and García-Navarro, P. "Two dimensional dam break flow simulation". *Int. J. Numer. Meth. Fluids*, 33, 35-57 (2000).
- [iv] Michaud, J., Johnson, C., Iokepa, J. and Marohnic, J. Methods for Estimating the Impact of Hypothetical Dam Flood Analysis. *Environmental Sciences Research*, Vol. 59, *Chemistry for the Protection of the Environment*, 4, 195-199 (2005)
- [v] Bladé, C. E. and Gómez, V.M. Modelación del flujo en lámina libre sobre cauces naturales. *Análisis integrado en una y dos dimensiones*. Monografía CIMNE No. 97, U.P.C., Barcelona, Spain, 227 (2006).

## AN INTERFACE FOR AN *HP*-ADAPTIVE FINITE ELEMENT PACKAGE USING GID

**Daniel Garcia-Doñoro<sup>a</sup>, Luis E. Garcia-Castillo<sup>a</sup>, and Ignacio Gómez-Revuelto<sup>b</sup>**

<sup>1</sup> <sup>a</sup>Dep. Teoría de la Señal y Comunicaciones, Universidad Carlos III de Madrid  
Escuela Politécnica Superior(Edificio Torres Quevedo), Avenida de la Universidad, 30  
28911 Leganes - Madrid, Spain. Phone: +34-91-6249171, Fax: +34-91-6248749  
Email: [dgdonoro,luise]@tsc.uc3m.es

<sup>b</sup>Departamento de Ingeniería Audiovisual y Comunicaciones, Universidad Politécnica de Madrid  
Email: igomez@diac.upm.es

**Key words:** finite elements, *hp*-adaptivity, geometrical modeling, user interface

**Abstract.** *This paper presents an interface between GiD and GMP, the Geometrical Modeling Package of the fully automatic *hp*-adaptive FE (Finite Element) software, developed at ICES (University of Texas at Austin). GiD is used to construct a tessellation of the problem domain into FE-like regions (blocks in GMP terminology), and the interface obtains and transfers all the topological and geometrical information to GMP. Then, GMP automatically constructs a parameterization for each FE-like region of the GMP mesh, which later can be used to generate the actual FE-mesh and support geometry updates during mesh refinements.*

### 1 Introduction

Finite element *hp*-adaptivity is a technology that allows for very accurate numerical solutions by simultaneously varying the size  $h$  and the polynomial order  $p$  of the elements of the mesh. It is worth noting a fully automatic *hp*-adaptive implementation, [1], [2], developed at ICES (University of Texas at Austin), in which some of the authors of this paper have contributed.

An *hp*-mesh obtained with the mentioned automatic adaptivity is shown in Fig. 1(d). Color indicates, according to the scale on the right, the polynomial order  $p$  of the finite elements (the dark blue being  $p = 1$  and the pink  $p = 8$ ). The mentioned *hp*-mesh is generated from the initial mesh shown in Fig. 1(c). It is observed how, despite the approximation of the quarter of a circle by two straight lines in the initial mesh, the adaptivity has been able to generate a mesh that provides a very good approximation of the curved contour. This is possible because geometry updates are allowed during mesh refinements. That important feature requires the knowledge of the exact geometry of the structure. For that purpose the so called Geometrical Modeling Package (GMP), [3], is used by the *hp*-code to support geometry information, independently of the mesh. GMP models structures as a combination of blocks (triangles, rectangles, prisms, hexahedrons, etc), each block being defined in terms of explicit or implicit parameterizations. Thus, a FE-like mesh is obtained. An example in 2D is shown in Fig. 1(a). However, it is

---

<sup>1</sup>This work has been supported by the Ministerio de Educación y Ciencia of Spain under projects TEC2004-06252/TCM and TEC2007-65214/TCM, and Air Force Research Laboratory under agreement number FA8655-07-1-3041



important to note that the actual FE-mesh for the analysis is generated from GMP information by using a multi-block *hp*-mesh generator integrated in the *hp*-code.

Information about the different block is entered into GMP by a text file (ASCII) that can be written in several formats. This file can be generated by hand. However, for complex engineering structures, this process is very slow and costly.

In this context, the automatic generation of the GMP file arises as an important objective in order to improve the usability of the *hp*-code. This paper presents an interface between GiD and GMP. A module (*problem type*, in GiD terminology) named *GiDtohp* has been developed. A tessellation of the problem domain into FE-like regions (blocks in GMP terminology) is constructed using GiD tools extended by *GiDtohp* module. Once the blocks are defined, the logic implemented in *GiDtohp* obtains and transfers all the topological and geometrical information to GMP (by writing the GMP text file mentioned above).

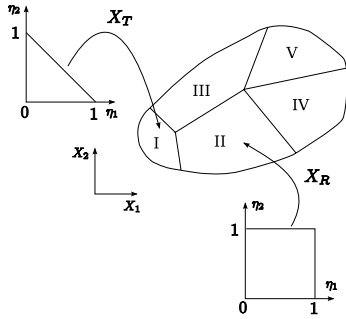
## 2 Interface features

There are two main working modes for *GiDtohp* interface. In one of the modes, each one of the FE-like regions or blocks (surfaces in 2D and volumes 3D) are created directly by the user employing available GiD draw tools and utilities. This mode is named *geometry mode* as the user is basically in GiD's *geometry view*. Figure 1(b) shows an example of this working mode in which GiD points, lines, and surfaces, can be seen. Those GiD entities, and the connectivity information associated to them, are transformed into GMP points, curves, and rectangles (and triangles), and connectivity information compatible with GMP. Parameterizations for each triangle or rectangle (the blocks for the 2D case) are constructed by GMP. From them, an initial *hp*-mesh is generated (see Fig. 1(c)).

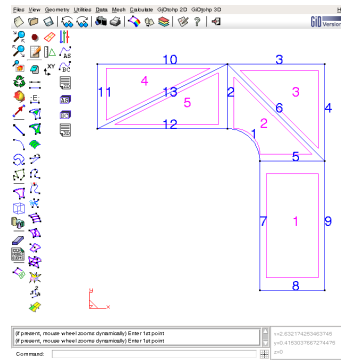
The module contains specific procedures using TCL-TK and TKWidget, providing a graphical and comfortable environment to the user for several tasks. For instance, the assignment to each block of the number of subdivisions that will be used to generate the initial *hp*-mesh is illustrated in Fig. 2(b). Note that two subdivisions (on each direction) have been created at each original block for the example of Fig. 1(c). The polynomial order associated to each block, which will be used later to set the order of the FE of the initial *hp*-mesh, is also introduced by using the same window. Note that the polynomial order has been set in the example to one for all blocks. Analogously, the interface provides graphical procedures to assign boundary conditions (see Fig. 2(c)). Other GMP and *hp*-code parameters needed for the analysis are also introduced by using specific windows. Due to paper length constraints they are omitted.

Once the user has completed the definition of the blocks, the user may execute the option to generate the GMP text files. That is performed by selecting the *geometry mode* button on the left part of window shown in Fig. 2(a). An example of *hp*-mesh generated by the *hp*-code from initial mesh of Fig. 1(c) is shown in Fig. 1(d). Geometry refinements around the curved are observed.

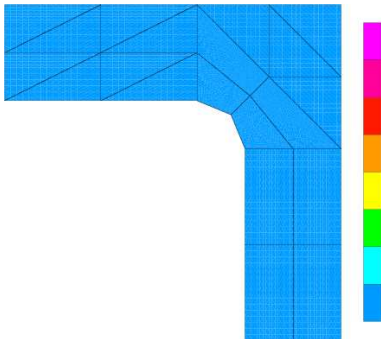
The other mode is oriented to structures in which the number of blocks needed in order to define them is large enough that is not practical to manually define each of them. In this mode, a mesh is generated by GiD using the boundary of the present geometry. This mode is named *mesh mode* because it makes use of the mesh capabilities of GiD. An example is shown in Fig. 1(e). Each of the finite elements of the GiD mesh will become a block for GMP. That is



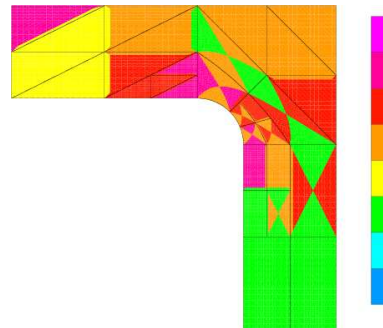
(a) GMP modeling of 2D structure



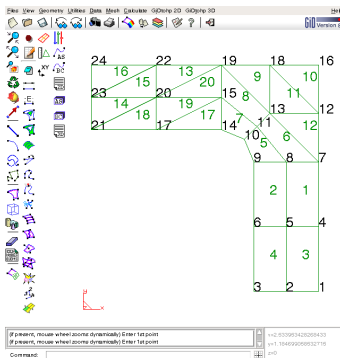
(b) Geometry mode for 2D structure



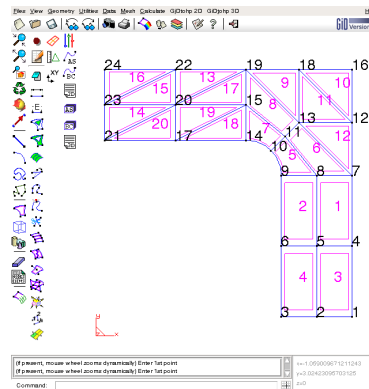
(c) Initial  $hp$ -mesh



(d)  $hp$ -mesh provided by  $hp$ -code

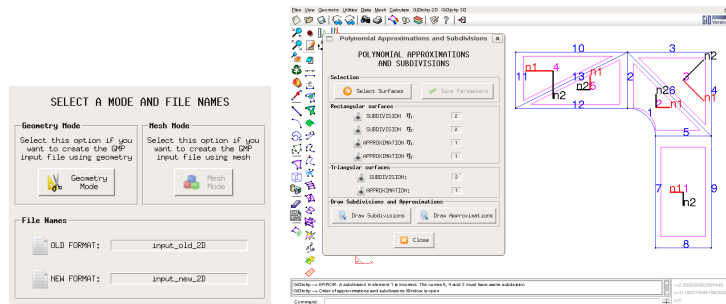


(e) Mesh mode for 2D structure

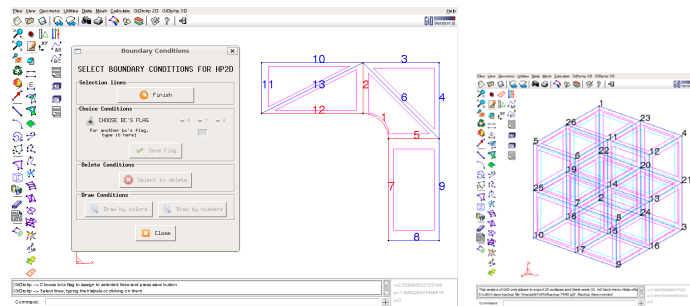


(f) Auxiliary geometry of mesh mode

Figure 1: Screenshots (Part I)



(a) 2D modes selection window (b) Assignment of subdivisions and polynomial order



(c) Assignment of boundary conditions

(d) Geometry mode for 3D

Figure 2: Screenshots (Part II)

done when selecting the *geometry mode* button on the right part of window shown in Fig. 2(a). An auxiliary geometry is created (although not visible by the user, it is shown in Fig. 1(f)). From that auxiliary geometry the GMP text files are generated following pretty much the same procedures that when in geometry mode.

The 2D version of the interface supports straight lines, arcs and NURBS lines. The 3D version, at the moment, does not support non planar surfaces. An example of 3D structure (known as Fichera's corner) created with *GiDtoh* in geometry mode is shown in Fig.2(d).

## References

- [1] L. Demkowicz, *Computing with hp Finite Elements. I. One- and Two-Dimensional Elliptic and Maxwell Problems*. Chapman & Hall/CRC Press, Taylor and Francis, Oct. 2006.
- [2] L. Demkowicz, J. Kurtz, D. Pardo, M. Paszynski, W. Rachowicz, and A. Zdunek, *Computing with hp Finite Elements. II Frontiers: Three Dimensional Elliptic and Maxwell Problems with Applications*. Chapman & Hall/CRC Press, Taylor and Francis, 2007.
- [3] D. Xue and L. F. Demkowicz, "Geometrical modeling package. version 2.0," Tech. Rep. 30, Institute for Computational Engineering and Sciences, Aug. 2002.

## APPLICATION OF GID TO GENERATE THE 3D FINITE ELEMENT MESH FOR THE STUDY OF MARINE CIRCULATION IN THE BAY OF BISCAY

Arnel L. German<sup>\*</sup>, Manuel Espino<sup>\*</sup>, Jordi Blasco<sup>†</sup>, Manuel Maidana<sup>\*</sup>,  
Enrique Escolano<sup>\*\*</sup> and Miguel Pasenau<sup>\*\*</sup>

<sup>\*</sup> Laboratory of Maritime Engineering (LIM)  
Universidad Politécnica de Cataluña  
Campus Nord UPC, 08034 Barcelona, Spain  
e-mail: arnel.german@upc.edu , web page: <http://lim-ciirc.upc.es/>

<sup>†</sup> Department of Applied Mathematics I  
Universidad Politécnica de Cataluña  
Campus Sud UPC, 08028 Barcelona, Spain  
e-mail: jorge.blasco@upc.edu , web page: <http://www.ma1.upc.edu/~blasco>

<sup>\*\*</sup> International Center for Numerical Methods in Engineering (CIMNE)  
Universidad Politécnica de Cataluña  
Campus Nord UPC, 08034 Barcelona, Spain  
e-mail: escolano@cimne.upc.edu , web page: <http://www.cimne.com/>

**Key words:** Unstructured Mesh Grid, Finite Element Mesh, Vertical Triangular Prism Generation

**Abstract.** *A 3D finite element mesh has been generated using GID to study the marine circulation in the Bay of Biscay. The surface of the study domain is discretized using unstructured mesh consisting of triangular elements. The triangular elements are then projected vertically to the bottom of the study area to generate vertical triangular prism columns. The lateral faces of the generated prismatic elements are vertical while the superior and inferior bases are not necessarily horizontal. The resulting computational grid describes faithfully the geometric complexities of the study area and at the same time, it complies with the numerical requirements of the ocean model.*

### 1 INTRODUCTION

Mesh generation is vital in computational field simulation of ocean dynamics because it has a tremendous influence in its accuracy and efficiency. In this context, mesh generation becomes a crucial step in numerical simulation and people from various backgrounds are working to develop meshing software models capable of generating both structured and unstructured meshes. Structured meshes, characterized by its regular connectivity, are ideal for finite difference because this numerical method can take advantage of the regular nature of

the grid for fast identification of neighboring cells. Unstructured meshes which have irregular cell arrangements are ideal for finite element simulation of irregular domains and complex geometries similar to coastal areas. With the recent advances in algorithm and computer hardware, unstructured mesh approach has been used for a wide range of ocean dynamics field simulation with better computational accuracy and cost<sup>i,ii,iii</sup>.

In this paper, the generation of a three dimensional finite element mesh for a marine environment using GiD is presented. In Section 2, we present the geometric requirements and numerical constraints that will govern the mesh construction. Section 3 discusses the methodology used by GiD to generate the horizontal and vertical ocean mesh. Some results are presented in Section 4 while Section 5 enumerates the conclusion.

## 2 STATEMENT OF THE PROBLEM

The objective of this work is to generate a spatial discretization which approximates the geomorphological characteristics of the Bay of Biscay (Figure 1) and complies with the constraints of the governing equation of the numerical model.



Figure 1: The Bay of Biscay with the location of the study area enclosed in a box

The mesh generation starts with the surface that describes the extent of the domain. While surface grid generation is a simple process, the uneven coastline of the bay has to be represented. The generated surface mesh is extended in 3D and considers the complex bathymetry of the bay in volume mesh generation. The bathymetry is very uneven due to the presence of canyons, sea cliffs and sea mounts.

Volume grid generation can be done using different three dimensional elements but the construction of the mesh in 3D must be given special attention especially with regards to the type of hydrodynamic problem being resolved. Normally for rigid-lid type oceanic problems, 3D mesh generation is constructed using tetrahedral or hexahedral elements. But in barotropic problems, where the free surface elevation is accounted for, or in baroclinic problems where horizontal gradients of density are important, vertical triangular prism elements are needed. For the latter case, the presence of the barotropic term involves volume integral of the product of the derivative of the bidimensional surface shape function and the tridimensional volume shape function. The computation of this integral is done elementwise and this is feasible only if the elements are ordered and stored in vertical columns<sup>iv</sup>.

Considering these criteria, the target volume discretization of the study area is an unstructured three dimensional mesh with the horizontal surface, composed of triangles of various dimensions adapted to the irregular geometry of the coastline and for the vertical, layers of vertical triangular prisms.

### 3 MESH GENERATION

The starting point of mesh generation is the given surface representation of the Bay of Biscay. The underlying principle used by GiD<sup>v</sup>, the software used to generate the mesh, is the advancing front method which is widely used for generating triangle and tetrahedral meshes.

The construction of the 3D mesh is done by dropping vertically each node of the previously generated triangles until it reaches the bottom as shown in Figure 2. All lateral faces of the resulting triangular prisms must be vertical to comply with the numerical requirements of barotropic and baroclinic problems. The superior and inferior bases of the generated triangular prisms are not necessarily horizontal.

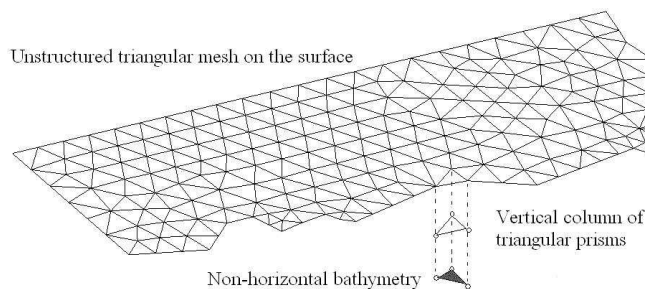


Figure 2: Volume generation using columns of vertical prisms

### 4 APPLICATIONS

In this section, some initial applications are presented to show the efficiency of the generated 3D mesh. The grid used is composed of 51,996 elements, 33,235 nodes and has four vertical layers. It is utilized to interpolate the initial conditions of temperature, salinity and water density in the Bay of Biscay. These parameters are interpolated in all nodes of the computational grid using known sets of data gathered from specific reading stations. The results for the bottom layer interpolations are shown in Figure 3 together with the computational grid.

### 5 CONCLUSIONS

An unstructured finite element mesh of the ocean topography of the Bay of Biscay has been presented in this paper. The computational grid is generated using advancing front method to discretize the surface into triangles and the vertical mesh is composed of vertical triangular prisms. The resulting computational grid describes more precisely the geometric complexities of the study area and at the same time, it complies with the numerical requirements of the ocean model. For this reason, it is expected that during the simulation of the marine circulation in the Bay of Biscay, the mesh will be an efficient tool to accurately represent this complex phenomena.

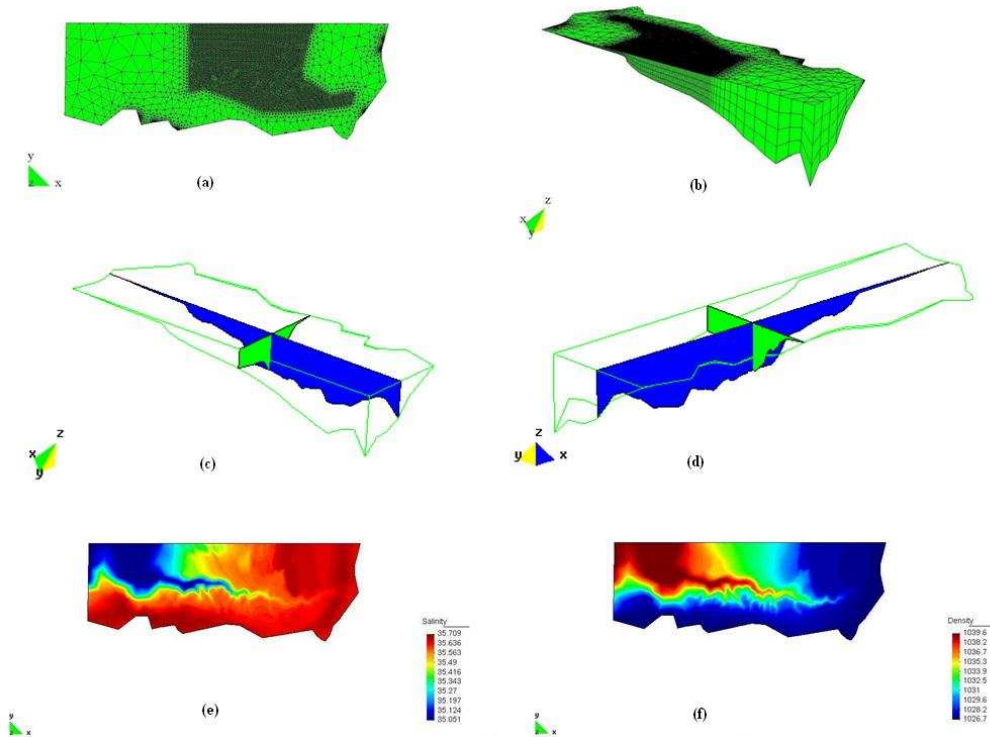


Figure 3: The Bay of Biscay Model: (a) 3D computational mesh; (b) Isometric view; (c) Rear cross section; (d) Front cross section; (e) Salinity and (f) Density at the bottom of the bay

## REFERENCES

- [i] R.J. Labeur and J.D. Pietrzak. "A fully three dimensional unstructured grid non-hydrostatic finite element coastal model", *Ocean Modelling*, **10**, 51-67 (2005).
- [ii] R.A. Walters. "Coastal ocean models: two useful finite element methods", *Continental Shelf Research*, **25**, 775-793 (2005).
- [iii] R.A. Walters. "Design considerations for a finite element coastal ocean model", *Ocean Modelling*, **15**, 90-100 (2006).
- [iv] M.A. Maidana, *Desarrollo de un modelo numérico en elementos finitos para las ecuaciones de Navier-Stokes. Aplicaciones oceanográficas*. Tesis doctoral UPC, (2007).
- [v] CIMNE, *GiD the personal pre and postprocessor Reference Manual Version 8*.

## **GiD LS-DYNA GRAPHICAL INTERFACE**

**González.H Sergio**

International Center for Numerical Methods in Engineering (CIMNE)  
Universidad Politécnica de Cataluña  
Campus Norte UPC, 08034 Barcelona, Spain  
e-mail: sergiog@cimne.upc.edu - web page: <http://www.cimne.com/>

**Key words:** Graphical Interface, Crash Test, LS-DYNA

**Abstract.** *Graphical interface between GiD and the general purpose finite element code LS-DYNA is presented. GiD can be used in both preprocessing and postprocessing of LS-DYNA simulations. LS-DYNA is developed by LSTC (Livermore Software Technology Corporation) and it is used to analyze the large deformation dynamic response of structures including structures coupled to fluids. GiD-LS-DYNA interface is focused on crash test problems and its capabilities are discussed in this paper.*

### **1 INTRODUCTION**

The graphical interface between GiD and LS-DYNA has been developed by CIMNE in collaboration with COMPASS and includes both the transfer of GiD preprocessing data into LS-DYNA and the transfer of simulation results from LS-DYNA into GiD for postprocessing. It has been programmed with a new interface development method based on a XML tree (which makes easier data processing) and takes advantage of both programming languages: TCL/TK for its graphical representation capabilities and C++ in order to work with elements and nodes data.

LS-DYNA is a general purpose finite element code that is developed by LSTC (Livermore Software Technology Corporation). It is used to analyze the large deformation dynamic response of structures including structures coupled to fluids. The main solution methodology is based on explicit time integration. Specialized capabilities for airbags, sensors and seatbelts have tailored LS-DYNA for applications in the automotive industry. The software accurately predicts a car's behavior in a collision and the effects of the collision upon the car's occupants, so it is a powerful tool to analyze vehicle designs.

### **2 GiD LS-DYNA INTERFACE**

Even if the interface is loaded from GiD as a classical problemtype, it offers a completely graphical environment powered by a *Toolkit for problemtypes creation* developed by Compass



Ingeniería y Sistemas S.A. With this new programming method, problem and groups data is always displayed on the left side of the screen during preprocessing (Figure 1), making its management easier for the user. In the same way, some options are displayed in an additional data tree during postprocessing to make faster results analysis (Figure 2).

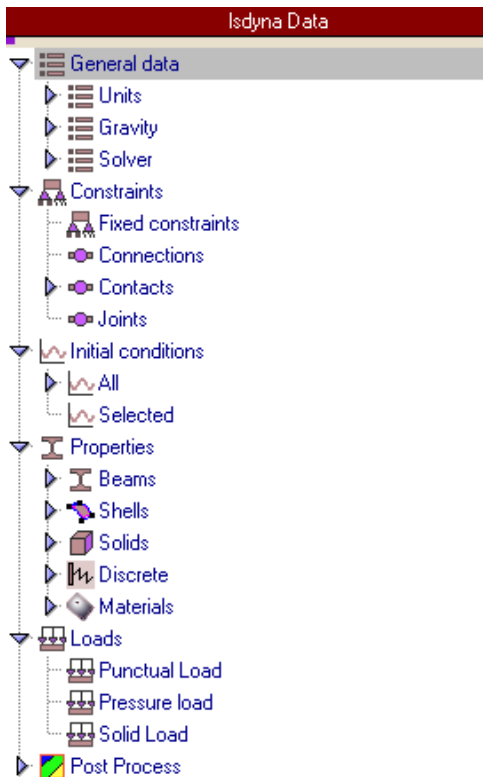


Figure 1: Preprocess options

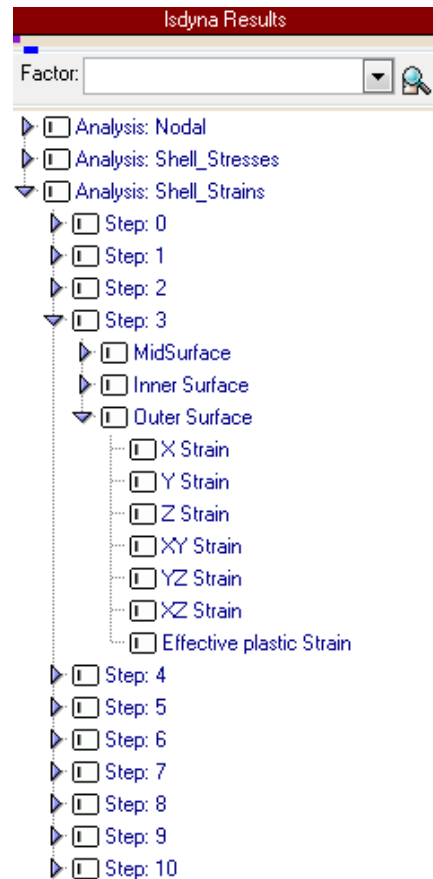


Figure 2: Postprocess options

Groups are defined by their mesh elements or geometry entities, and they can be created and edited in an easy way with the help of a groups edition window (Figure 3).

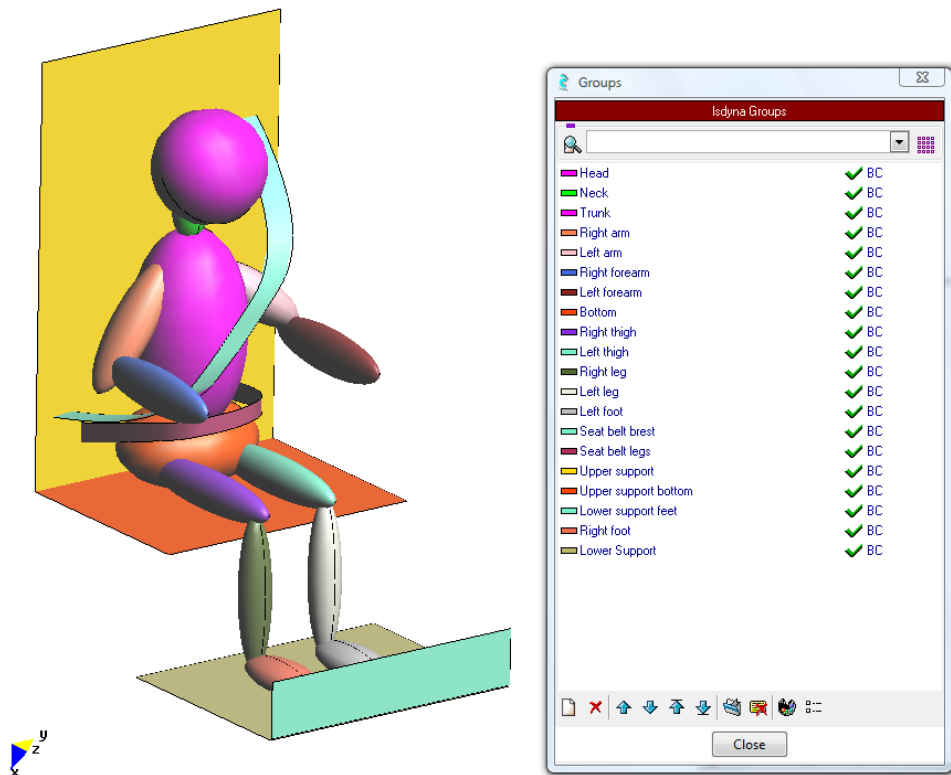


Figure 3: Groups edition window

The aim of the interface is to define crash test problems, which is the main LS-DYNA application as stated earlier. It is able to completely define and to work with several elements (beams, shells, solids, dampers and springs) as well as elastic, plastic and anisotropic materials. Dynamic loads and constraints have been implemented as well. Interface development has been focused in both contacts and joints definition, which are two of the most important problems during crash test problems preprocessing.

Some simple crash tests have already been simulated with GiD-LS-DYNA interface, showing up its performances. Next implementation phase will provide the interface with seat belts and airbags definition tools. Therefore, the interface will be a very powerful tool to pre and postprocessing the majority of crash test problems.

## 2.1 Benefits of GiD-LS-DYNA interface

LSTC develops its own pre and postprocessor (named LS-PREPOST), which is always provided for free with LS-DYNA licenses. This software works with every kind of LS-DYNA problems, but it has two important weaknesses. On one hand its 3D elements meshing capabilities (LS-PREPOST is focused on 2D mesh generation) and on the other hand its not

too much user-friendly graphical interface. In order to satisfy these requirements some graphical interfaces with other commercial pre and postprocessors (as Hypermesh or Oasys) have been developed by other societies.

### 3 CONCLUSIONS

There are many reasons why GiD is an excellent addition to these available softwares. First, the GiD LS-DYNA user-friendly interface allows the user to apply the whole problem conditions and to analyze its results in a completely graphical environment. Moreover, GiD improves LS-PREPOST meshing capabilities and it is also able to import a large number of CAD and mesh formats. Its relative inexpensive cost together with these technical performances make GiD an attractive choice as a pre and postprocessor for LS-DYNA simulations.

In summary, GiD users have with this interface the opportunity to work with one of the most popular commercial solvers for nonlinear dynamics analysis. On the other hand, LS-DYNA experienced users could be attracted by its completely user-friendly environment, which makes easier and faster crash tests definition.

### 4 ACKNOWLEDGEMENTS

Presented software is also the result of COMPASS staff and GiD team efforts. Their help made possible the development of this software, and their knowledge introduced me to an exciting new field.

### REFERENCES

---

- [i] LSTC official web page, <http://www.lstc.com/>
- [ii] LSTC, "LS-DYNA theoretical manual" (May 1998)
- [iii] LSTC, "LS-DYNA keyword user's manual", Version 971 ( May 2007)
- [iv] E.Oñate, "Cálculo de Estructuras por el Método de Elementos Finitos", *CIMNE* (1992)

## THE GENERAL PURPOSE SOFTWARE XFINAS 3.0 FOR ANALYSIS OF BRIDGE

Ki-Du Kim<sup>1</sup>, Songsak Suthasupradit<sup>2</sup>, Panot Chobsilprakob<sup>3</sup>, Pramin Norachan<sup>4</sup>,

Tae Young Kim<sup>5</sup>

<sup>1,2,3,4</sup> Department of Civil & Environmental System Engineering, Konkuk University, Hwayangdong, Seoul, 135-781, Korea

<sup>5</sup>Hanyoung Foreign Language High School, Sangil-dong, Seoul, 134-090, Korea

Email: <sup>1</sup> [kimkd@konkuk.ac.kr](mailto:kimkd@konkuk.ac.kr),

**Keywords:** General purpose, software, shell, solid, frame, contact elements, GID

**Abstract.** *The solutions of both geometric and material nonlinear problems have been greatly facilitated by the development of powerful and efficient finite element software. Thus, the general-purpose finite element software XFINAS has been developed to solve problems ranging from simple static, to highly advanced nonlinear dynamic problems, with the capability of supporting large sets of elements. Its user-friendly graphical interface was developed using the pre/post processor software, GiD. The current version of XFINAS has been developed at AIT and Konkuk University in Korea. It is the result of extensive research and development of the finite element program FINAS, which was originally developed in Imperial College, London. Because of its high accuracy, efficiency and robustness, it has become a very attractive modern computer tool for civil and mechanical engineers for the analysis of structures and continua and is suitable for both research and professional applications. In the following, a brief features and bridge examples of XFINAS are presented.*

### 1. INTRODUCTION

The program based on the nonlinear finite element method, FINAS which is capable of the elasto-plastic stability assessment of thin walled structures, was developed on a CDC-Main frame and UNIX environment, at Imperial College, London by Trueb (1984), Bates (1987) and

Kim (1992). The general purpose software, XFINAS which is an eXtended version of FINAS, has been developed on Window Operating system in AIT and Konkuk University (2007). XFINAS to enables a powerful nonlinear dynamic structural analysis , taking into account of material and geometric nonlinearity. A large number of numerical testing has been carried out for the validation of XFINAS elements, which shows the good agreement with the references by Kim (2006). The pre- and post processing of XFINAS can be carried out by using GiD. Thus, the new program will be efficient and powerful tool in design and research of the structures.

XFINAS provides a series of solution strategies for nonlinear analysis. Both force and displacement loading can be applied in static analysis. An automatic selection of constraint equation and arc-length control are available for highly nonlinear problems. The solution procedure uses either full or modified Newton-Raphson method. The solution features of XFINAS are given in Table 1.

Table 1 Solution feature of XFINAS

<p><b>Linear and Nonlinear Static Analysis</b>  <b>Dynamic Time-history analysis</b> (Central difference Method, Newmark-beta, Wilson-theta and HHT Methods)  <b>Mode superposition method for linear dynamic analysis with damped and undamped system</b> (Eigenvector, Loaddependent Ritz vector)  <b>Seismic analysis</b> (Time integration method, Mode superposition method, Response spectrum methods , Multiple supports analyses)  <b>Co-rotational method for nonlinear shell element</b>  <b>Nonlinear solution control algorithm</b>(Load control, Displacement control. Constant arc-length , Automatic arc-length control method)  <b>Geometrical nonlinearity</b> (Updated Lagrangian Method)  <b>Elasto-plastic material</b> (Von-Mises with strain hardening, Ilyushin-Ivanov with strain hardening, Mohr-Coulomb , Drucker-Prager, Tresca)  <b>Fiber-reinforced composite materials with the progressive failure analysis</b> (Maximum stress, Tsai-Wu, Tsai-Hill, Modified Puck Criterion Theory)  <b>Postbuckling analysis of frame, plate and shell</b>  <b>Eigenvalue analysis</b>  <b>Buckling and natural frequency analysis</b>  <b>Vibration control using viscous damper</b> Base-isolation with friction  <b>Concrete Creep and shrinkage</b> (CEB-FIP Model Code 90, ACI)  <b>Offset, Pin&amp;Hinge</b> (end release) connection</p>	<p><b>Nonlinear link element</b> (Gap, Hook &amp; Gap-Hook)  <b>Bond-link element</b> (1D,2D &amp; 3D Anchor)  <b>Contact element</b> (2D &amp; 3D, Steel-concrete, Soil-structure)  <b>Automatic Bridge moving load</b> (AASHTO, Korean Influence line analysis (frame element and shell element)  <b>Standard steel section property</b> (Korean-code, Euro-code)  <b>3D dynamic analysis of bridge-vehicle interaction</b> <ul style="list-style-type: none"> <li>• Moving axle loading</li> <li>• Articulated high-speed train (TGV/KTX)</li> <li>• Independent car-train (Shinkansen/Taiwan HST)</li> </ul> <b>Nonlinear Coupled analysis of Pressure-Soil interaction</b> <ul style="list-style-type: none"> <li>• 2-D Biot Consolidation</li> <li>• 3-D Biot Consolidation</li> </ul> <b>Heat Transfer analysis</b>  <b>Optimization of cable tension</b>  <b>Concrete hydration analysis</b>  <b>Loss of prestressing in pre-tensioned and post-tensioned structures</b> (Instantaneous loss: elastic shortening, friction and anchor slip, Time dependent loss: creep, shrinkage and relaxation)  <b>Construction analysis of long span bridge</b></p>
--	---

## 2. APPLICATION OF XFINAS IN BRIDGE ANALYSIS

Several bridge analysis modules is implemented into the general purpose Non-linear Dynamic Finite element package, XFINAS, developed in Konkuk univ. in Korea and AIT in Thailand for PC. To demonstrate the capability of the bridge analysis module and to identify its limitation, a variety of bridge problems are tested.

### 2.1 Construction analysis of 3-span continuous bridge using shell element

The following example is the same three-span bridge designed by Kechum (1986). The bridge is constructed using the cantilever method. The girder segments are cast-in-place using a traveling formwork, while the girders near the abutments are conventionally erected. The structural behavior of the bridge under dead load, construction loads and prestressing is traced through the construction phase and over a 27-year service period thereafter. The use of shell elements in modeling will allow the inclusion of the effects of transverse tendons and cross-section deformations.

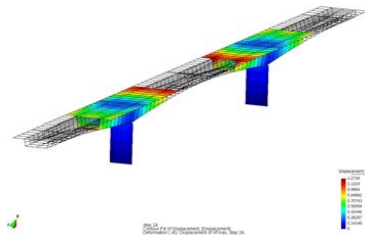


Fig.1. Construction analysis of 3-span continuous bridge

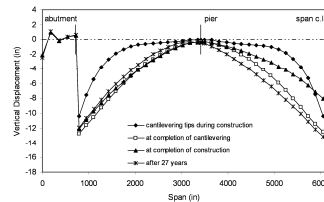


Fig.2. Vertical displacement at the center of bottom slab

The main differences between frame and shell model is that the cross-section properties of the girders are changed by its deformation which cannot be observed in the beam model.

### 2.2 Automatic live load analysis of double cell-two span continuous bridge

The grillage model subjected to AASHTO HS20 truck load. The grillage model loading and conditions are shown in figures 3. The bridge consisting of four lane with 3 m width. Various load conditions has been investigated using XFINAS automatic vehicle load option. The maximum response of each load case also given by XFINAS.

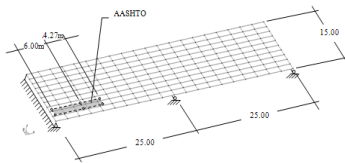


Fig.3. Loading condition

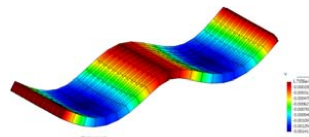


Fig.4. Total displacement

### 2.3 Three dimensional analysis of high speed bridge-train interaction

A high-speed independent-car train passing over a bridge of two-spanned concrete girder with box section shown in Fig.5 is considered. The train system consist of a front power car, eight passenger cars and rear power car moving at a constant speed over ther bridge.

The vertical displacement history of middle of first span at peed 300 km/h calculated by the new 3-D bridge-train mudule in XFINAS is perfectly match with that of the validated 2-D model in Fig.6.

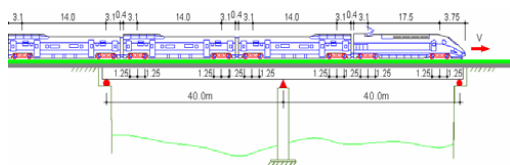


Fig.5. General of train and bridge

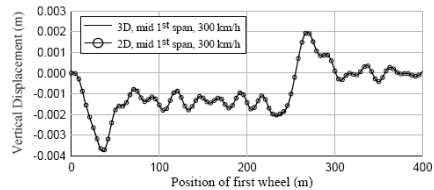


Fig.6 Comparison of vertical displacement at mid span Between 2D and 3D models

### 3. CONCLUDING REMARKS

Although a lot of general purpose softwares are available for the structural research and design, there are still rooms to improve the solution with accuracy, stability, robustness and computational efficiency. For this purpose, XFINAS system is developed based on the most efficient formulation. The advanced module of bridge analysis in XFINAS was also developed to overcome the increasing demand of advance analysis and design of bridges. The algorithm for bridge analysis such as construction analysis and three dimensional bridge-train interaction are applicable for complex bridge structures, thus the XFINAS can be used for the design and research of bridge applications.

**Acknowledgement:** This research was supported by a grant(06건설핵심D05) from Innovation of Construction Technologies Program funded by Ministry of Construction & Transportation of Korean government and Brain Korea 21 (BK21). And this work supported by the Korea Research Foundation Grant funded by the Korean Government (KRF-2006-학06A2101).

### REFERENCES

- [i] [www.xfinas.com](http://www.xfinas.com)
- [ii] K.D.Kim, G.R. Lomboy, A Co-rotational Quasi-Conforming 4-Node Assumed Strain Shell Element for Large Displacement of Elasto-plastic Analysis, Computer Methods in Applied Mechanics and Engineering, 195 (2006) 6502-6522, September
- [iii] K.D. Kim, G.R. Lomboy. G.Z. Voyiadjis A 4-Node Assumed Strain Quasi-Conforming Shell Element with 6 D.O.F., International Journal for Numerical Methods inEngineering, Volume 58, Issue 14, (2003), 2177-2200

## SPHERE PACKING FOR DISCRETE ELEMENT SIMULATION ON GID

Carlos Labra, Eugenio Oñate and Enrique Escolano

International Center for Numerical Methods in Engineering  
Technical University of Catalonia  
Gran Capitan s/n, 08034  
Barcelona, Spain

e-mail: clabra@cimne.upc.es, onate@cimne.upc.es, escolano@cimne.upc.es

**Key words:** Discrete Elements, Sphere Packing, Mesh Generation.

**Abstract.** *In the last years, the Discrete Element Method (DEM) became a very useful tool for the simulation of geomechanic and particle movement processes. The first step in a discrete element simulation is the discretization of the domain into a set of particles. The cost of generating a good cylindrical or spherical packing has resulted in a great number of approaches during the last years. A new algorithm is proposed for high density packing using a scheme which minimizes the distance between each particle. Using the support of a finite element mesh, less time is needed in order to achieve a low porosity configuration. In addition, a boundary constraint is introduced. The application of the same optimization scheme is used as a condition to force a good surface definition. The results obtained present a high efficiency for the generation of low porosity packing, achieving values smaller than 10% in 2D cases and 30% in 3D cases. This technique is implemented in GiD, where the creation of the new element type Circle (2D) and Sphere (3D) allow the generation of discrete element models. An extra support for the analysis of the generated mesh, as volumen, porosity or coordination number is created in order to obtain a better management of the meshes.*

### 1 INTRODUCTION

In the last years, the discrete Element Method (DEM) became a very useful tool for the simulation of geomechanic and particle movement processes<sup>1-4</sup>. The technique requires the discretization of the media by a finite set of particles. The present work proposes an alternative technique for the generation of very dense particle distributions. The idea is to use a fast algorithm for an initial generation, like some of the ones presented previously and densify the



package by an optimization algorithm. In particular, a finite element mesh based scheme is used.

## 2 THE ALGORITHM

The main idea of the method is to *improve* a given particle assembly in order to obtain a lower porosity configuration.

Given an initial particle distribution, a high porosity exists when the neighbouring particles are not in contact. The reduction of porosity condition can be written as a non-linear square problem where the function to be minimized is given by the distance between neighbouring particles of the original configuration. This allows the inclusion of boundary constraints to ensure a good reproduction of the boundaries, a feature which constitutes a mayor advantage in all the cases in which the friction between surfaces is important<sup>4</sup>.

### 2.1 Internal contacts

A low density initial assembly is assumed in order to define the existence of neighbouring particles without contact. The low density is produced by the void areas where the contacts are not achieved. A modified distance function is defined between all neighbouring particles, where the existence of the contact pair is introduced by a triangulation. In a local neighbourhood for one particle the distance function between particles  $i$  and  $j$  can be defined as

$$d_{ij} = \|\vec{x}_i - \vec{x}_j\|^2 - (r_i + r_j)^2 \quad (1)$$

where  $\vec{x}_k$  is the coordinate center of the particle  $k$  and  $r_k$  its radius. The square of the values is used for the sake of simplicity, because a derivative function is required and the minimum of this modified distance is equivalent to the standard function.

In order to find the minimum of void areas or interstitial spaces, the function needs to be minimized for all the particles in the assembly. For that purpose, a global function is defined using a minimum square scheme, where the global function is written as

$$\min F = \sum_{i=1}^m \sum_{j=1}^m \delta_{ij} d_{ij}^2 \quad (2)$$

where  $\delta_{ij}$  is a Kronecker delta function which defines the existence of the contact pair  $[i,j]$ . These connectivities are achieved by the edges of the triangulation over the initial assembly. The square of  $d_{ij}$  is used because the minimum of any contact pair is required, and the use of a linear system may cause some negative values in the radii of the particles.

The system can be now solved for an initial assembly, where the final compactation degree allows a very low porosity level. The convergence rate of the scheme depends on the initial configuration. A good result is however obtained in few iteration steps.

### 2.2 Treatment of boundaries

A boundary constraint or boundary condition is proposed with the same argument as in the previous section. A modified function of the distance between the contour of the geometry and

the external particles is used in order to obtain a homogeneous contour in the external of the assembly. In the external zone of the domain it is possible to establish the distance between the particle  $i$  and some boundary line  $k$  as

$$R_{ik} = \|\vec{d}_i\|^2 - r_i^2 \quad (3)$$

where  $\vec{d}_i$  is the vector joining the center of the particle with the closest boundary point.

We will assume in the following that the algorithm is finite element mesh based. Hence only the inner nodes of the mesh are particles, while the outer nodes define the boundary mesh.

With the introduction of this new condition, a modified version of the equation (2) is written.

$$\min F = \sum_{j=1}^n \sum_{j=1}^n \delta_{ij} d_{ij}^2 + \sum_{i=1}^n \sum_{k=1}^n \delta'_{ik} R_{ik}^2 \quad (4)$$

The resolution of this system for a set of particles is able to solve the density problem and a good boundary definition for the final configuration of the assembly.

### 2.3 Initial generation of the media

For the generation of the initial configuration, it is possible to use any algorithm proposed in the literature. However the finite element mesh based techniques offer better conditions for the algorithm proposed in this work. This is because very developed algorithms exist and the generation of complex geometries is achieved easily. One of the necessary considerations for the initial mesh is the structuration of the elements, because very regular elements produce a regular number of contacts for the different particles and a homogeneous package of particles is found. In order to safe the problem, an initial preprocess is made over the mesh, where random local displacements over the node position is used to generate a random configuration.

## 3 EXAMPLES

An example for a 2D generation with refinement is shown in Figure 1. An application

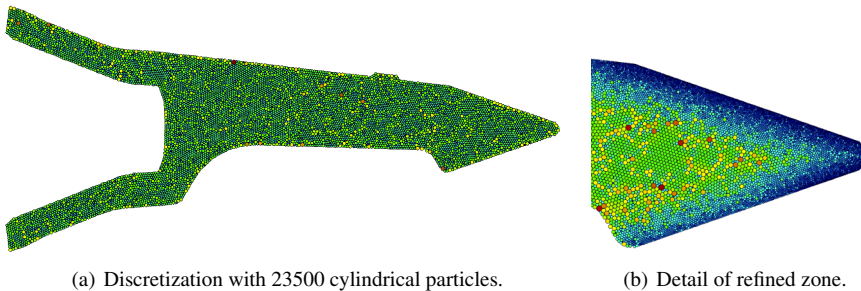


Figure 1: Tooth of excavation machine discretized with cylindric particles and refinement in the interaction surface. example in 3D is shown in Figure 2. Similar to the 2D example, a tooth of an excavation machine is discretized with 25000 particles. A good result of the generation process can be observed. The final porosity in the example is 30.77%.

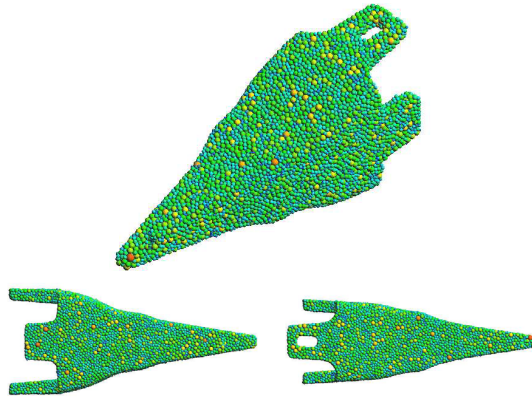


Figure 2: Tooth of excavation machine. 3D discretization.

#### 4 GID SUPPORT OF CIRCLE AND SPHERE ELEMENTS

This algorithm has been implemented in the GiD kernel. New *Circle* and *Sphere* element type can be handled. Basic support features for this elements include drawing, selection, mesh generation, scripting access, postprocess, and element's quality.

#### 5 CONCLUSION

- A new dense sphere particle packing algorithm has been presented.
- A boundary constraint is included in order to obtain a good surface definition, allowing the discretization of complex geometries.
- The comparison with other algorithms shows a good result for the porosity and coordination number, with a considerable speed.
- This technique is a good candidate for problems which require a high density packing.

#### REFERENCES

1. P. A. Cundall. Formulation of a three dimensional distinct element model—part i. a scheme to detect and represent contacts in a system of many polyhedral blocks. *Int. J. Rock Mech., Min. Sci. Geomech. Abstr.*, 25(3):107–116, 1988.
2. P. A. Cundall and O. D. L. Strack. A discrete numerical method for granular assemblies. *Geotechnique*, 29:47–65, 1979.
3. F. Zarate J. Rojek, E. Oñate and J. Miquel. Modelling of rock, soil and granular materials using spherical elements. In *2nd European Conference on Computational Mechanics ECCM-2001*, Cracow, June 2001.
4. F. Zarate J. Rojek, E. Oñate and J. Miquel. Thermomechanical discrete element formulation for wear analysis of rock cutting tools. Technical report, CIMNE, Barcelona, 2004.

## ARTIFICIAL NEURAL NETWORKS FOR OPTIMAL AIRFOIL DESIGN

R. López, R. Flores, E. Escolano and E. Oñate

International Center for Numerical Methods in Engineering (CIMNE)

Universidad Politécnica de Cataluña

Campus Norte UPC, 08034 Barcelona, Spain

E-mail: [rlopez@cimne.upc.edu](mailto:rlopez@cimne.upc.edu), [rflores@cimne.upc.edu](mailto:rflores@cimne.upc.edu), [escolano@cimne.upc.edu](mailto:escolano@cimne.upc.edu) and [onate@cimne.upc.edu](mailto:onate@cimne.upc.edu)

Web page: <http://www.cimne.com>

**Key words:** Neural Networks, Multilayer Perceptron, Optimal Shape Design, Aeronautical Applications

**Abstract.** A neural networks approach is proposed in this work for the designing of airfoil profiles with maximum aerodynamic efficiency. A practical application is solved by integrating the software tools Flood, GiD and PUMI for neural networks, pre and postprocessing and computational fluid dynamics, respectively.

### 1 INTRODUCTION

The aerodynamic efficiency is the amount of lift generated by a wing or vehicle compared to the drag it creates by moving through the air [1]. It can therefore be defined as the  $C_l / C_d$  ratio, where  $C_l$  and  $C_d$  are the lift and drag coefficients, respectively.

Improvement of the efficiency is one of the major goals in wing design. Indeed, since a given aircraft's needed lift does not change, delivering that lift with lower drag leads directly to better fuel economy, climb performance and glide ratio.

In order to obtain high efficiency it is essential to design airfoils using shape optimization techniques [2]. The use of neural networks within a variational formulation provides a direct method for the solution of optimal shape design problems [3].

Neural networks have been widely applied in aeronautics. For instance, an aerodynamic design procedure that incorporates that computational tool is described in [4]. However, the approach here is different since an extended class of neural network is used to define the airfoil shape, and not a response surface for the objective function.

The method is applied to the designing of the shape and the flight conditions of a transonic airfoil. The results demonstrate that the approach is very useful for optimization, since the constructed neural network is able to represent an extensive family of airfoils for any flight condition.

## 2 PROBLEM STATEMENT

An airfoil can be generated using analytical equations that describe the camber (curvature) of the mean-line (geometric centerline) of the airfoil section,  $y_c(x)$ , as well as the section's thickness distribution along the length of the airfoil,  $y_t(x)$ , for  $x \in [0,1]$ . This will provide us with the final coordinates for the airfoil upper surface  $(x_u, y_u)$  and lower surface  $(x_l, y_l)$  [1].

A suitable airfoil must hold some conditions. The camber distribution must be zero at both borders of the airfoil,  $y_c(0) = 0$  and  $y_c(1) = 0$ . On the other side, at the left border, the thickness must be zero,  $y_t(0) = 0$ , and its derivative must be infinite,  $y_t'(0) = \infty$ . At the position of maximum thickness  $p$ , the thickness distribution must take the maximum thickness value  $m$ ,  $y_t(p) = m$ , and the derivative here must be zero,  $y_t'(p) = 0$ . Finally, at the right border, the thickness must be zero,  $y_t(1) = 0$ , and its derivative can not be infinite,  $y_t'(1) \neq \infty$ .

The aim is to determine the shape and the angle of attack,  $\alpha$ , of an airfoil with given thickness and under transonic flight conditions, providing maximum aerodynamic efficiency. The maximum thickness is here set to  $m = 0.15$ , and the free-stream Mach number to  $M_\infty = 0.85$ . The flow is assumed to be Eulerian [5].

## 3 NUMERICAL RESULTS

The optimal shape design problem stated in the preceding Section is approached in this one using a variational formulation for an extended class of multilayer perceptron [3] [6].

### 3.1 Selection of function space

A neural network with a sigmoid hidden layer and a linear output layer is used here to represent the camber and the thickness distributions [3]. It must have one input,  $x$ , and two outputs,  $y_c$  and  $y_t$ . Three neurons are set in the hidden layer. Figure 1 is a graphical representation of this network architecture.

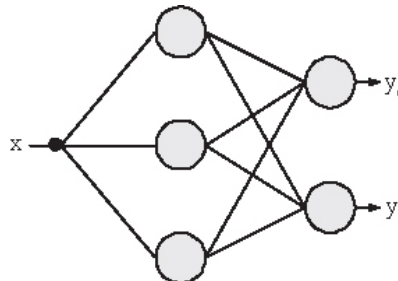


Figure 1. Network architecture representing the airfoil.

On the other hand, this multilayer perceptron must be extended with two independent parameters, the position of maximum thickness,  $p$ , and the angle of attack,  $\alpha$ . The total set of free parameters is thus  $\underline{\beta} = (\underline{\omega}, p, \alpha)$ , where  $\underline{\omega}$  is the vector of biases and synaptic weights

in the multilayer perceptron [6].

Finally, the camber must hold the conditions  $y_c(0) = 0$  and  $y_c(1) = 0$ . Also, the thickness needs to satisfy  $y_t(0) = 0$ ,  $y_t'(0) = \infty$ ,  $y_t(p) = m$ ,  $y_t'(p) = 0$ ,  $y_t(1) = 0$  and  $y_t'(1) \neq \infty$ . For that purpose, a suitable set of particular and homogeneous solutions for the camber and the thickness,  $\varphi_{0c}(x)$ ,  $\varphi_{0t}(x)$ ,  $\varphi_{1c}(x)$  and  $\varphi_{1t}(x)$ , is chosen [6].

Such a neural network spans a family  $V$  of parameterized functions  $(y_c, y_t)(x; \underline{\beta})$  of dimension  $s = 14 + 2$ , being 14 the number of biases and synaptic weights in the neural network and 2 the number of independent parameters.

Multilayer perceptron neural networks are a class of universal approximators [7]. In this way, the function space constructed in this Section can be considered a very suitable family of airfoils.

### 3.2 Formulation of variational problem

The statement of this problem is then to find a function  $(y_c, y_t)^*(x; \underline{\beta}^*)$  for which the functional  $F[(y_c, y_t)(x; \underline{\beta})] = C_l / C_d$ , defined on  $V$ , takes on a maximum value.

Evaluation of the objective functional is performed in three steps. First, an airfoil is proposed by the neural network using Flood [8]. Second, a GiD batch file is automatically written to create the geometry, apply the boundary conditions, generate the mesh and write the fluid solver input file. Third, the lift and drag coefficients are calculated by solving the Euler equations using PUMI [5]. Figure 2 shows the activity diagram for the evaluation of the objective functional.

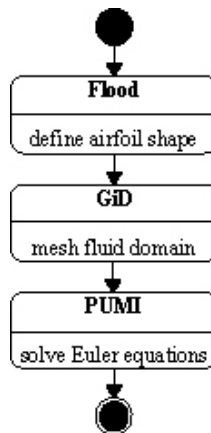


Figure 2. Activity diagram for evaluating the objective functional.

### 3.3 Solution of reduced function optimization problem

An evolutionary algorithm with linear ranking fitness assignment, stochastic universal sampling selection, intermediate recombination and normal mutation is applied for training the neural network [8]. The dimension of each individual is 16, the population size is set to 160 and the number of generations is set to 100. The total number of evaluations performed is thus 16000.

The upper and lower coordinates of the most efficient airfoil found by the neural network

are plotted in Figure 3, together with the corresponding pressure coefficient colour map and velocity vector field. These have resulted in a supercritical airfoil with  $C_l / C_d = 4.894$ . The best performance is for an angle of attack  $\alpha = 3.890^\circ$ .

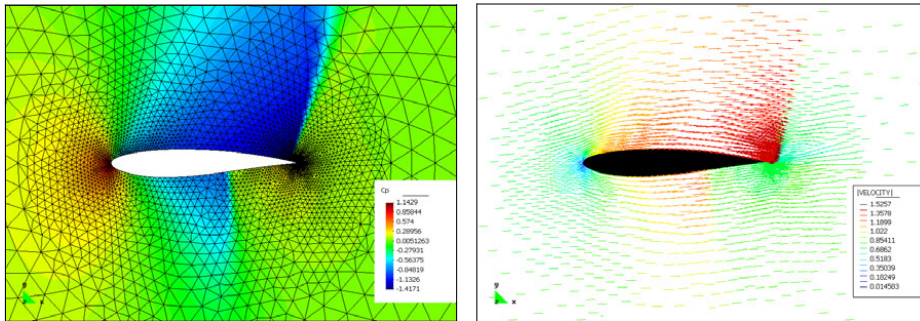


Figure 3. Pressure and velocity fields for the optimal airfoil design, with  $\alpha = 3.890^\circ$ .

#### 4 CONCLUSIONS

A multilayer perceptron extended with independent parameters and boundary conditions is able to represent a very complete family of airfoils. This neural network has been used here to find an optimal design with given thickness and under for transonic flight conditions, which has resulted in a supercritical airfoil.

Future work relies on distributing the computation over a cluster, in order to decrease computational time and to achieve better training results.

#### REFERENCES

- [1] H. Ashley, Engineering Analysis of Flight Vehicles, Dover Publishing (1992).
- [2] D. Bucur and G. Buttazzo, Variational Methods in Shape Optimization Problems, Birkhauser (2005).
- [3] R. Lopez, E. Balsa-Canto and E. Oñate, "Neural networks for variational problems in engineering", International Journal for Numerical Methods in Engineering, in press (2008).
- [4] M.M. Rai and N.K. Madavan, "Aerodynamic design using neural networks", AIAA Journal, 38(1), 173-182 (2000).
- [5] E. Ortega, R. Flores and E. Oñate, "An edge-based solver for compressible flow", CIMNE (2005).
- [6] R. Lopez and E. Oñate, "An extended class of multilayer perceptron", Neurocomputing, in press (2008).
- [7] K. Hornik, M. Stinchcombe and H. White, "Multilayer feedforward networks are universal approximators", Neural Networks, 2(5), 359-366 (1989).
- [8] Flood: An open source neural networks C++ library, [www.cimne.com/flood](http://www.cimne.com/flood) (2008).
- [9] GiD – The personal pre and postprocessor, [www.gidhome.com](http://www.gidhome.com) (2008).

**GID PRE/POST PROCESSING SYSTEM  
AS AN INTERFACE FOR  
PARALLEL RESERVOIR SIMULATOR (PARSI)**  
M. Abedi, S. Farnoush, R. Fatehi, M.A. Fayazbakhsh, H. Naderan,

**M.T. Manzari\***

Center of Excellence in Energy Conversion  
School of Mechanical Engineering  
Sharif University of Technology

\* Corresponding author  
Email: mtmanzari@sharif.edu

**Key words:**

**Abstract.** GiD pre/post processing system is used to provide a user friendly interface for our Parallel Reservoir Simulator (PaRSi), which is completely designed and programmed by the Reservoir Simulation Group at Sharif University of Technology sponsored by Pars Oil and Gas Company. PaRSi is a three dimensional parallel simulator for analysis of multiphase fluid flows in a petroleum reservoir. The simulator is based on a finite volume formulation and uses a newly developed high resolution central scheme as its underlying numerical method. The program is able to use both structured and unstructured grids along with either cell-centered or cell-vertex approach. GID provides powerful tools for both geometry modelling and mesh generation to the system as well as a well organized interface for assigning initial and boundary conditions. These are integrated as a new Problem Type. The simulation program is run by clicking an icon in the GID preprocessor. GID's postprocessing tools are also employed to visualize the computational results such as streamlines, variations of physical properties in space and time and to create relevant animations.

**1 INTRODUCTION**

Numerical simulation of flows in hydrocarbon reservoirs is a powerful tool which can be used for the management of production from such systems. Well placement and operation schedule can be optimized using a fast and accurate simulator. To this end, multiple non-linear partial differential equations must be solved numerically on typically large physical domains for a long period of time, which frequently exceeds several years. [1] As the simulations are very time consuming, one must use parallel computing techniques to obtain the required solutions within a reasonable time.



PaRSi is a parallel reservoir simulator software which can simulate three dimensional multiphase flows in petroleum reservoirs based on the so-called black-oil model. The software uses facilities incorporated in GiD as its pre and postprocessor. In the following, the basic features of the simulation software are briefly described and the dialogue boxes used for communication between GiD and the simulator are explained.

## 2 SOLVER

The heart of PaRSi simulator is its solver which is based on the black-oil model. This solver uses a volume balance formulation [1,2], in contrast to the customary pressure-saturation formulation. This simplifies dealing with various under-saturation states that occur during the production history. The volume balance formulation results in a nonlinear parabolic equation for pressure and a set of non-convex degenerate hyperbolic equations for fluid compositions. The equations are split to facilitate the use of a segregated approach.

During each time-step, the pressure equation is solved implicitly from which, fluid velocities are calculated. Then, fluid compositions are calculated using the component transport equations. A novel high resolution central scheme is used for the solution of component transport equations [2,3]. The main advantage of this method is that its accuracy is comparable with the more sophisticated higher-order Godunov schemes while retaining the simplicity of the traditional central schemes [3].

Time-step size is calculated based on several conditions. The first one is the CFL condition which ensures the stability of the solution. The second condition controls the maximum change in components which limits the splitting error associated with the pressure and component transport equations. The third condition is a user specified maximum time-step size which is activated when the above two conditions give unacceptable time-step sizes.

## 3 GEOMETRY AND MESH GENERATION

As GiD provides both structured and unstructured grids, the software was design to work with both types. Unstructured mesh can be used for more complicated geometries and enables PaRSi to resolve complex flow features more accurately especially near production or injection wells. GiD also has the capability to generate different output mesh files and assigning several conditions to elements, nodes or faces of elements [4] which is acknowledged by PaRSi's solver.

## 4 PARSI PREPROCESSOR PROBLEM TYPE

All data and parameters for the PaRSi's solver are set in the GiD environment. PaRSi uses a new Problem Type in GiD which enables the software to use most features of GiD. A general view of GiD's environment with the Problem Type used by PaRSi is shown in Figure 1. Below a brief description for each window is given.

### 4.1 PaRSi- Materials

Reservoirs may have different layers with material properties. The associated window in GiD can set various properties including rock compressibility, porosity, and absolute permeability in three dimensions. Also, relative permeability and capillary pressure of each layer can be defined as functions of water and gas saturations via tables, correlations, or specified data files.

#### 4.2 PaRSi- Initial conditions

Water and gas initial saturations, assigned to either elements or nodes, can be set in the initial conditions window.

#### 4.3 PaRSi- Boundary conditions

Boundary conditions, either an active aquifer or an impermeable wall, should be assigned to boundary faces of the volume in this window.

#### 4.4 PaRSi- Well conditions

Well properties and production scenarios are defined through either injection or production well condition windows and then assigned to the well elements (in a cell based method), or nodes (in vertex based method).

#### 4.5 PaRSi- PVT

General properties of reservoir fluids including gas, water, saturated oil, and under-saturated oil, are entered in this window. These properties contain density of fluid at standard conditions, compressibility of fluid and variation of some properties of fluids such as viscosity, density, formation volume factors, etc. which can be entered through table, correlations, or specified data file as a function of pressure.

#### 4.6 PaRSi- general data

Reservoir's initial pressure, temperature and reference depth are given in this window. Also, in this window one can choose between the vertex-based or the cell-based methods.

#### 4.7 PaRSi- stopping criteria

Constraints containing total time of production, total gas oil ratio and total oil production are defined in this window in order to determine the simulation duration.

### 5 GiD AS A POSTPROCESSOR FOR PARSI

Several visualization facilities exist in GiD. These can be any or all of the followings: contours plots of different parameters, vectors, animations of variation of variables with time, viewing results on different sections of the geometry and also graphs of variation of variables with time or position. Typical results for a SPE comparative study are shown in Figure 2.

#### REFERENCES

[1] Trangenstein, J.A. and Bell, J.B., "Mathematical Structure of the Black Oil Model for Petroleum Reservoir Simulation", *SIAM Journal of Applied Mathematics*, Vol. 49, pp. 749-783, 1989.

[2] Naderan, H., Manzari, M.T., Hannani, S.K., "Application and Performance Comparison of High Resolution Central Schemes for the Black Oil Model", *Int. Journal of Numerical Methods for Heat and Fluid Flow*, Vol. 17, No. 7, pp 736-753, 2007.

[3] Karimi A., Naderan H., Manzari M.T., and S.K. Hannani, "A Comparison between

High Resolution Central and Godunov-based Schemes for the Black-oil Simulation”. Submitted to International Journal for Numerical Methods in Heat and Fluid Flow, 2007.

[4] Ribó, R., de Riera, M. and Solano, E., “GiD Reference Manual”, Ed. CIMNE, Spain, 1999.

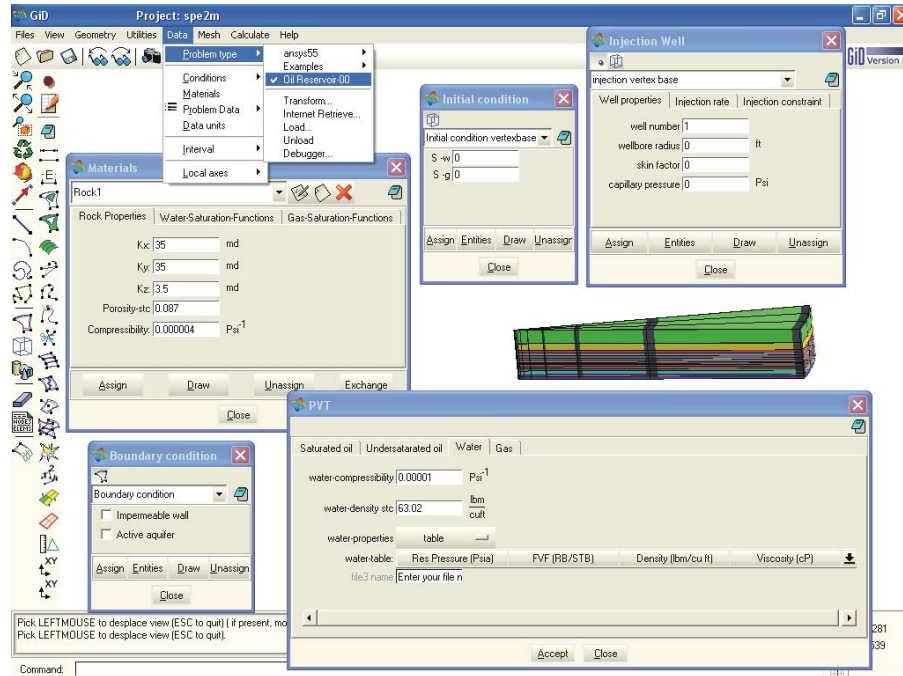


Figure 1: A view of GiD while preparing data for a problem



Figure 2- Pressure contour plots for the SPE test case

## MULTIPHYSICS SIMULATIONS USING NACS IN COMBINATION WITH GID

Martin Meiler<sup>\*</sup>, Hermann Landes<sup>\*</sup> and Manfred Kaltenbacher<sup>\*</sup>

<sup>\*</sup>SIMetris GmbH  
Am Weichselgarten 7  
91058 Erlangen, Germany  
Email: [info@simetris.de](mailto:info@simetris.de) – Web page: <http://www.simetris.de>

**Key words:** Simulation, Multiphysics, Finite Element Analysis, NACS, GiD Interface

**Abstract.** *An interface between the finite element software NACS and GiD has been developed by SIMetris recently. NACS (Numerical Analysis of Coupled Systems), which is developed and marketed by SIMetris, has been designed as a finite element software for the efficient solution of multiple coupled field problems. Currently, it provides solution facilities for piezoelectric, acoustic, magnetic, and mechanic problems as well as combinations of those. In the presentation the required adaptations within GiD's graphical user interface (GUI) to support NACS will be described. Furthermore, we will present the implementation of a scripting facility which allows an easy-to-use generation of parametric models using dedicated GiD input scripts. Finally some demonstration examples will be presented.*

### 1 INTRODUCTION

In this paper, the use of GiD in combination with the finite element software NACS (Numerical Analysis of Coupled Systems), which has been developed by SIMetris, will be demonstrated. In order to support NACS, a special interface has been developed for GiD which does not follow the customization as proposed by GiD, but introduces a completely redesigned GUI adaptation.

NACS is a multiphysics finite element software whose single field applications cover magnetics, mechanics, electrostatics and acoustics. Since NACS has been developed with regards to coupled fields, nearly arbitrary combinations of these single fields may be solved including, but not limited to piezoelectric, magneto-mechanic or, acoustic-mechanic tasks. This allows the simulation of sensors, actuators or even complete systems with applications reaching from medical systems, power transformers to small sensor systems like piezoelectric transducers.

Since NACS does not include a pre- or postprocessor, interfaces to for commercial software packages which provide this kind of functionality are required. GiD is a good choice as pre- and postprocessor since it allows the user to generate models easily and in an intuitive way. The GiD interface will be presented in the following chapter.

## 2 GiD INTERFACE FOR NACS

The GiD interface for NACS has to provide two basic functionalities. First, a geometric model has to be generated. Based on this geometric model the simulation setup of NACS is specified. This includes the selection of the computational domains, the definition of the analysis type, selection of included physics types, boundary conditions as well as the results that shall be obtained and stored during the simulation.

Two different approaches can be followed when trying to generate the simulation files. The first relies on using the GUI and working interactively with the program whereas the second approach requires the use of script files.

Regardless of the chosen method, the output files of the preprocessing consist of a mesh file, which is stored as a HDF5-file, and of a parameter file, which is stored as a xml-File. HDF5 is a standard file format that allows an efficient storage of large amounts of data.

The GiD interface itself is split into two separate parts. The first part is implemented in Tcl/Tk as an extension to GiD, whereas the second part consists of an external SOAP-Server, that allows a client-server communication with the localhost. The server process manages all settings according to the simulation setup. The choice of boundary conditions or results presented to the user depends on the previously selected analysis, geometry and physic types and is preselected by the server process.

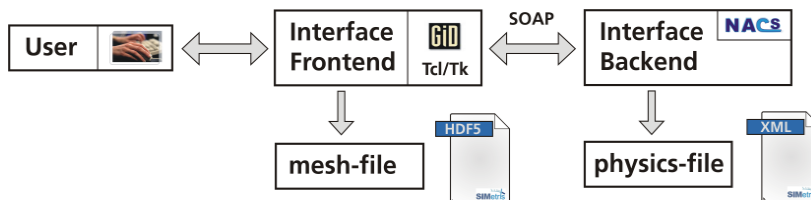


Figure 1: Work Principle of the NACS Interface for GiD

### 2.1 Graphical User Interface (GUI)

Using the GUI the user can interactively create the model and learn to use GiD as well as options and features NACS offers him. Therefore a Computation Wizard has been implemented guiding the user through the definition of the physical setup. This includes the selection of the geometry type, analysis type, physic types, couplings, boundary conditions, results, and solver. At the end of the model generation process the simulation input files will be created and the simulation can be started.

Figure 2 shows a sketch of the reworked GUI and includes the region definition window at the upper left corner of the display, the wizard, that guides the user through the parameterization process, in the lower left corner and the NACS command line at the upper right corner. The geometric model which consists of a steel plate with two piezo actuators on its surface can be seen in the upper right corner.

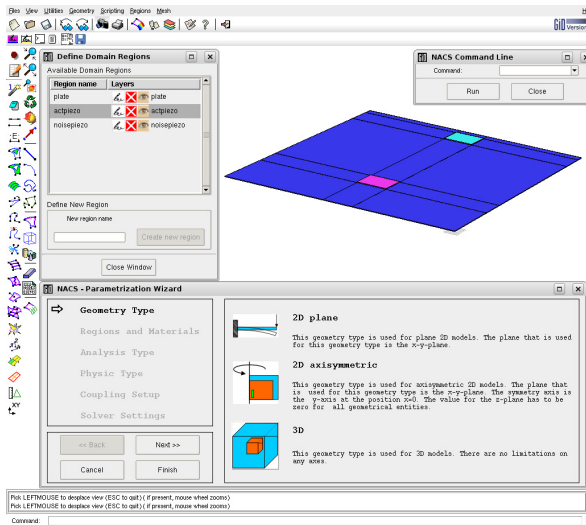


Figure 2: GUI of NACS Interface for GiD

```

...
## Region Definition
region plate plateLayer
## Surface Region Definition
surfregion fix Surfaces "1:10"
## Physical Setup
setgeometry 3d
matfile mat-nacs.xml
material plate st37
# Analysis Type
harm 1 linear 2 230 267.5
# Physic Type
physicreg 1 mech plate
# Boundary Conditions
bc 1 mech fix disp x 0
bc 1 mech fix disp y 0
# Results
result 1 mech disp "" all
# Create Mesh and write files
mesh
writemodel plate 1e-3

```

Figure 3: Scripting Example

## 2.2 Scripting Interface

The second approach, which relies on the use of script files including the process of model generation, meshing, and the definition of the physical setup of the simulation, will be the preferred method for most users. The main advantage of this method for creation of the simulation setup consists of the fact that it provides a reproducible way to generate models even from the command line, by using GiD in batch mode. Furthermore, parameter variations can easily be carried out by changing the corresponding values in the script file.

A part of a scripting file is shown in figure 3. Within this part of the script the computational region plate is defined. Then the surface region fix is defined, consisting of all surfaces from nr. 1 to 10. After this step the geometry type is set to 3d, the material file is defined and the material of type st37 (steel) is set for the region plate. A harmonic analysis will be performed at two frequencies (230 Hz and 267,5 Hz). The physical simulation setup consists of a simple mechanics calculation in region plate with displacement boundary conditions specified for the x- and y-displacements in the surface region fix. Finally, the result type is specified (mechanics displacement), the meshing process is initiated, and the simulation files are written.

### 2.3 Post-Processing

The results obtained from a simulation run with NACS can easily be examined using GiDs post processing functionality. Only results that may not be displayed on the simulation grid like integral quantities, i.e. the electric charge or energy results, have to be examined with external tools.

### 3 EXAMPLE

A short example will illustrate the impact of piezoelectric transducers that are applied on a thin steel plate<sup>i</sup>. Whereas one of the transducers is used to excite the vibrations of the plate, the second transducer acts as a vibration cancellation actuator and tries to minimize the amplitude of the vibration. The model has been generated using the scripting interface for GiD. Parts thereof are displayed in figure 3 as well as the geometric model in figure 2.

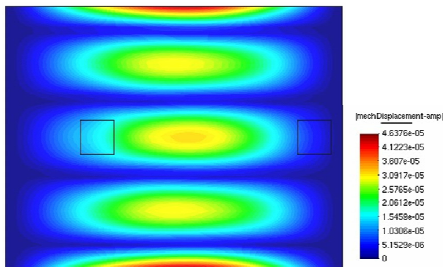


Figure 4: Vibrating Steel Plate excited by the Noise Actuator

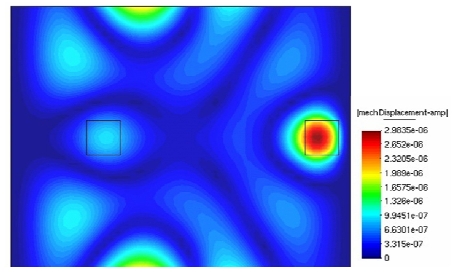


Figure 5: Vibration Result with applied Active Vibration Cancellation Actuator

Figure 4 shows the plate vibrations as excited by the first piezoelectric transducer. The result in figure 5 depicts the reduced vibration amplitude due to the presence of the active vibration cancellation actuator.

### 4 CONCLUSIONS

In this paper a GiD interface for NACS has been introduced. It was pointed out that GiD represents an intuitive and easy-to-use pre- and postprocessor for finite element simulations. Therefore the GUI has been adapted and a Tcl-based scripting interface has been developed in order to provide a dedicated interface for NACS.

The shown examples emphasize the capabilities of NACS in combination with GiD.

<sup>i</sup> M. Meiler, L. Messner, A. Dantele, M. Kaltenbacher, T. Hegewald, „Active Noise Cancellation with Smart Structures Analyzed by an Enhanced Finite Element Scheme for Non-linear Piezoelectricity“, Proc. ANSYS Conference & 25th CADFEM Users Meeting

## SIMULATION OF COUPLED ELECTROMAGNETIC-MECHANICAL SHEET FORMING

R. Mendez, A. Ferriz, O. Fruitos

International Center for Numerical Methods in Engineering (CIMNE)  
Campus Nord UPC, 08034 Barcelona, Spain  
e-mail: metalform@cimne.upc.edu

**Key words:** Electromagnetic sheet forming, regularization of Maxwell equations, ERMES, Stampack®, meshing tools, display simulation results.

**Abstract.** The finite element method has characteristics that do it a powerful tool to solve electromagnetic problems. In this paper low frequency industrial electromagnetic-mechanical forming applications of code based in the regularization of Maxwell equations will be presented. Analytic and experimental validations will be described. Standard and specific developments, supported on GID platform, are described too.

### 1 INTRODUCTION

Electromagnetic Forming (EMF) is a metal working process that relies on the use of electromagnetic forces to deform metallic workpieces at high speeds. The EMF pieces can be used alone or combined with the usual mechanic methods. In this process, a transient electric current is induced in a coil using a capacitor bank and high-speed switches. This current induces a magnetic field that penetrates the nearly conductive workpiece where an eddy current is generated. The magnetic field, together with the eddy current, induces Lorentz forces that drive the deformation of the workpiece. In an EMF process, the material can achieve velocities in the order of 100 m/s in less than 0.1 ms. The dynamics of this event, including die impact, enhance the formability of the workpiece and reduce springback [1].

With the current state of the art of software, the EMF problems consist in two separate analysis. CIMNE works is working into coupling the two analysis in only one process.

The authors thank the Spanish “Ministerio de Educación y Ciencia” their funding in the SICEM project (Simulación multifísica para el diseño de conformado electromagnético) It is coordinated by CIMNE and with the participation of LABEIN, Tecnalia.

### 2 ELECTROMAGNETIC PROBLEM

ERMES is a FEM Electromagnetic code that solves Ecuaciones de Maxwell Regularizadas en Presencia de Singularidades [i][ii]. Its pre and postprocessor resources are based on the GID platform (see ERMES bar in fig.1 and two of the menus in fig. 2).





Figure 1: ERMES icons Bar in GiD platform

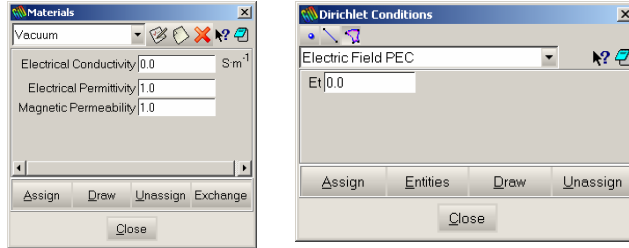
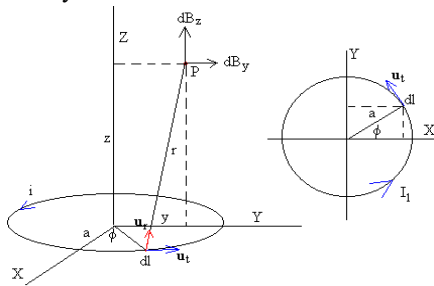


Fig. 2: Input material data and Dirichlet conditions

In order to validate this electromagnetic code, which is in development, the numerically simulated model with the one spire analytic solution was compared. The formulations of the analytic model are:



$$B_z = \frac{\mu_0}{2 \cdot \pi} \cdot i \cdot a \cdot \int_{\pi}^0 \frac{-(a - y \cdot \cos(\theta))}{(a^2 + y^2 + z^2 - 2 \cdot a \cdot y \cdot \cos(\theta))^{3/2}} d\theta \quad (1)$$

$$B_y = \frac{\mu_0}{2 \cdot \pi} \cdot i \cdot a \cdot z \cdot \int_{\pi}^0 \frac{-\cos(\theta)}{(a^2 + y^2 + z^2 - 2 \cdot a \cdot y \cdot \cos(\theta))^{3/2}} d\theta \quad (2)$$

$$\begin{aligned} H_z &= \frac{B_z}{\mu_0} & H_y &= \frac{B_y}{\mu_0} \\ H &= \sqrt{H_z^2 + H_y^2} \end{aligned} \quad (3)$$

The expressions (1) and (2) have been solved with the explicit mathematical program Mathcad®.

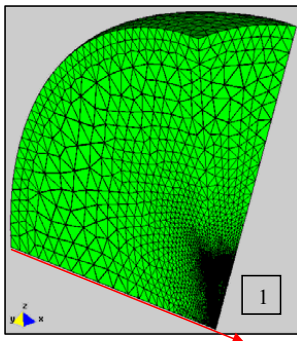


Fig. 3: Simulation mesh

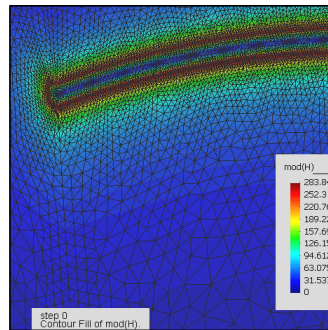


Fig. 4: Numerical results

Figures 3 and 4 show the mesh used and the simulation results respectively. Graph 1 shows the comparison between analytic and simulated results into the spire revolution axis (Label 1 fig. 3), which illustrate a good agreement between them.

A cone benchmark laboratory validation test [iii] was selected too. In fig. 5, the initial domain and coil geometry is shown (30° sector only). In this example, the Perfect Electric Conductor (PEC) condition was supposed to the sheet. The IGES and Bach format files make possible to build the model in an easy way.

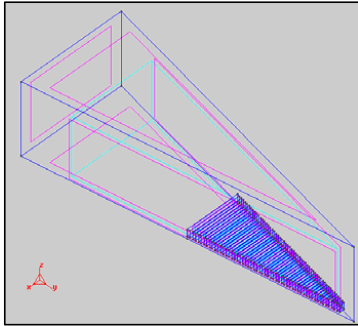
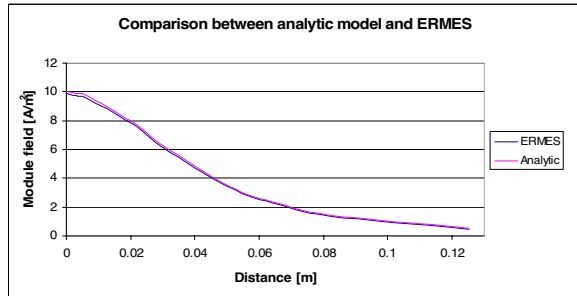


Fig. 5: Geometry of electromagnetic model



Graph. 1: Magnetic field vs. distance (respect the plane of the spiral) in numerical and analytic problem.

CIMNE has worked calculating the EM problem and the mechanical problem iterating manually. Thus, the need to do an automatic iterative simulation was analysed. The figures 6, 7 and 8 show the succession of the magnetic field in three different steps of forming simulation.

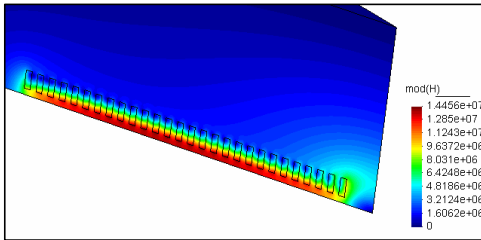


Fig. 6: Distribution of the magnetic field in the first iteration.

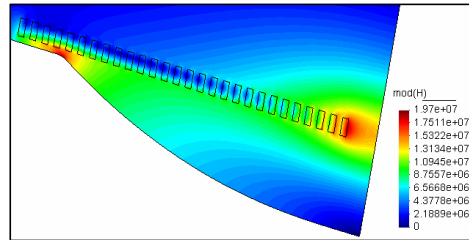


Fig. 7: Distribution of the magnetic field in the second iteration.

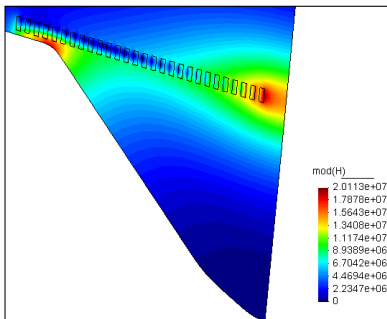


Fig. 8: Magnetic field in 3<sup>rd</sup> iteration

The field value decreases quickly as the distance to sheet increases. In the second and third step, the magnetic field is concentrated in the matrix accordance radius and in the magnetic coil axis.

Magnetic pressure (P) in PEC conditions is function of the magnetic field module (H) (equation (3)) and the vacuum magnetic permeability ( $\mu_0$ ):

$$P = \mu_0 \cdot \frac{|H|^2}{2} \quad (4)$$

### 3 MECHANICAL PROBLEM

The mechanical code used is Stampack<sup>®</sup>. Its pre-postprocessors resources also are implemented in the GiD platform. In order to modelling the problem, it's necessary also to import the initial and posterior sheet configurations from EM code. Due to the benchmark axisymmetry, the mechanical model is in 2D. Only 2D top line nodes of the sheet in deformed position in the time  $t_i$  is the input of the EM problem in time  $t_{i+1}$ . The experimental and the simulated results are shown in the figures 9 and 10.

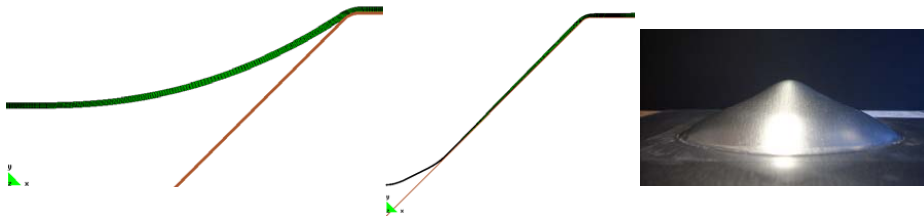


Fig. 9: Deformed in two different times and the experimental sheet formed (Courtesy of LABEIN-Tecnalia)

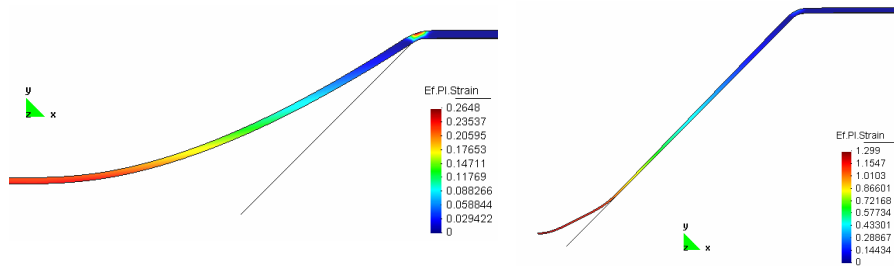


Fig. 10: Effective plastic strains in two different times of the process

### 4 CONCLUSIONS

- Pre and postprocessor GiD platform is useful to work with simple or complex geometries in iterative manually coupled problems. The IGES, bch or dxf files, simplify the geometry transfer between EM and mechanical modules.
- The small gap between the sheet and the coil difficult the meshing. The use of tools like “unstructured size transitions” combined with “structured lines and surfaces” improves the control of non structured mesh generation in this zone. The automatic loops implementation at the moment is not possible.
- The standard visualisation tools of the results are used. The calculus of magnetic pressure is possible in user interface level. Specific visualization tools (calculus and visualization of volumetric forces) are under develop.
- To confirm the correct adjust of experimental results at lower and higher energy and frequency levels new benchmarks will be necessary.

### REFERENCES

- [i] R. Otín, J. Mora, “El Método de los Elementos Finitos Aplicado a las Ecuaciones de Maxwell Regularizadas en Presencia de Singularidades”, CIMNE, 2007, Barcelona.

- 
- [ii ] A. El-Azab, M. Garnich, A. Kapoor “Modeling of the electromagnetic forming of sheet metals”, ELSEVIER 2003, Amsterdam.
- [iii] P.Jimbert, I.Eguia,M. Gutierrez, B. , “Conformado electromagnético: una nueva posibilidad para la deformación en automoción”, IMHE Suplemento Deformación, Ed. IZARO, 2006, Bilbao.



## MODELING THE STRUCTURAL AND ACOUSTIC BEHAVIOR OF SONAR TRANSDUCER WITH ATILA CODE AND GiD

H.Mestouri, A.Loussert, and G.Keryer

Laboratoire ISEN Brest-Département d'instrumentation  
Institut Supérieur de l'Électronique et du Numérique (ISEN)  
20 rue Cuirassé Bretagne, C.S. 42807  
29228 Brest Cedex 2, France  
Email: hind.mestouri@isen.fr- Web page : <http://www.isen.fr>

**Key words:** Transducer Arrays, Finite Element Method, ATILA FEM Code, GiD Graphical Interface, Crosstalk, Fluid Pressure.

**Abstract.** *Many important issues in transducer arrays design, such as crosstalk, cannot be accurately studied using analytic method due to the complexity of the partial differential equations involved. Finite element method (FEM) is the only appropriate way to gain more detailed information. In this paper, a 2D finite element model is constructed to modeling the structural and acoustic behaviour of transducer arrays, using ATILA code and GiD graphical interface. Several different analyses were designed to examine a different aspect of acoustic behaviour of sonar transducer. It was found that crosstalk affect pressure fields in fluid (water).*

### 1 INTRODUCTION

The active sonar is a system that allow transmitted and received acoustic signals, it is consisting of both a projector and hydrophone. Figure 1 shows the geometry of transducer arrays considered in this paper [1], it is a low frequency transducer arrays developed for shallow water with 300 kHz resonance. It is composed of six piezoelectric elements, and mounted in a housing whose main function is to provide mechanical support for array, separated by an acoustically and electrically inactive material (Filler) which prevents acoustic wave propagation between elements. A waterproof material is used to protect the piezoelectric transducer elements; this material is usually selected to possess approximately the same acoustic properties than water to reduce energy loss at the water interface. The matching layers at the front face are used to adapt the different acoustic impedances of piezoelectric and water respectively, there are one or more (usually two) matching layer to increase the bandwidth [2]. The typical center-to-center spacing between transducer elements is  $d=\lambda/2$ . Usually, these transducers operate at their resonant frequency. If the resonant frequency is  $f_r=300$  kHz,  $c=1500$  m/s speed of sound in water, then the wavelength, is  $\lambda=0.5$  cm.

Due to crosstalk through transducer arrays structure, sonar beam patterns are distorted and a low level sensitivity can also be obtained. Much study of this problem can be found in literature [2]. Several approaches based on numerical methods and experimental methods

have been proposed [3]. In this work, we built several array with and without structure, with and without matching layers, and using classical housing (Aluminum). A 2D finite element model is constructed to modeling the structural and acoustic behaviour of sonar transducer using ATILA code and GiD graphical interface.

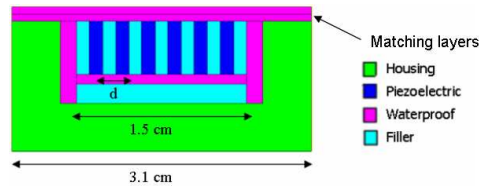


Figure 1: Geometry of the transducer arrays

## 2 MODELING TOOLS

Finite element method is widely used for the modeling of piezoelectric transducers. It is a method of transforming a continuum system to its equivalent discretized system in which the system is divided into elements [4]. ATILA (Analysis of Transducers by Integrating Laplace equations) is a user interactive finite element code originally developed by many French scientists and engineers during 1980s, and is specifically developed for modeling of two or three dimensional elastic, piezoelectric, magnetostrictive and fluid structures [4]. With ATILA, you can perform static, modal, harmonic and transient analyses of your active structures. Because the formulation is organized around a strong electrical/mechanical coupling and a strong fluid/structure coupling, ATILA is a very efficient design tool for all types of active materials applications: actuators, transducers, sensors, and so on. The program modules are independent, which means that we can customize the software configurations to meet your specific needs. Different types of materials can be used for the design of heterogeneous 2D and 3D structures, and multiple excitation sources (electrical potentials, currents into inductors, displacements, forces and pressures) can be used at the same time. Applications include sonar and acoustic transducers (piezoelectric and magnetostrictive), piezoelectric transformers, piezoelectric and magnetostrictive motors and most piezoelectric and magnetostrictive actuators and sensors (piezoelectric valves, magnetostrictive pumps, piezoelectric accelerometers, magnetostrictive torque sensor).

Due to complexity of creating data files of ATILA code, we used GiD graphical interface to creating data files by defining geometry we want to study, the materials it is composed, and constraints. He allows generates a mesh (for finite elements, finite differences or other methods) and transfers geometric data [5].

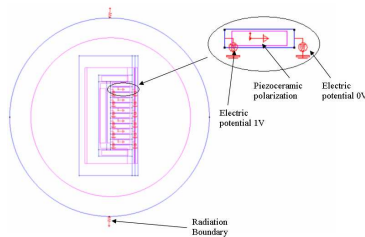


Figure 2: Boundary condition and piezoelectric polarization

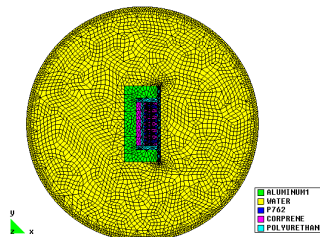


Figure 3: Automatic meshing of transducer arrays

### 3 SIMULATION RESULTS

The proposed procedure to modeling sonar transducer is to use GiD for creating data file; we choose the geometry described in Figure 1. A 2D plane strain condition is considered, that imply the absence of strain in the third geometrical dimension, which physically means a structure with either a very thin (plane stress) or an infinitely long (plane strain) third dimension [6]. For this simulation we use harmonic analysis with loss. A non reflecting boundary condition to the fluid domain (water) is applied; it creates a limit (not infinite) on the finite element mesh of the fluid. This condition and piezoelectric polarisation are shown in Figure 2. After choosing quadrilateral finite element type to describe the region under study, and size of mesh spacing that is related to the smallest acoustic wavelength used, GiD allows the use of an automatic mesh generator which creates node coordinates and element topologies Figure 3. Finally, when the data file is created, ATILA can run, provides a results file and some file containing arrays for post processing. A graphic display of the directivity patterns and sensitivity can be easily obtained graphically. Animated views of the vibrating structure or of the pressure in the fluid are also available on graphic terminals.

Due to symmetry of the problem it is sufficient to simulate only the half of the device when we excite all element with the same excitation at the same time. In this work, we are interested in modeling complete transducer arrays, in order to use beamformer which is to send sounds in one direction  $\theta$ . The beamformer is due to applying of a time delay between adjacent elements  $\tau_n$  (1) [7], where  $n=[0, \dots, N-1]$ ,  $N$  denotes total number of element, and  $\theta$  is the angle between transmitting direction and the direction of the array. We excite each elements by an electric potential of magnitude 1V, and phase  $\varphi_n$  (2).

$$\tau_n = \frac{nd}{c} \cos \theta \quad (1)$$

$$\varphi_n = 2\pi f \tau_n \quad (2)$$

Figure 4 shows the modeling of six piezoelectric elements in water without other materials. We found the exact direction that we have imposed. In the purpose, to display the effect of matching layers, Figure 5 shows the modeling of transducer arrays without matching layers, and Figure 6 shows the results of complete transducer arrays at the direction  $\theta=30^\circ$ . Comparing these results, we can see that matching layers increase the bandwidth, but the crosstalk is important. On the other hand, Figure 7 shows the results of complete transducer arrays at the direction  $\theta=60^\circ$ . In this time, we observe that crosstalk increase respectively with transmitting direction, and we find important side lobes.

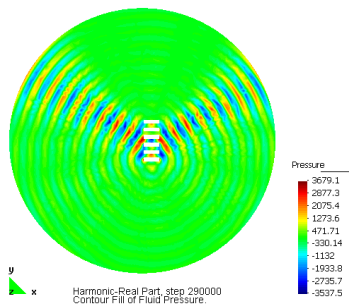


Figure 4: Fluid pressure of six elements without structure  $\theta=30^\circ$

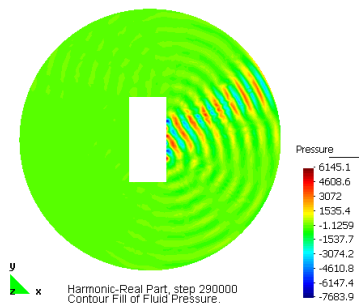


Figure 5: Fluid pressure of transducer arrays without matching layers  $\theta=30^\circ$



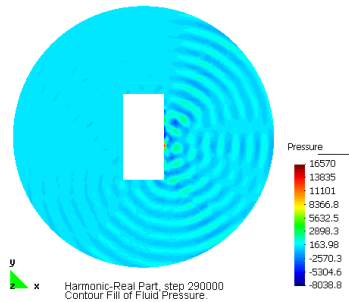


Figure 6: Fluid pressure of six elements with structure  $\theta=30^\circ$

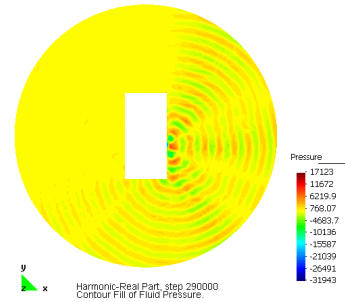


Figure 7: Fluid pressure of six elements with structure  $\theta=60^\circ$

#### 4 CONCLUSIONS

In this paper the effect of crosstalk due to sonar structure was investigated. A 2D finite element model to analyze crosstalk, using ATILA code and GiD graphical interface has been shown. Future applications will also handle complete transducer arrays including environmental noise and the role of sonar dome.

#### REFERENCES

- [1] J.S Bird, S. Asadov, and P. Kraeutner, "Improving arrays for multi-angle swath bathymetry", *OCEANS 2003. Proceedings*, Vol. 4, pp. 2085 – 2092, Sept 2003.
- [2] Z. Shiwei, L. Gregory, Wojcik, and John A. Hossack, "An Approach for Reducing Adjacent Element Crosstalk in Ultrasound Arrays", *IEEE Transactions on Ultrasonics, Ferroelectrics, and Frequency Control*, vol.50, pp. 1752-1761, Dec. 2003.
- [3] A. Caronti, R. Carotenuto, G. Caliano, E. Cianci, and M. Pappalardo, "A finite element study of cross coupling in 1-D capacitive micromachined ultrasonic transducer arrays", *Proc. IEEE Ultrason. Symp.*, pp. 1032-1035, 2002.
- [4] A. C. Hladky-Hennion, R. Bossut, S. Alkoy, P. Lopath, R. E. Newnham, "Finite Element Modeling of Transduction Materials with Application to Piezoelectric Hollow Sphere Transducers", *Proc. IEEE International Frequency Control Symposium*, pp. 709-714, May 1998.
- [5] <http://www.gid.cimne.upc.es>
- [6] R. Lerch, "Simulations of Piezoelectric Devices by Two- and Three-Dimensional Finite Elements", *IEEE Trans. on Ultras., Ferroel. and Freq. Control*, Vol. 37, No. 3, pp. 233 - 247, 1990.
- [7] I.S.D. Solomon, A.J Knight, "Spatial processing of signals received by platform mounted sonar", *Oceanic Engineering, IEEE Journal*, Vol. 27, Issue 1, pp. 57 – 65, Jan 2002.

## NUMERICAL TOPOLOGY OPTIMISATION USING GID

J.A. Oliveira, J. Pinho-da-Cruz, A. Andrade-Campos and F. Teixeira-Dias

Departamento de Engenharia Mecânica  
Universidade de Aveiro, Campus Universitário de Santiago  
3810-193 Aveiro, Portugal  
e-mail: jalex,jpc,gilac,ftd@ua.pt

**Keywords:** Finite Element Method, Homogenisation, Topology Optimisation

**Abstract.** *The overall mechanical behaviour of a given structure depends not only on the materials it is built from but also on its shape and topology. Therefore, the design of a material microstructure might improve the behaviour of the macrostructure, as well as significantly change the way its optimisation is performed. In this scope, a typical topology optimisation approach can be extended to optimise structures built from materials such as composite materials, functionally graded materials or cellular materials.*

*In this scope, the authors apply topology optimisation methods on a multiscale problem using variations of a power-law method. The main goal is to optimise the topology of a given macroscale. The optimisation problem is solved over the macroscale in a classical fashion, while the periodic microscale problem is approached using the Asymptotic Expansion Homogenisation (AEH) method to solve a Representative Unit-Cell (RUC) linear elasticity homogenisation problem.*

*The authors also show the usage of GiD as a pre- and post-processor. All the process data (both for the macro- and microscale problems) are introduced in dedicated problem types with a graphical user-friendly interface (GUI) developed within GiD. Post-processing is also carried out with GiD, enabling the analysis of the results of multiscale optimisation problems.*

### 1 INTRODUCTION

Recent developments in structural applications and innovative products lead to increasing demands for significant structural performance and material properties. The design of structures and composite materials gathers substantial attention in engineering due to their capability of attaining the desirable functions, where the configuration of structures and materials can be purposely designed. In this sense, the use of computer simulation techniques can generate flexible and efficient solutions. In fact, computational topology optimization has become a prevalent tool in the fields of structural and material design<sup>i,ii,iii</sup>.

The authors show that different spatial orientations of the same orthotropic composite material influence the optimal behaviour of the global structure. The material properties are calculated with an asymptotic expansion homogenization procedure, while the optimal macrostructure is the result of a topology optimization procedure. Due to the specificity of

each of the multiscale problems presented, the need to fine tune both the pre- and postprocessing stages of the numerical simulation procedures means that there are several advantages on the usage of GiD<sup>®</sup>.

## 2 ASYMPTOTIC EXPANSION HOMOGENISATION

The asymptotic expansion homogenisation (AEH) method is used to solve problems that involve physical phenomena on continuous media with periodic microstructures. This useful technique can be used to study the behaviour of structural components built from composite materials. In this method, the material microstructure is approximated by the spatially periodic distribution of a representative unit-cell (RUC). Applying loads to these materials results in periodic oscillations of the resulting displacement, stress or deformation fields. These oscillations derive from the periodicity of the microstructural heterogeneities and lead to the assumption of the existence of two separate dimensional scales, linked to material behaviour phenomena at the macroscale and microscale levels. The macroscale problem is transformed into a common finite element problem, using a homogenized set of material properties that result from the microscale problem solution. This solution is a homogenized elasticity matrix, averaged through the representative unit-cell with periodicity boundary conditions. This is done solving six finite element problems, in which the material property gradients within the composite material are used to determine the RUC eigendeformations. These natural deformation modes – three linear and three angular modes – represent the microstructural oscillations that render the influence of the material heterogeneities on the overall material properties<sup>iv</sup>.

## 3 TOPOLOGY OPTIMISATION

When designing a structure intended to support a specific set of loads, a fundamental topology can be found using optimization procedures. Starting from known loads, boundary conditions and the maximum design space available, the result is a design concept which is as light as possible, while resulting in the desired minimum compliance design<sup>ii</sup>. A common and efficient approach is a power-law method called Solid Isotropic Material with Penalization (SIMP). In this material distribution method, the objective function is the density of material. Note that this is not density in the usual physical sense but a value that interpolates between 0 and the effective material properties. The material properties are modelled as the relative material density raised to some power (penalty) times the material properties of the solid material<sup>ii,v</sup>. This means that, for a given volume restriction, the method results in a black and white design, representing areas with and without material.

In this work, the authors used a variation of this method in which the density values act upon the homogenised elasticity matrix instead of a given set of material properties. This way, the optimisation procedure gives way to the optimal macrostructure for a given microscale, *i.e.* a given material component distribution.

## 4 MULTISCALE PROCEDURE

The overall multiscale procedure is composed of a homogenisation step and a set of three topology optimisation calculations, as shown in Figure 1. The authors used a representative unit-cell of a continuous parallel fibre reinforced composite material, with a reinforcement volume fraction  $f_f=47\%$ . Applying the asymptotic expansion homogenisation procedure led to an elasticity matrix for this three-dimensional composite material structure. Three different

bidimensional elasticity matrices were derived, each representing the material properties of the composite material for each of the three main orthogonal orientations. This resulted in the two orthogonal orthotropic and one isotropic orientations illustrated in Figure 1. These material properties were then used in the macroscale topology optimisation problem with the set of boundary conditions shown in Figure 1.

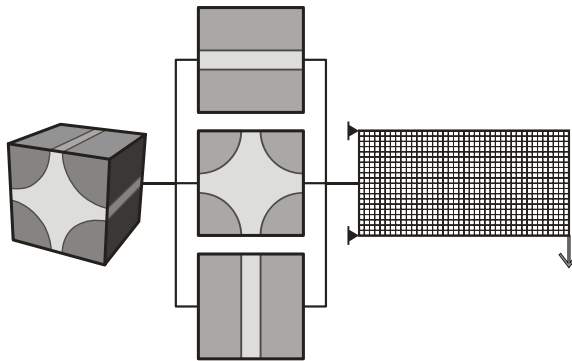


Figure 1: Overall multiscale procedure.

## 5 RESULTS

The metal matrix composite material (see Figure 1) is made of an Aluminium (Al) matrix and Boron (B) reinforcement fibres. The elastic modulus of the matrix material is 68.3 GPa and the elastic modulus of the reinforcement material is 379 GPa. The Poisson coefficient is 0.3 for the matrix material and 0.1 for the reinforcement.

In Figure 2 it is possible to see the six eigendeformations that resulted from the AEH procedure. The overall results are shown in Figure 3. It is clear that, for a constant reinforcement volume fraction, the microscale topology has a major influence on the optimal macrostructure design. Furthermore, the two orthotropic examples act as bounds for the isotropic case. It is also possible to verify the influence of the reinforcement orientation on the optimisation results.

## 6 CONCLUDING REMARKS

The main conclusion of this work is that the topology optimisation procedure reacts to changes in the material microstructure. In addition, the macroscale optimized geometry changes in order to make better use of the higher stiffness orientations of the composite material.

As for the pre- and post-processing stages, GiD proved a highly valuable tool. All the process data are introduced in GiD's dedicated problem types, showing its flexibility over multidisciplinary numerical simulations. Moreover, the variety of different requirements in the way that the results are presented is easily fulfilled with the extensive customisation options provided.

## 7 ACKNOWLEDGEMENTS

The authors acknowledge the financial support provided by FCT – Fundação para a Ciência e a Tecnologia – and by the FSE – Fundo Social Europeu – within the III Quadro de

Apoio Comunitário.

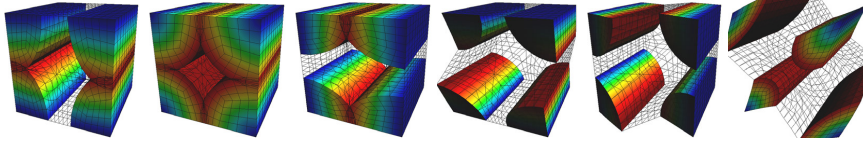


Figure 2: Set of eigendeformation modes of the selected representative unit-cell.

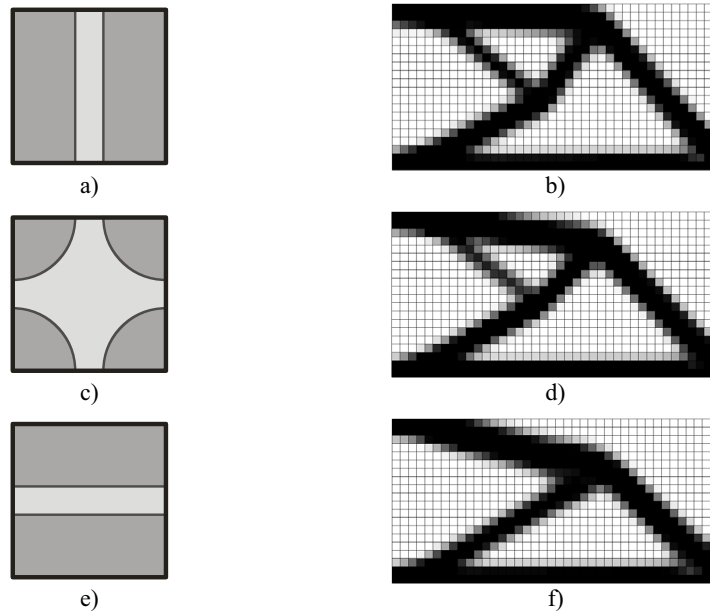


Figure 3: Optimisation results (b, d and f) using different reinforcement orientations (a, c and e).

## REFERENCES

- [i] N. Kruijff, S. Zhou, Q. Li and Y. Mai, "Topological design of structures and composite materials with multiobjectives", *International Journal of Solids and Structures*, **44**, 7092-7109, (2007).
- [ii] M.P. Bendsøe and O. Sigmund, *Topology Optimization: Theory, Methods and Applications*, 2<sup>nd</sup> Ed., Springer Verlag, (2003).
- [iii] G. Allaire, *Shape optimization by the Homogenization Method*, Springer Verlag, (2002).
- [iv] P. Chung, K. Tamma and R. Namburu, "Asymptotic expansion homogenisation for heterogenous media: computational issues and applications", *Composites Part A*, **32**, 1291-1301, (2001).
- [v] O. Sigmund, "A 99 line topology optimization code written in Matlab", *Structural and Multidisciplinary Optimization*, **12**(2), 120-127, (2001).

## **Coupled THM problems in geotechnical engineering using CODE\_BRIGHT-GiD**

Sebastià Olivella, Jean Vaunat, Benoit Garitte and Nuria M. Pinyol

*Department of Geotechnical Engineering and Geosciences, ETSECCPB, UPC*

### **Abstract**

CODE\_BRIGHT is a finite element program that solves coupled THM problems in geological materials. There are a number of questions involved when a module has to be developed to use it as a problem-type in GiD. The variety of constitutive laws that can be used in such a program and the variety of boundary and initial conditions require a development of pre-process and post-process with a sufficient degree of generality. The paper shows examples of applications that cover different types of geotechnical and environmental engineering problems.

### **1. INTRODUCTION**

The program CODE\_BRIGHT solves the coupled THM problems in geological materials using the finite element method. Customization to use GiD as pre- and post-process of CODE\_BRIGHT was performed and this permits to tackle a number of problems in the field of geotechnical and environmental engineering.

The program CODE\_BRIGHT couples the thermal (multiphase heat transport in porous media), hydraulic (two phase flow of liquid and gas in porous media including vapour), mechanical (unsaturated soil mechanics under isothermal conditions) problems and the solute transport. These problems require a number of constitutive laws and these have been organized accordingly in the interface. Since the number of material properties and parameters is large, it is useful to import sets of parameters if they are similar in other applications, so this is a convenient utility in GiD.

A number of improvements have been done in the code since its early development (Olivella et al 1996). One of them is the construction/excavation which is handled by activating and deactivating sub domains. For construction, an intermediate state is considered during which the weight of the layer under construction is applied linearly. While construction permits the described smooth process, excavation is more complicated as removing a layer causes changes of variables (stresses, pressures) in the remaining material which are fast and strongly coupled.

The examples shown in this paper are in 2D and 3D. The highly nonlinear coupled problems handled by the program are sometimes the limiting factor as the number of time steps to be solved is very large (for instance: small time steps during heating periods, after excavation, after fluid injection or pressure changes). So, one has to think in the space and time dimensions.

## 2. GENERAL DESCRIPTION OF CODE\_BRIGHT

A porous medium composed by solid grains, water and gas is considered. Thermal, Hydraulic and Mechanical aspects are taken into account, including coupling between them in all possible directions. As illustrated in Figure 1, the problem is formulated in a multiphase and multispecies approach.

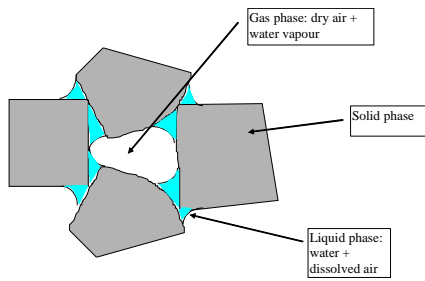


Figure 1. Schematic representation of an unsaturated porous material

The three phases are:

- solid phase (s):
- liquid phase (l): water + air dissolved + solute
- gas phase (g): mixture of dry air and water vapour

The three species are:

- solid (-): mineral
- water (w): as liquid or evaporated in the gas phase
- air (a): dry air, as gas or dissolved in the liquid phase
- solute (c): in the liquid phase

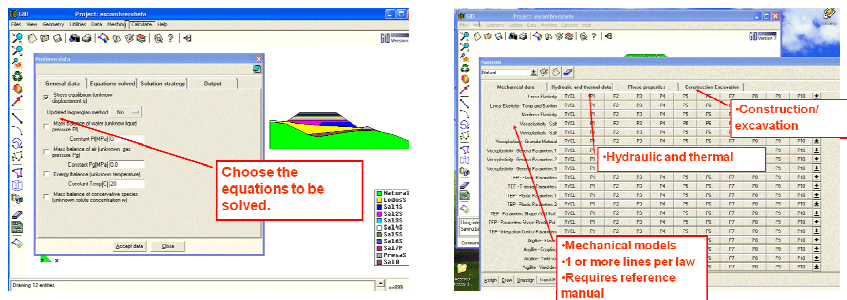


Figure 2. a) Customized window where the equations to be solved are selected. Solution strategy and Output sections contain default values (e.g. for tolerances that control convergence of nonlinear iterations). b) Customized window for material parameter input. ITYCL is used to decide types of laws inside a constitutive law (e.g. Viscoplasticity for granular materials may have different options of flow rules).

The program CODE\_BRIGHT solves the following equations:

Equation: mechanical equilibrium equations (1, 2 or 3 dimensions):

$$\nabla \cdot \boldsymbol{\sigma} + \mathbf{b} = \mathbf{0}$$

Unknown: displacements,  $\mathbf{u}=(u_x, u_y, u_z)$

Equation: water mass balance:

$$\frac{\partial}{\partial t} (\rho_l \omega_l^w S_l \phi + \rho_g \omega_g^w S_g \phi) + \nabla \cdot (\mathbf{j}_l^w + \mathbf{j}_g^w) = f^w$$

Unknown: liquid pressure,  $P_l$  (MPa)

Equation: air mass balance:

$$\frac{\partial}{\partial t} (\rho_l \omega_l^a S_l \phi + \rho_g \omega_g^a S_g \phi) + \nabla \cdot (\mathbf{j}_l^a + \mathbf{j}_g^a) = f^a$$

Unknown: gas pressure,  $P_g$  (MPa)

Equation: internal energy balance:

$$\frac{\partial}{\partial t} (E_s \rho_s (1-\phi) + E_l \rho_l S_l \phi + E_g \rho_g S_g \phi) + \nabla \cdot (\mathbf{i}_c + \mathbf{j}_{Es} + \mathbf{j}_{El} + \mathbf{j}_{Eg}) = f^e$$

Unknown: temperature,  $T$  (°C)

Equation: solid mass balance:

$$\frac{\partial}{\partial t} (\rho_s (1-\phi)) + \nabla \cdot (\mathbf{j}_s) = 0$$

Unknown: porosity,  $\phi$  (-)

Equation: solute mass balance:

$$\frac{\partial}{\partial t} (\rho_l \omega_l^s S_l \phi) + \nabla \cdot (\mathbf{j}_l^s) = f^s$$

Unknown: solute concentration,  $\omega_l^s$  (-)

The resulting system of PDE's (Partial Differential Equations) is solved numerically. The numerical approach can be viewed as divided into two parts: spatial and temporal discretizations. Finite element method is used for the spatial discretization while finite differences are used for the temporal discretization. The discretization in time is linear and the implicit scheme uses two intermediate points,  $t^{k+\epsilon}$  (for nonlinear terms) and  $t^{k+\theta}$  (for gradient terms) between the initial  $t^k$  and final  $t^{k+1}$  times. Finally, since the problems are non-linear, the Newton-Raphson method was adopted to find an iterative scheme.

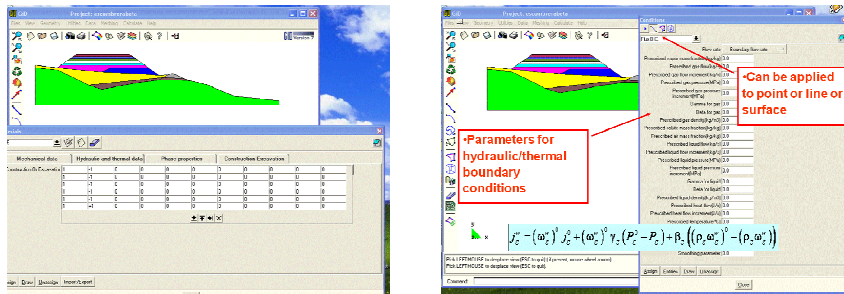


**Figure 3. a) Customized window for layer/material construction. b) Customized window for hydraulic boundary condition application. For 2D problems the condition can be applied to node/line/surface. Parameter list contains several items as the thermo hydraulic boundary condition equations are complex (evaporation/radiation/rain/...)**

Figure 2 and 3 show the aspect of the interface with different windows customized and incorporated in GiD. Figure 2a shows the **Problem data** window. The equations to be solved are chosen here. There is no restriction on the combination of equations to be solved. The number of degrees of freedom ranges from one to seven depending on the dimensions and equations chosen. Figure 2b shows the customized **Materials** window. Once in the window the mechanical, hydraulic and thermal, the phase properties and the



construction/excavation sections are displayed. This part is continuously growing and changing as research activity in this field requires new modifications.

Figure 3a shows the construction of a given layer at the time interval number 6 (the layer is inactive during the preceding 5 intervals i.e. with a value of -1). The **time intervals** in CODE\_BRIGHT are sequential time periods defined by an initial time a final time and a given time discretization parameters (initial time step and upper bound time step). Finally, figure 3b shows the customized window for the hydraulic and thermal boundary conditions (**Conditions**). These are intimately related with the construction/excavation as some contours which are exposed to atmosphere at some time intervals become internal in some others. Hydraulic and thermal boundary conditions are defined in a comprehensive way to account for evaporation, heat radiation, convection, infiltration, constant pressure and constant temperature.

### 3. APPLICATION OF CODE\_BRIGHT TO GEOTECHNICAL ENGINEERING PROBLEMS.

In this section some examples that have been solved with CODE\_BRIGHT are briefly described. These examples are related to different research activities at the Department of Geotechnical Engineering and Geosciences (UPC).

Figure 4 refers to an analysis of an experiment simulating radioactive waste disposal in an unsaturated rock. Heating up to 200 °C implies water evaporation around the drift and this manages to dry the rock. The different properties of the rock matrix and the rock fractures produce different desaturation of the pores and consequently different permeability. The heating also produces volumetric (compressive and dilatative) and shear deformation in the rock. These deformations induce changes in the intrinsic permeability. Both hydraulic and mechanical processes induce changes in permeability. This affects the flow of water and gas which in turn influences the heat transport and the temperature (Olivella and Gens, 2005).

Figure 5 shows a series of calculations related to behaviour of a 50 m high earth dam. These geotechnical structures should be analyzed using coupled hydro-mechanical equations. There are aspects related to unsaturated soils (unsaturated flow and collapse deformations) which are not considered in engineering practice. Figure 5 shows the pressure distribution in the natural ground and the clay core after construction. Construction is a process which should be necessarily modeled in order to obtain in a realistic way the water content, the stresses and the density of the materials. Deformability and strength are a function of these variables. Pore water pressure distribution and displacements at the end of the impoundment are also indicated in the figure.

Rapid drawdown may induce failure of earth dams due to high pore pressures in the upstream shoulder (Figure 6). However, pore pressure calculation requires the solution of a coupled problem as both pore pressure and stresses change on the upstream earth dam boundary. In some classical methods, the pore pressure is determined considering only the flow problem but this implies an overestimation of pressures which is not realistic (Alonso and Pinyol, 2008; Pinyol et al, 2008).

Figure 7 is another example related to radioactive waste disposal. Gas generated in wastes may migrate by diffusion and advection. In the case of two phase flow, the pore pressure generated may be high enough to induce discontinuity opening. This produces permeability variations which can only be properly determined by solving coupled hydro-mechanical problem. Figure 7 shows an experiment of gas migration in a scheme that contains a barrier made of sand-bentonite. The complex protocol of construction / water pressurization / gas injection requires several steps of modeling. For this type of problems the restart option is very convenient, otherwise the complete simulation of the problem requires long term calculations as time steps are relatively small (time step is controlled by the worse equation in terms of error). See more details in Olivella and Alonso (2004).

Simulation of coupled problems is also carried out at the level of laboratory experiments. Figure 8 shows the modelling of gas injection in a soil (initially saturated) with permeability variations induced by changes in degree of saturation (water content) and deformations. In this case the Experimental set up and laboratory investigations have been performed by Harrington and Horseman (2003). Similar tests are currently performed in the Geotechnical Laboratory of the UPC.

Figure 9 shows the analyses that are currently performed (Garitte et al, 2008) as desing calculations for the future TED experiment. The experiment will be launched after the excavation of the GED gallery (foreseen in October-November 2008), an extension of an existing GMR gallery. The excavation of a small niche is planned in the GED drift, from which the heater boreholes and the instrumentation boreholes will be drilled. One of the objectives of the design work is also the determination of the optimal instrumentation pattern.

#### 4. CONCLUSIONS

This paper reviews a number of applications of CODE\_BRIGHT-GiD. Although most of the problems are related to waste disposal, which in fact was the original field of work, problems related to civil engineering geotechnical problems appear and should also be considered and analyzed.

#### 5. REFERENCES

- Alonso E.E. & N. M. Pinyol (2008) Unsaturated Soil Mechanics in Earth and Rockfill Dam Engineering. First European Conference on Unsaturated Soils. Durham, United Kingdom. In print.
- Garitte, B. Vaunat, J. and A. Gens (2008). Thermo-Hydro-Mechanical Design Calculations for the TED Experiment, Internal Report for ANDRA (France), Department of Geotechnical Engineering and Geosciences.
- Harrington, J.F., and S.T. Horseman (2003) Gas Migration in KBS-3 Buffer Bentonite: Sensitivity of Test Parameters to Experimental Boundary Conditions, SKB Technical Report TR 03-02, 2003.
- Olivella, S., A. Gens, J. Carrera & E. E. Alonso (1996) Numerical formulation for simulator (CODE\_BRIGHT) for coupled analysis of saline media. *Engineering computations*, 13(7): 87-112.
- Olivella, S. & E. E. Alonso (2004). Modelling the hydro-mechanical behaviour of GMT in situ test including interface elements, GMT Report. UPC-NAGRA.
- Olivella, S. & A. Gens (2005). Double structure THM analysis of a heating test in a fractured tuff incorporating intrinsic permeability variations. *Int. J. Numer. Anal. Met. Geomech.* 42, 667-669.
- Pinyol, N.M., E.E. Alonso & S. Olivella (2008) Rapid drawdown in slopes and embankments. *Water resources research*. In print.

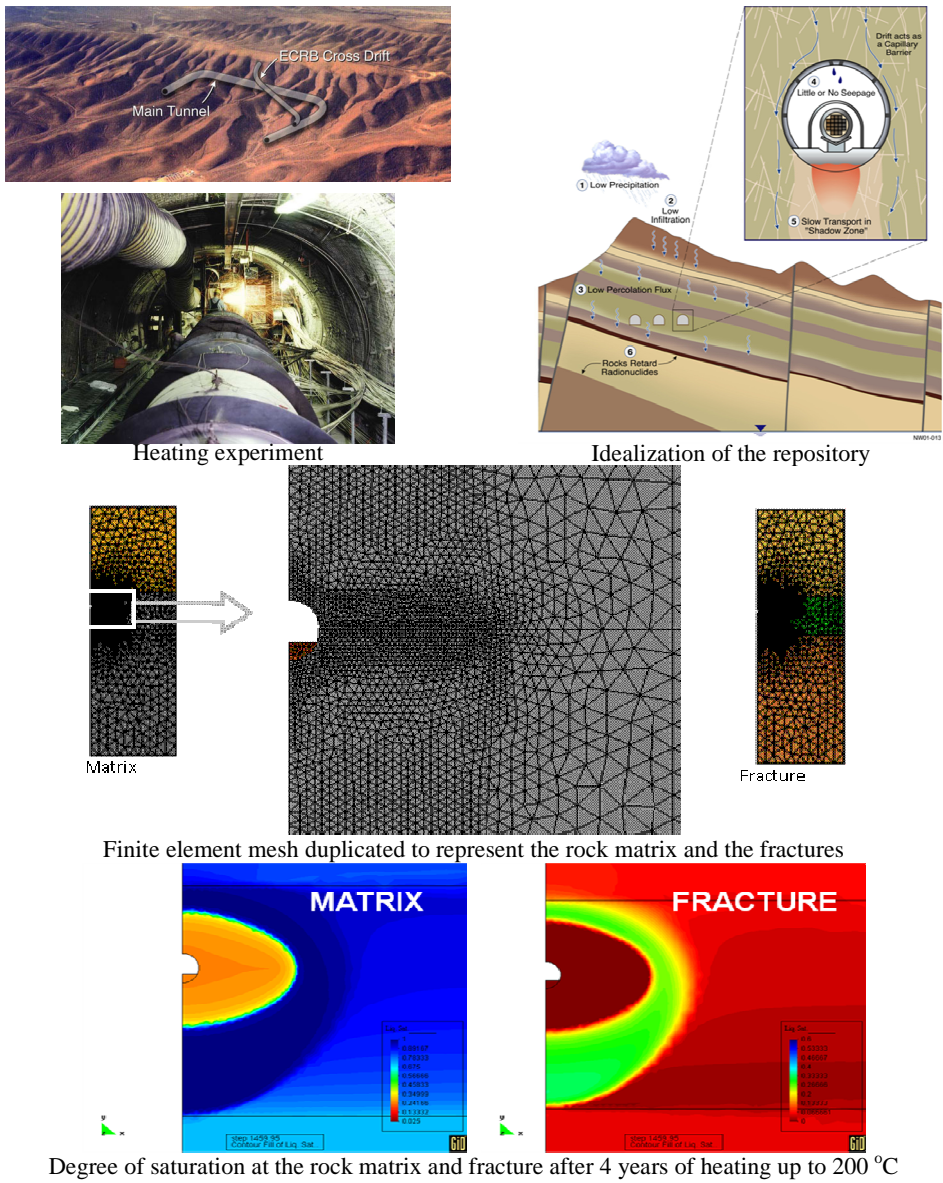
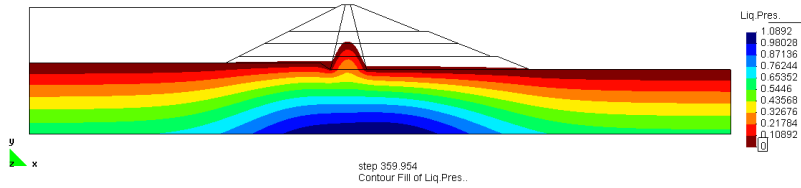
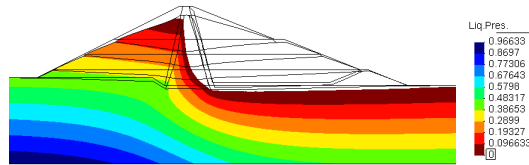


**Figure 4. Modelling THM response of a fractured rock (Yucca Mountain, Nevada) using a double structure approach. A total of 5 dof/node are solved in a monolithic way ( $u, p_l, p_g, T$ ).**

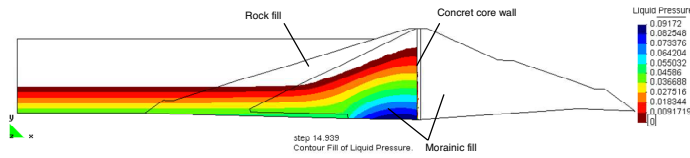


Pore pressure distribution after construction (only positive)

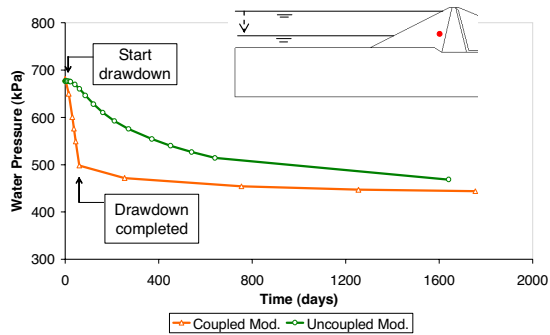


Water pressure (only positive) and deformed mesh after reservoir impoundment

**Figure 5. Modelling earth dams. Construction generates pore pressure, stress increments and accumulated plastic strains.**



Water pressure after rapid drawdown (only positive)



Pore pressure evolution for coupled and uncoupled analyses

**Figure 6. Modelling rapid drawdown in earth dams.**

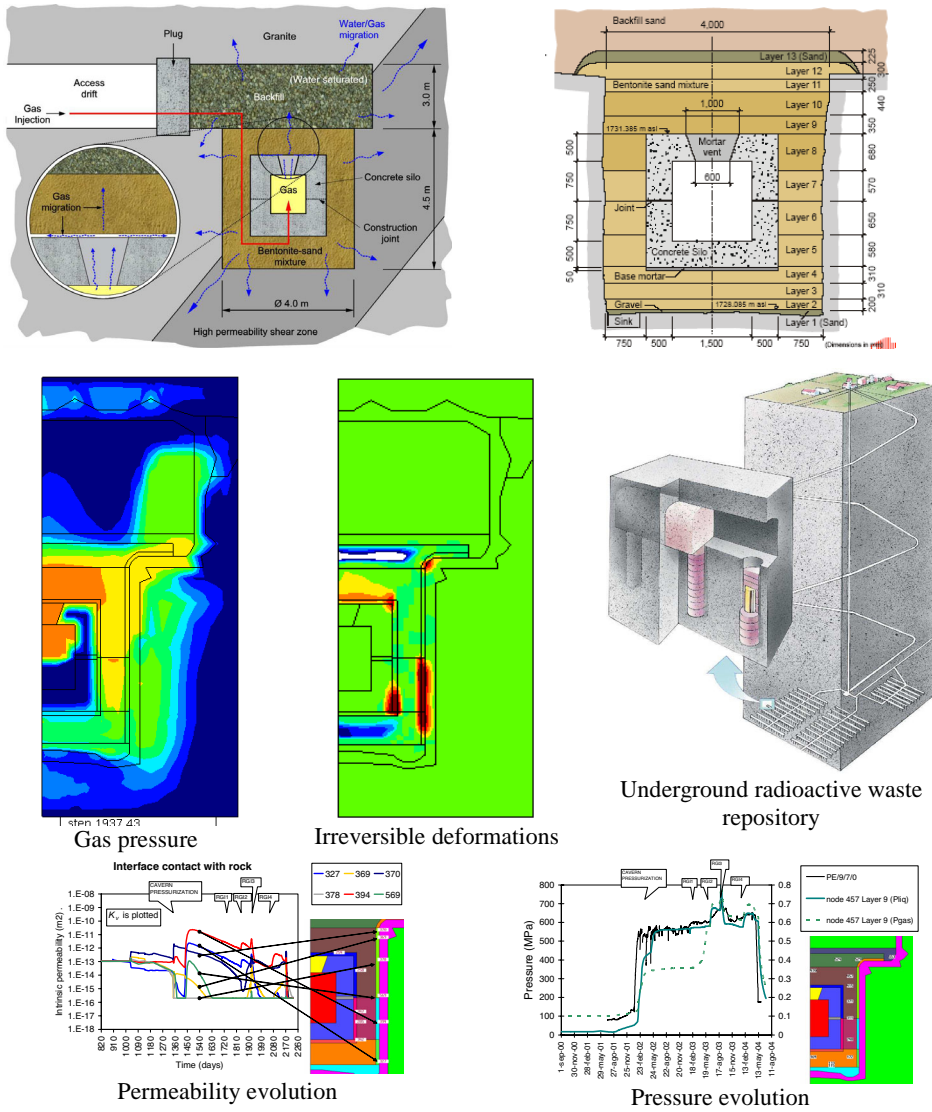


**Figure 7. Modelling gas generation (due to waste degradation) and flow through geological materials**

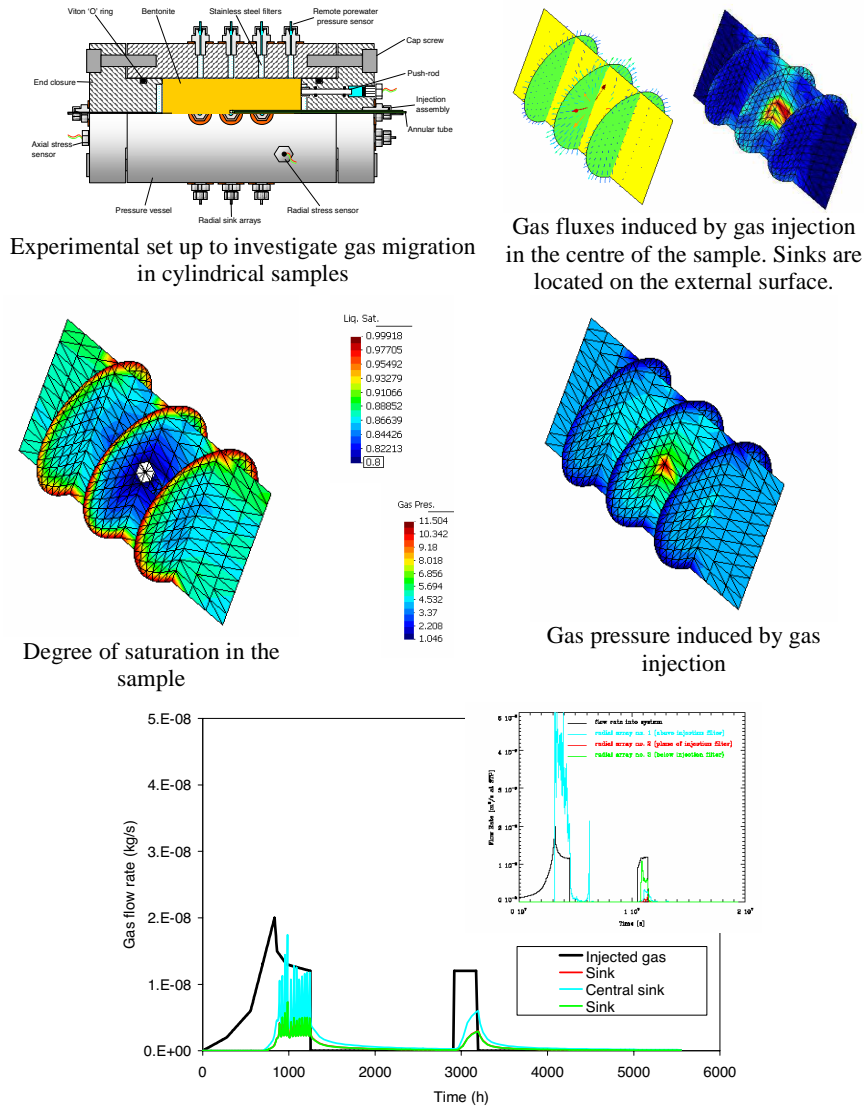
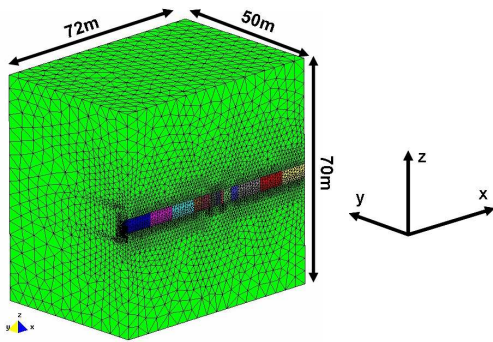
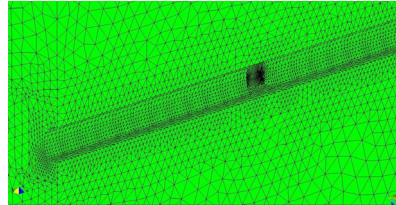


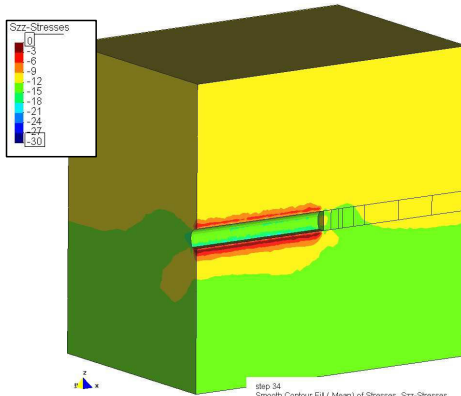
**Figure 8. Gas flow is simulated using a coupled formulation to account for permeability variations induced by deformations (Experiments from Harrington and Horseman, 2003)**



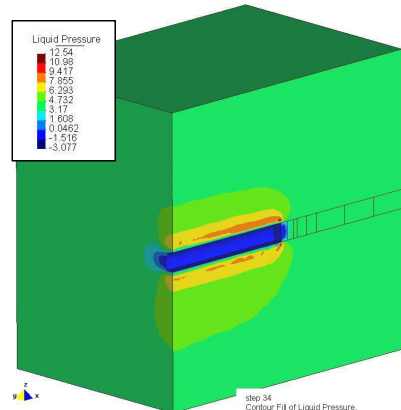
The domain includes the host rock, drift excavation and borehole



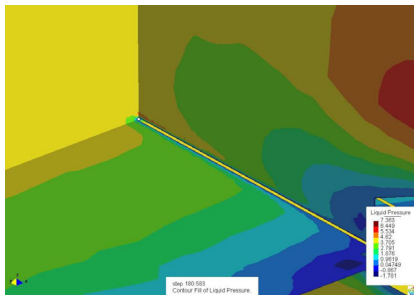
Detail of the drift and the zone where the borehole is drilled



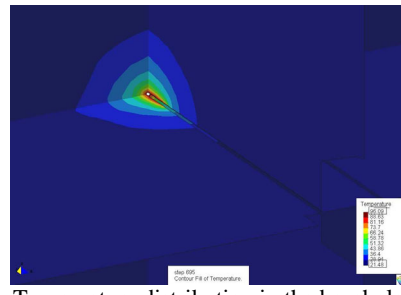
Vertical stress during drift excavation



Pore pressures during excavation



Pore pressure during borehole drilling



Temperature distribution in the borehole

**Figure 9. Design calculations of TED in situ experiment to be performed in Bure (France) by ANDRA. The modeling includes drift excavation, borehole drilling and heating phases**

## LUNG AUTOMATIC RECONSTRUCTION ALGORITHM FOR CFD SIMULATIONS

Julien Penneçot<sup>\*</sup>, Lars Krenkel<sup>†</sup> and Claus Wagner<sup>†</sup>

<sup>\*</sup> Deutsche Zentrum für Luft- und Raumfahrt (DLR)  
AS-FS  
Bunsenstrasse 10,  
37073 Göttingen, Germany  
e-mail: [julien.pennecot@dlr.de](mailto:julien.pennecot@dlr.de)

<sup>†</sup> Deutsche Zentrum für Luft- und Raumfahrt (DLR)  
Email: [lars.krenkel@dlr.de](mailto:lars.krenkel@dlr.de)

<sup>†</sup> Deutsche Zentrum für Luft- und Raumfahrt (DLR)  
Email: [claus.wagner@dlr.de](mailto:claus.wagner@dlr.de)

Key words: Reconstruction, Segmentation, CFD, Lung, Skeletonization, Mesh generation.

**Abstract.** In this paper, the outline of a program generating almost fully automatically the surface mesh of a bronchial tree based on medical CT image data is presented. For the whole process, required user input is reduced to a minimum. Particularly of importance is the implementation of a skeleton algorithm in order to determine the generation of each bronchial branch and to cut the branches to obtain the outlet markers. No repetitive pixel painting or triangle picking tasks are needed during the surface mesh generation process.

### 1 INTRODUCTION

Most of the patients admitted in the intensive care unit need artificial ventilation. A better comprehension of the processes involved in air transport within the lungs is necessary in order to optimize the artificial ventilation techniques. Nowadays, computational fluid dynamics (CFD) allows for efficient and robust simulation of flows in highly complex geometries like the human upper or the central airways. However, as an input for CFD software, a spatially discretised computational domain representing the physical domain of interest, i.e. human respiratory system, a numerical volume mesh, has to be generated. The mesh generation process is normally long and cumbersome and need many manual interventions. In this paper, a program for automatised geometric segmentation and surface mesh generation based on medical computer tomography (CT) image data is presented. The main objective was to reduce the required interactive user input to a minimum.

The program consists of two major modules. One image processing module which allows geometry segmentation out of a staple of 2D medical CT images and a second module, a surface mesh generation module, for generating a triangle based surface mesh of the



segmented geometry. In this case, the algorithm has been applied to a CT dataset of an isolated pork lung for reconstruction of the central airways.

## 2 SEGMENTATION AND SURFACE MESH GENERATION

The image processing is performed on all images simultaneously using the standards segmentation techniques such as cropping, blurring, sharpening, thresholding and edge detection<sup>i</sup>. Then, a region growing advancing front method is used to obtain a single set of connected voxels. It allows for capturing the entire bronchial tree and to differentiate the latter from the pulmonary blood vessels. Statistical filters as well as expanding and shrinking techniques are applied in order to remove undesired small details and concavities within the geometry. User input is only required to determine some global values such as the grey level used during the thresholding algorithm, to select the region of interest, and finally to define the desired number of generations which are going to be reconstructed. By superposition of the segmented geometric bodies with the original image the level of detail resolution as well as the quality of the overall segmentation process can be checked by optical means (Figure 1).

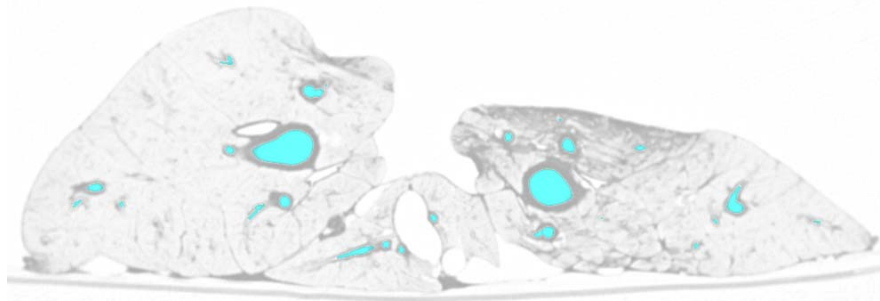


Figure 1: Superposition of the segmented lung with the original image. All small branches are captured by the segmentation algorithm (cyan patches), while the blood vessels are excluded from the computational domain.

The user input for the second module, the surface mesh generation, is limited to the definition of the inlet location. The initial surface mesh is generated using a marching cube method. A non shrinking smoothing algorithm<sup>ii</sup>, is used on the initial mesh to obtain a smooth surface and finally a polygon reduction algorithm<sup>iii</sup> allows to reduce significantly the number of triangles while keeping the form of the surface mesh. The triangles at the inlet plane (trachea) are flagged during the mesh generation process. All other branches finish with a dead end. They need to be cut perpendicularly to their axis in order to apply a pressure outlet condition at each end for the CFD simulation. This is done with the help of the compact line-like 1-D representation of the segmented 3D bronchial tree, the so-called skeleton.

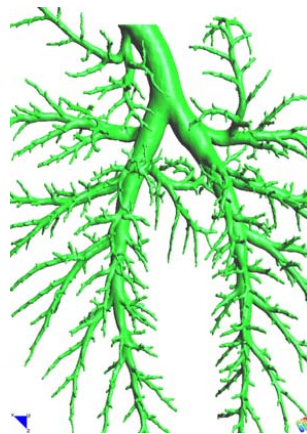


Figure 2: Initial Surface meshes

### 3 SKELETIZATION AND BRANCH CUTS

For each branch, the CFD simulation needs to have an identified set of outlet triangles. These triangles should be coplanar. Therefore all branches need to be cut perpendicularly to its axis and the triangles resulting from the cut need to be flagged as outlet. This is done with the help of a skeleton algorithm.

The voxels of the skeleton of the bronchial tree (Figure 3) are extracted from the stack of images using an algorithm based on two discrete distance fields<sup>iv</sup>. A boundary seeded distance field is computed to determine the distance between a voxel and the closest boundary. This distance field is used to center the skeleton line along a branch. A point seeded distance field determines the distance between a voxel and the seed point (here at the beginning of the trachea) following a path fully inside the segmented lung. The local maxima of the point seeded distance field are branch ends and are used as starting points for the acquisition of the skeleton. The size of the neighbourhood for the local maxima search is chosen in order to capture all physical branches while reducing the number of phantom branches (created by noise on the boundary of the segmented lung). The skeleton is then stored using a hierarchic branch structure. The position, direction and path as well as the length and children of each branch are stored in this data structure. The generation of each branch can be also derived using this structure.

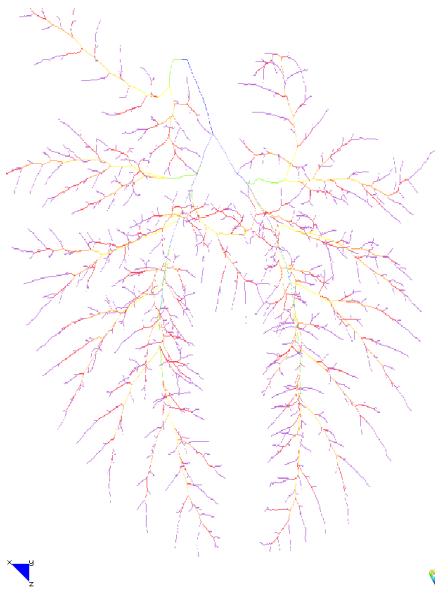


Figure 3: Skeleton of the bronchial tree. All branches are described by a thin line, the generation of the branch is colour coded.

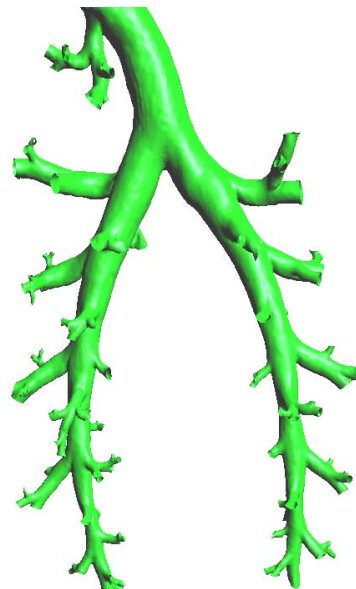


Figure 4: Final surface mesh with 4 generations. The branch cuts are performed automatically and perpendicularly to each branch.

The branch ends are then cut using the information delivered by the skeleton. The user can choose how many generations of branches the lung model should have (Figure 4). The cuts can be performed either at the end of each branch thus keeping the full network of branches resolved through the underlying CT images or they can be performed further up in the lung model in order to reduce the model to a specified number of generations. The position and the normal vector of the plan used for cutting the branches is delivered primarily by the skeleton, but these values are iteratively optimized in order to cut each branch as perpendicularly to the branch axis as possible. Triangles located behind or being directly cut by the cut planes are erased and the corner points of the resulting triangle front are projected onto the cutting plane. Outlet markers are set at the branches ends. The volume meshes can then be created with standard unstructured or pseudo-structured grid generators such as e.g. NETGEN or CENTAUR™.

#### 4 CONCLUSION

The presented process chain allows for an almost automatised reconstruction of a complex surface mesh from high resolution medical CT image data. Geometry reconstruction of bronchial trees with four to eight generations of branches can be quickly generated from standard 1024x1024 pixel CT scans with slice spacing of 0.6mm and 50% overlap. During the whole mesh generation process, only little user input is necessary. User input is needed in order to define global constants such as the thresholding and sharpening values. It is also needed in order to select a seeding point for the region growing algorithm as well as the point seeded distance field. The surface mesh generation, the smoothing, and the triangle reduction algorithm are fully automatised. Finally, the geometry of the bronchial tree is reduced to the desired level of central airway generations by fully automatic branch cutting and additionally the outflow planes are flagged as outflow markers.

The applied algorithms allow to reduce the time used for geometry reconstruction and mesh generation. The skeleton technique is efficient for the upper and central airways which are organised in a tree structure, but it can also be easily applied to other bio-medical applications such as blood vessels or rhino pharyngeal flow investigations after only minor adaptations.

#### REFERENCES

- [i] R. Löhner and J.R. Cebral, "From medical images to CFD meshes", Proc. 8<sup>th</sup> International Meshing Roundtables, (1999).
- [ii] G. Taubin. "A signal processing approach to fair surface design", Computer Graphics Proceedings, Pages 351-358, (1995).
- [iii] S. Melax., "A simple, fast and effective polygon reduction algorithm", Game developer, Pages 44-49, (1998).
- [iv] Y. Zhou and A.W. Toga, "Efficient skeletonization of volumetric objects", IEEE transactions on visualization and computer graphics, Vol. 5. No. 3. (1999).

## A NEW SYSTEM FOR PROBLEMTYPES CREATION

M. R. Peyrau<sup>1\*</sup>, R. Ribó<sup>2\*</sup>

Compass Ingeniería y Sistemas  
Tuset 8, 7 2  
08006 Barcelona, Spain

1: E-mail: peyrau@compassis.com, web page: <http://www.compassis.com>  
2: E-mail: ramsan@compassis.com, web page: <http://www.compassis.com>

**Key words:** Problemtypes, Interface creation, Finite element method

**Abstract.** *In order to use GiD to prepare data for a specific analysis program, it is necessary to customize it. The customization involves the predefinition of all the information that must be entered by the user, as well as the definition of the way the final information is given to the corresponding solver. The configuration process is performed by means of a problemtype, which is a collection of files used to configure GiD for a particular analysis. In this way, the traditional GiD problemtype is defined with a directory and a set of files, which contains the full functionality for customizing the preprocess. The new Toolkit for problemtypes creation is based on these features and files, but uses additional capabilities provided with the Toolkit and does not need most of the original files anymore. Therefore, the new problemtype is also defined with a directory and a set of files, which contains a main XML configuration file, a main TCL file with the initialization routines, a file defining the way in which the final information has to be written inside the input files that will be read by the corresponding solver and several other TCL files. In order to add conditions, materials, general data or units systems information to the problem type, it will be necessary to modify the main configuration file, which is defined in XML format and contains all the definition of all the data (except the geometry) that must be filled by the user to perform the analysis. In this way, the Toolkit permits to process easily XML documents on a physical tree view inside the GiD window, to couple entities into groups using standard windows and to edit their properties. This powerful tool also groups all the common features of the different problemtypes, which facilitates its creation. A realistic application example of the Toolkit is the Plaxis-GiD interface program, which performs the simulation of 3D geotechnical problems by means of the finite element method.*

### 1 INTRODUCTION

When GiD is to be used for a specific type of analysis, it is necessary to predefine all the input data required from the user like geometry properties and boundary conditions

(i.e. constraints, loads, velocities). It is also necessary to define the way in which this information should be given to the solver. In this way, the customization is done by creating a problemtype, which is a collection of files used to configure GiD for a particular analysis program. In fact, the traditional GiD problemtype is defined with a directory with the problemtype name and the extension .gid containing several files, where most of them have the same name than the directory with different file extensions referring to their particular functions. A new system for problemtypes creation has been developed, which is based on these original capabilities, but uses additional capabilities provided with the so called Toolkit.

## 2 THE NEW PROBLEMTYPES STRUCTURE

The new problemtype is defined using a directory with the problemtype name, but does not need most of the original files. In this way, the main configuration file with .spd extension is defined in XML format and contains the definition of all the data (except the geometry) necessary to perform a numerical analysis. Therefore, it is necessary to modify this XML file in order to add conditions, general data or units information to the problemtype. Moreover, a TCL file has to be introduced in the directory scripts containing the way in which the output information has to be written inside the input files that will be read by the solver. It is also possible to create new sophisticated windows, menus or new functionalities to the program inside the initialization file using the TCL/TK programming language. Table 1 shows the use of the main files in the new problemtypes system.

File extension	Description	Problemtype with Toolkit
name.prb	Problem and intervals data	Not used
name.cnd	Conditions definition	Used, should not be modified
name.mat	Material properties	Not used
name.bas	Information for data input file	Not used, should be void
name.tcl	Main TCL file, initialization	Used
name.default.spd	Main configuration file, XML-based	Used

Table 1: Main files that configure the new problemtypes with the Toolkit

## 3 WHY A NEW SYSTEM FOR PROBLEMTYPES CREATION?

There are various motivations for using the new Toolkit for problemtypes creation. On the one hand, XML is a W3C<sup>[3]</sup> standard, endorsed by software market leaders, it supports Unicode and it is becoming more and more popular in the area of storing and describing information<sup>[1],[4]</sup>. On the other hand, the syntax rules of XML are very simple, logical and easy to use. Moreover, XML documents are human-legible and reasonably clear. Besides,

using the Toolkit the information is stored in plain text format in a self-describing syntax, which facilitates the aggregation of data. It should be important to note that the elements in an XML document form a tree structure that starts at "the root" and branches to "the leaves" with different relationships between the properly nested elements. XML 'elements' are defined using not predefined "Opening and closing tags" and can have 'attributes', which provide additional information<sup>[3],[4],[5]</sup>. In fact, the tree structure of XML allows to aggregate efficiently elements and the new Toolkit permits to convert automatically XML documents to its physical tree view in the GiD window for interfaces creation. In this way, the Toolkit allows to hide parts of the data tree for specific types of analysis or to couple entities into a same 'group' using standard windows inside the interface. Moreover, the Toolkit permits to edit easily the 'group' properties. Furthermore, this tool is coupling all the common features of the different problemtypes, which facilitates the problemtypes creation.

#### 4 TOOLKIT CONVENTIONS

Due to XML tags are not predefined, the Toolkit defines its own tags in order to create automatically a tree view and simple windows on the left of the GiD window, which facilitates the aggregation of data. In this way, we call 'field' to the 'Element name' and 'parameter' to the 'attribute'. Therefore, all data is contained in fields and parameters, where the parameters can contain a literal value, a xpath expression or a [TCL command]. It should be emphasized here that XPath is used for addressing parts of a XML tree. In fact, XPath is based on a tree representation of the XML document and provides the ability to navigate through its hierarchical structure selecting nodes from the tree<sup>[5]</sup>. In the case of considering a xpath expression, a search is performed in the tree and the result is substituted in the parameter when necessary. In the case of using a [TCL command], the command between brackets is executed when necessary and the return value is replaced inside the parameter. Typically, the TCL procs called 'proc' are defined at the end of the XML document. An realistic example of the Toolkit applications in order to create a tree view, interface windows and to simplify data storage is the Plaxis-GiD program, which is showed in Figure 1.

#### 5 CONCLUSIONS

A new Toolkit has been developed for problemtypes creation in order to facilitate the introduction of all the input data to transfer to a specific analysis program. It is based on a XML hierarchical structure and a physical tree view on the GiD window. In order to add conditions, materials, general data or units systems to the problemtype, it is necessary to modify a XML tree inside the main configuration file, which contains all the data (except the geometry) necessary to perform a numerical analysis. The Toolkit permits to process easily XML documents on a physical tree view, but it also allows to hide parts of the data tree if this is convenient for a particular type of analysis. It also permits to couple

entities into groups using standard windows inside the interface and to edit their own properties easily. Summarizing, using the Toolkit it is possible to create tree interfaces easily and to store data more efficiently and automatically due to this tool is coupling all the common features of the different problemtypes. Thus, the Plaxis-GiD program is a realistic application of this powerful tool.

## 6 ACKNOWLEDGEMENTS

The authors wish to thank all those from Plaxis BV, who provide the project geometry and input dates given in Figure 1.

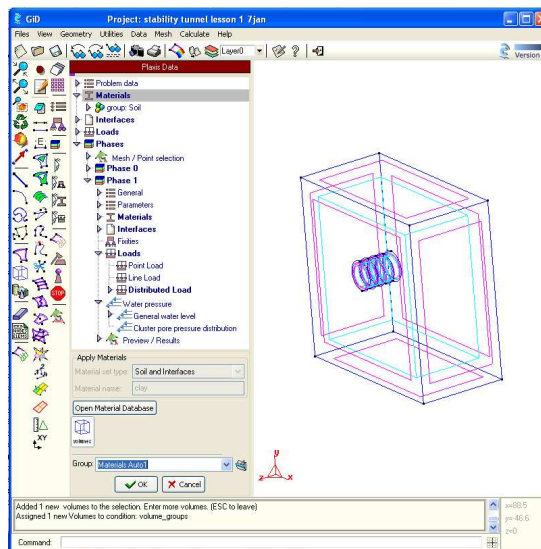


Figure 1: Problem data tree structure in the Plaxis-GiD interface program. A group is applied to volume entities using the Toolkit for windows creation

## REFERENCES

- [1] R. Light, *Presenting XML*, Sams. Net Publishing, (1997).
- [2] C. F. Goldfarb and P. Prescod *The XML Handbook*, Prentice Hall, (1998).
- [3] World Wide Web Consortium (W3C), available from [www.w3.org](http://www.w3.org).
- [4] M. Kay *XPath 2.0 Programmers's Reference*, Wiley Publishing, (2004).
- [5] A. Skonnard, M. Gudgin *Essential XML QuickReference*, Addisonj-Wesley, (2001)

## GID-PAK INTERFACE

Dragan Rakic<sup>\*</sup>, Aleksandar Nikolic<sup>†</sup>, Miroslav Zivkovic<sup>†</sup>, Radovan Slavkovic<sup>†</sup>

<sup>\*†</sup>Faculty of Mechanical Engineering  
Sestre Janjic 6, 34000 Kragujevac, Serbia  
e-mail: [drakic@kg.ac.yu](mailto:drakic@kg.ac.yu), web page: <http://www.fempak.kg.ac.yu/>

**Key words:** GiD, PAK, Program interface, FEM

**Abstract.** GiD-PAK interface is a user interface between programs for pre and post processing – GiD and PAK program package. Basic instructions for developing the interface between the programs are given in the paper, with a specific review on PAK-S module. PAK-S is the program for linear and nonlinear static and dynamic structural analysis based on the Finite Element Method. Several Finite Element types are implemented in this program module as well as several material models. Developing GiD-PAK interface we get a powerful program tool for complex structural analysis.

### 1 INTRODUCTION

GiD-PAK Interface is a user interface between programs for pre and post processing – GiD<sup>i</sup> and PAK<sup>ii</sup> program package. Software package PAK is on the level of world-known packages for structural analysis. There are built-in finite elements and material models according to the state-of-the art theoretical achievements. Program PAK-S includes modulus for solving static and dynamic analysis of constructions, geometrically and materially nonlinear problems, fracture mechanics, etc. Connecting of all PAK program modules and software for pre and post processing GiD is in process.

### 2 DESCRIPTION OF PAK-S INTERFACE SOFTWARE GID

Scheme of problem solving applying software GiD<sup>iii</sup> and PAK-S, using developed interface described in this paper, is given on the figure 1.

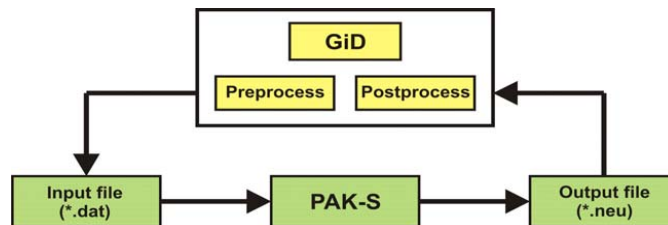


Figure 1 : The communication of GiD and solver PAK-S



After model defining in the mode for pre processing of program GiD, we get an ASCII file with the `.dat` extension on the output. This file is sent to solver PAK-S and on its output we get a `.neu` extension file that contains the results of the previously done analysis. Obtained result can be post processed now in the mode for post processing of GiD program.

In order to unite pre and post processor GiD and solver PAK-S into one program package where it is possible to do the complete analysis, as previously mentioned, it is necessary to create an interface that connects these two parts.

Create a new folder with the solver name (PAK<sup>iv</sup> in this case) within the existing **Problemtypes** folder. This way PAK submenu will appear in GiD program **Problem type** menu. Then create **PAK-S.gid** folder within PAK folder. The entire translator that contains the following files will be placed in **PAK-S.gid** folder:

#### Configuration files

- PAK-S.cnd
- PAK-S.mat
- PAK-S.prb

#### TCL extension files

- PAK-S.tcl

#### Template files

- PAK-S.bas

### 3 ANALYSIS OF GID-PAK-S INTERFACE FILES

#### 3.1 Configuration files

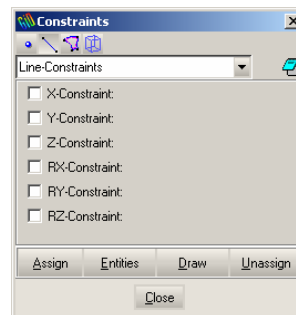
File with the `.cnd` extension has the information about problem boundary conditions (constraint and load). An important characteristic of **Conditions** file is that it must be defined through which geometrical entities the boundary conditions are given (over points, over lines, over surfaces, over volumes or over layers), and which way these parameters are assigned to finite elements (over nodes, over face elements or over body elements). The structure of **PaK-S.cnd** file is briefly described in the following text.

There are two parts defined with the name **BOOK** within this file; **Constraints** and **Static\_Loads**. The part of the code that refers to **BOOK Constraints** is next given, whereas a dialog window that creates this part of the code in GiD program graphical interface is presented on the picture next to the code.

```

NUMBER: 2 CONDITION: Line-Constraints
CONDTYPE: over lines
CONDMESHTYPE: over face elems
QUESTION: X-Constraint:#CB#(1,0)
VALUE: 0
QUESTION: Y-Constraint:#CB#(1,0)
VALUE: 0
QUESTION: Z-Constraint:#CB#(1,0)
VALUE: 0
QUESTION: RX-Constraint:#CB#(1,0)
VALUE: 0
QUESTION: RY-Constraint:#CB#(1,0)
VALUE: 0
QUESTION: RZ-Constraint:#CB#(1,0)
VALUE: 0

```



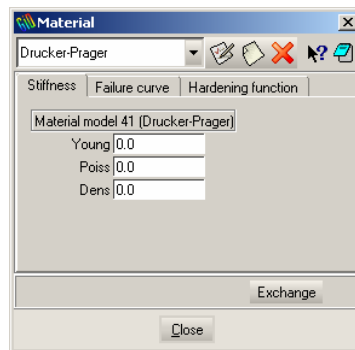
File with the `.mat` extension has the information about different material models (**Material**) as well as the definitions of different finite element types with their characteristics

(Property). This file is divided into two parts as well: **BOOK Material** and **BOOK Property**, so that material models are independent from the finite element types and their characteristics. The part of the code that defines material characteristics of one of the material models implemented in PAK-S program and the dialog window that this code creates in GiD graphical interface follows.

```

NUMBER: 41 MATERIAL: Drucker-Prager
TITLE: Stiffness
QUESTION: matID
VALUE: 41
STATE: hidden
COMMENT: Material model 41 (Drucker-Prager)
QUESTION: Young
VALUE: 0.0
HELP: Young's modulus (E)
QUESTION: Poiss
VALUE: 0.0
HELP: Poisson's ratio (ni)
QUESTION: Dens
VALUE: 0.0
HELP: Material density
TITLE: Failure_curve
...
END MATERIAL

```

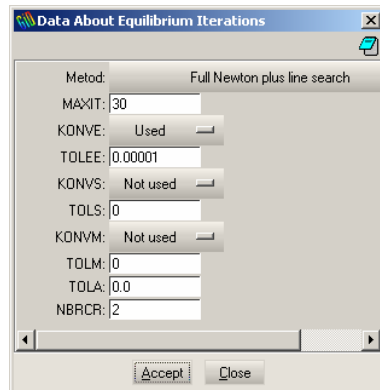


File with the **.prb** extension has the information about the analysis type, post processing options, equilibrium iterations, permanent constraints, body loads, imperfection, fracture mechanics etc. It is different from the two previous files because it does not depend on geometrical entities. The information being input here is used to set the solver parameters. The example of code that creates the dialog window for defining Equilibrium iterations in the GiD graphical interface follows as well as the dialog window created by this code in the GiD graphical interface.

```

BOOK: Data_About_Equilibrium_Iterations
QUESTION: Metod:#CB#(Elastic_tangent_matrix,...)
VALUE: Full_Newton_plus_line_search
...
QUESTION: KONVE:#CB#(Used,Not_used)
VALUE: Used
QUESTION: TOLEE:
VALUE: 0.0001
QUESTION: KONVS:#CB#(Used,Not_used)
VALUE: Not_used
QUESTION: TOLS:
VALUE: 0
QUESTION: KONVM:#CB#(Used,Not_used)
VALUE: Not_used
QUESTION: TOLM:
VALUE: 0
QUESTION: TOLA:
VALUE: 0.0
QUESTION: NBRCR:
VALUE: 2

```



### 3.2 TCL extension files

File with the **.tcl** extension automatizes any of the processes in GiD and new options can be assigned with it. The appearance of the entire PAK-S interface is defined within it, including the appearance of the created menu and submenu. **PAK-S.tcl** consists of numerous procedures that correspond to **TCL** language.

### 3.3 Template files

Within interface folder we create **PAK-S.bas** file that represents the main part of the interface between these two programs. After model defining it is necessary to write all the information in the input file with **.dat** extension that will be processed by PAK-S solver. This file describes format and data structure of the input file for the solver. It accepts solver data for the analysis in many cards that are divided into logical parts. The part of code template file that writes down the input file for PAK-S solver and refers to basic data for the problem defining follows.

```
C /4/ BASIC DATA FOR THE PROBLEM (6I2,3X,3I5)
C (IOPGL(I),I=1,6),NDIN,ISOPS,ICVEL
*if((strcmp(GenData(Static/Dynamic),"Static")==0))
*Set Var NDIN=0
*else
*Set Var NDIN=1
*endif
*if((strcmp(GenData(Eigenvalue),"0")==0))
*set var ISOPS=0
*else
*set var ISOPS=1
*endif
*set var ICVEL=1
*format "%2i%2i%2i"
*GenData(X-Constraint)*GenData(Y-Constraint)*GenData(Z-Constraint)\
*format "%2i%2i%2i%8i%5i%5i"
*GenData(RX-Constraint)*GenData(RY-Constraint)*GenData(RZ-Constraint)*NDIN*ISOPS*ICVEL
```

In this card of the input file for the PAK-S solver the following is defined: the analysis type (static or dynamic), setting eigenvalue calculations, global translation and rotation. Parameters that are read and written in this card are defined in **PAK-S.prb** file.

## 4 CONCLUSION

GiD-PAK interface represents the connection between programs for pre and post processing of GiD and PAK-S solver. Developing this interface we get a very powerful tool for solving different kinds of problems of structure strength analysis. The interface is the basis for the further upgrade that can be applied in the usage of different fields in FEM such as: geomechanics, heat transfer, biomechanics, fluid flow and fluid-fracture interaction, etc.

## REFERENCES

- [i] Ramon Ribó, Miguel de Riera Pasenau, Enrique Escolano, Jorge Suit Pérez Ronda, Abel Coll Sans, GiD - **Reference Manual Version 7**, CIMNE Barcelona, Spain.
- [ii] M.Kojić, R.Slavković, M.Živković, N.Grujović, **PAK-S, Program for FE Structural Analysis, USERS MANUAL**, Faculty of Mechanical Engineering of Kragujevac - Laboratory for Engineering Software, Kragujevac, 2003, Serbia.
- [iii] Ramon Ribó, Miguel de Riera Pasenau, Enrique Escolano, Jorge Suit Pérez Ronda, Abel Coll Sans, GiD - **User Manual Version 7**, CIMNE Barcelona, Spain.
- [iv] Aleksandar Nikolić, **PAK-T interface for software GiD**, Diploma work, Faculty of Mechanical Engineering, University of Kragujevac, 2007, Serbia.

## ONE-DIMENSIONAL NUMERICAL MODEL OF ARTERIES IN GID

**Eduardo Soudah and Eugenio Oñate**

International Center for Numerical Methods in Engineering (CIMNE)  
Universidad Polit cnica de Catalu a  
Campus Norte UPC, 08034 Barcelona, Spain  
e-mail: esoudah@cimne.upc.edu , web page: <http://www.cimne.com/biomedical>

**Key words:** Arterial model, finite element methods, blood flow, cardiovascular system.

**Abstract.** *According to WHO estimates, 17 million people around the globe die of Cardiovascular Disease (CVD) each year. About 600 million people with high blood pressure are at risk of heart attack, stroke and cardiac failure. In 1999 CVD contributed to one-third of global deaths. Low and middle-income countries contributed to 78 percent of CVD deaths. By 2010 CVD is estimated to be the major cause of death in developed countries. This huge impact has motivated the development of numerical models for arterial behaviour in order to study cardiovascular pathologies and interventions.*

### 1. INTRODUCTION.

The reason why one-dimensional models for the blood flow may be attractive is that full 3D computer simulations of the whole cardiovascular system and specific surgical interventions are quite prohibitive in terms of computational calculus. The aim of this work is to create and validate a new numerical scheme with experimental measures of the flow profile obtained by high resolution magnetic resonance and ultrasound techniques and compare these results with 3D simulations.

### 2. METHODOLOGY.

#### 2.1. Mathematical model.

We introduce a non-linear one-dimensional model to describe the flow motion in arteries and its interaction with the wall displacement. The governing system of equations (Eq.1-Eq.2-Eq.3) results from conservation of mass and momentum applied to a 1-D impermeable and deformable tubular control volume of incompressible and Newtonian fluid. The model has been deduced by making the following assumptions: axial symmetry, radial displacements, and constant pressure on each section, no body forces and dominance of axial velocity. Also, in the absence of branching, a short section of an artery may be considered a cylindrical compliant tube.

$$\frac{\partial A}{\partial t} + \frac{\partial Q}{\partial z} = 0 \quad (1)$$

$$\frac{\partial Q}{\partial t} + \frac{\partial}{\partial z} \left( \alpha \frac{Q^2}{A} \right) + \frac{A}{\rho} \frac{\partial P}{\partial z} + K_r \left( \frac{Q}{A} \right) = 0 \quad (2)$$

where the unknowns are  $A(z,t)$  is the cross-sectional area of the vessel,  $Q(z,t)$  is the mean flux,  $P$  is the average internal pressure over the cross-section,  $\alpha$  is the momentum-flux

correction coefficient,  $z$  is the axial coordinate along the vessel,  $t$  is the time,  $\rho$  is the density of the blood taken here to be  $1040 \text{ Kg}\cdot\text{m}^3$  and  $KR$  is the friction force per unit length, which is modelled as  $KR = 2\pi v(\gamma+2)$  according to Formaggia[1], with  $v$  the viscosity of the blood taken here to be  $4.5 \text{ mPa}\cdot\text{s}$ . In order to close the system equations (Eq.1-Eq.2), we provide a relation for the pressure completed with a pressure–area (Eq.3) relation previously. It assumes a thin, homogeneous and elastic arterial wall and it takes the form.

$$P = P_{ext} + \psi(A; A_o, \beta) \Rightarrow \psi = \beta \frac{\sqrt{A} - \sqrt{A_o}}{A_o} \Rightarrow \beta = \frac{Eh_o\sqrt{\pi}}{1-\xi^2} \quad (3)$$

where  $A_0$  and  $h_0$  are the sectional area and wall thickness at the reference state ( $P_0, U_0$ ), with  $P_0$  and  $U_0$  assumed to be zero,  $E$  is the Young's modulus and  $\xi$  is the Poisson's ratio, typically taken to be  $\xi=0.5$ , since biological tissue is practically incompressible. The parameter  $\beta$  is related to the speed of pulse wave propagation,  $c$  (Eq.4), through Formaggia[1],

$$c = \frac{\beta}{3\rho A_o} A_o^{\frac{3}{2}} \quad (4)$$

## 2.2 Boundary conditions and branching.

The hyperbolic system of partial differential equations (Eq.1-Eq.2-Eq.3) is solved in each arterial segment of Fig.1 with the following boundary conditions. At the proximal end of the ascending aorta (Fig1.Left.(A)) we enforce a real inflow rate  $Q(t)$  gives for the MRI measures in a cardiac cycle and for the rest of the arteries we impose the terminal resistance according to the reference Wang and Parker[2][Table1]. For the all branches the technique used is the domain-bifurcation of Quarteroni [3], the boundary conditions of the arterial segments joining at junctions are prescribed by enforcing conservation of mass and continuity of the total pressure.

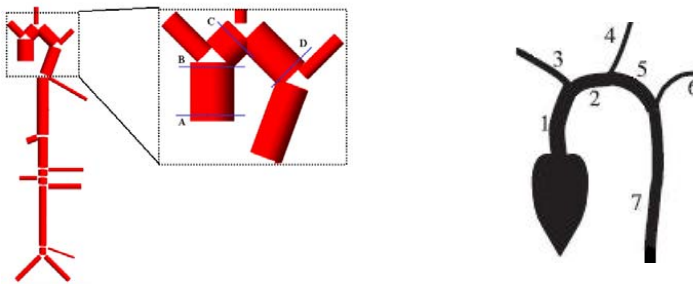


Figure 1: Schematic representation of the arterial network simulated, which includes the aorta, brachial, carotid, femoral and the main thoracic arteries (left). Numbers refer to names of the main arteries in the Table 1 of the area of study.

## 2.3 Numerical Scheme.

Eqs.(1-2-3) are solved using a second-order discontinuous Taylor-Galerkin spatial-discretisation scheme and a four-order explicit Runge-Kutta time-integration scheme, with an adaptive step-size control. This scheme is suitable for the 1-D formulation because it can propagate waves of different frequencies without suffering from excessive dispersion and

diffusion errors. Details on this algorithm can be found in F.Mussi,[4].The Taylor-Galerkin requires a time step limitation in order to keep the solution stable, the stabilization adopted is the method CFL (Courant-Friedrichs-Levy)[5]

$$\Delta t \leq \text{CFL} \min_{0 \leq i \leq N} \left[ \frac{l_i}{\max(\lambda_{1,i}, \lambda_{2,i})} \right] \quad (5)$$

where the  $\lambda_{1,i}$  means the eigenvalue  $\lambda_1$  at the mesh in the node  $i$  and  $\text{CFL}=0.577$ [5].

## 2.4 Physiological Data.

The physiological parameters used in each arterial segment are given in the Table1. Our model aims at representing the arterial geometry and elasticity of a healthy young adult. In the absence of detailed knowledge of these properties, the geometry and wall elasticity of the arteries are based on data published in Wang and Parker [2].

	Name	l (cm)	r (cm)	h (cm)	E (10 <sup>6</sup> Pa)	c (m/s)	R <sub>t</sub> (10 <sup>9</sup> Pa·s/m <sup>3</sup> )
1	Ascending Aorta	4.0	1.470	0.163	0.4	4.67	
2	Aortic Arch I	2.0	1.263	0.126	0.4	4.43	
3	Brachiocephalic	3.4	0.541	0.067	0.4	4.93	
4	Left. Ext Carotid	17.7	0.334	0.042	0.8	7.02	13.9
5	Aortic Arch II	3.9	1.195	0.115	0.4	4.35	
6	Left Subclavian I	3.4	0.474	0.066	0.4	5.23	6.01
7	Thoracic Aorta	5.2	1.120	0.110	0.4	4.39	

## VALIDATION OF RESULTS

We have presented a 1-D model of pulse wave propagation that is able to capture the main wave propagation features observed in vivo in the aorta and the arteries supplying them from the aorta. From the origin of the aorta, Fig 1 (Left) position A, our model predicts a continuous blood flow towards the arch aortic, Fig 1 (Left) positions B,C,D during all the cardiac cycles, which is in agreement with in vivo measurements (Fig 2). In order to validate the flow distribution between the different arteries, we also compare the flow with the physiological data obtained a correct distribution (1/3 of the volume flow is coming out from the heart to the upper-aortic circulation).

	Vessel name	Q(ml/sec)	% of the total Flow
3	Brachiocephalic	105	
4	Left. Ext Carotid	26	
6	Left Subclavian I	40	
7	Thoracic Aorta	171	34%
		350	66%
	Total	521	

## CONCLUSION

Furthermore, there is the possibility of developing one-dimensional models to understand perfectly how the flow propagates into all the cardiovascular system to use this information to set both inflow and outflow boundary conditions for 3D finite elements problems and could be helpful for the early detection, diagnosis and prevention of related arterial diseases

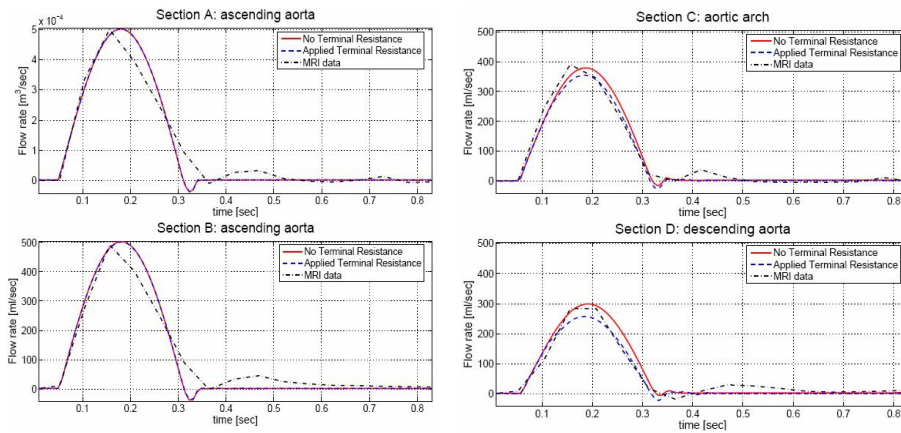


Figure 2: Flow velocity over one cardiac cycle in sections A,B,C,D to the Figure 1

## ACKNOWLEDGEMENTS

The authors would like to acknowledge Dr. Francesç Carreras for his contribution, and the Hospital de la Santa Creu i Sant Pau for the use of the images material.

## REFERENCES

- [1] L.Formaggia,D.Lamponi,and A.Quarteroni: One dimensional model for blood flow in arteries Journal of Engineering mathematics,47:251-276,2003.
- [2] J.Wang and K.H. Parker. Wave propagation in a model of the arterial circulation .J.Biomech, 37; 457-470, 2004.
- [3] A.Quarteroni and A.Valli. Domain decomposition methods for partial differential equations. Volume 118 of applied mathematical series. The Clarendon Press Oxford University Press, NewYork, USA,1999
- [4] F.Mussi, E.Soudah, E.oñate Cardiovascular System: A One-Dimensional fluid dynamic analysis using finite element method. Monograph Cimne, Barcelona, Spain, 2006.
- [5] L.Quartapelle. Numerical solution of the incompressible Navier-Stokes equations. Birkhäuser Verlag, Basel, 1993.

## BATCH CONTROLLED PRE-PROCESSING FOR SHIELD TUNNELLING PROBLEMS IN GID

\* **Janosch Stascheit and Günther Meschke**

Ruhr University Bochum, Institute for Structural Mechanics  
Universitätsstr. 150, D-44780 Bochum, Germany  
janosch.stascheit@rub.de, guenther.meschke@rub.de

**Key Words:** *automatic modelling, pre-processing, mechanised tunnelling, Finite Element Method.*

**Abstract.** *A set of programs and GiD customisations is presented, that are used to automatically perform the pre-processing for the numerical simulation of shield tunnelling [1,2] based on the Finite Element Method.*

*For the development of a simulation software for shield tunnelling within the European Integrated Project TUNCONSTRUCT [3], an efficient and user-friendly modelling tool is needed to generate the three-dimensional Finite Element model of the shield machine, the heading face support, the lining and the surrounding soil with often complex geological structures. As the simulation software is intended to be integrated into a large distributed design support software framework, several features were requested: The simulation software should be web-accessible by means of an apparent integration into the client software of the design support tool and it should require as little user interaction as possible.*

*In order to perform the pre-processing tasks needed for the simulation model, GiD was chosen. Two important features of GiD in this context are that GiD may be used in totally silent mode and that it is customisable to a high degree. This allows for a tailored system which may be batch-controlled for its usage on remote systems. This contribution is focussed on the GiD customisations made as well as on the set of scripts that are necessary for the remote invocation and setup of the pre-processor.*

### 1 INTRODUCTION

During the design phase of shield tunnelling projects numerical simulations are a useful (and often indispensable) tool to provide detailed information on the response of the tunnel-soil system for the considered design variants. However, three-dimensional time- and space-discrete analyses require large efforts for the modelling. Since the modelling effort usually imposes a significant obstacle against using advanced numerical models in order to improve the design of tunnelling projects, the numerical analysis of those projects is often limited to rather simple and in many cases two-dimensional models.

Within the European research project TUNCONSTRUCT [3], an integrated design support software (Integrated Optimisation Platform for Tunnelling, IOPT) is being developed, that gives



design engineers the possibility of conveniently considering different design variants and easily compare their advantages and disadvantages. As part of this design support software, an advanced three-dimensional Finite Element simulation software (**ekate**) has been developed. In this context, the modelling tool presented in this paper allows for a fully automatic generation of a Finite Element model for specific shield tunnelling projects using GiD.

## 2 WORKFLOW

Due to the fact that the modeller is intended to run automatically and without graphical user interaction, several features had to be implemented into the software that perform the required steps in a robust and silent way. For the implementation of the modeller, several customisations had to be made inside GiD. Beside the actual problemtype that allows for the generation of proper input files for the **ekate** simulation software, further measures have been taken of which the most interesting are described in detail in Section 3.

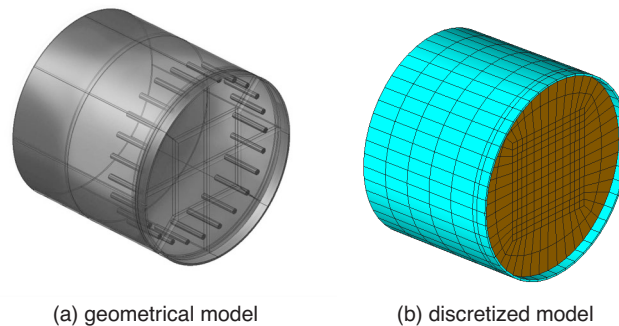


Figure 1: Finite Element model of the shield machine

Since only specific sections of the tunnel need to be simulated, only a limited domain of the tunnel is simulated at once. Hence, a simulation domain is generated and the complete ground model is accordingly adapted by means of a user-defined TCL function (see Section 3.1).

The tunnel excavation follows an alignment curve that is defined by a polyline, where each node is located in the centre of a segmented lining ring. Additionally, the diameters of the cutting wheel, the shield and the segmented lining elements are given input parameters. Section 3.2 gives an overview on how the tunnel geometry is generated with GiD. The shield machine is generated as a separate GiD project and included into the final model. It is modelled as a separate deformable body that interacts with the ground via frictional contact (see Figure 1).

After all geometrical features of the simulation model have been created, the boundary conditions are being applied and the mesh is generated by the automatic mesh generator of GiD. In order to apply the correct boundary conditions, a surface selection algorithm has been implemented as a user-defined TCL function in the GiD problemtype (see Section 3.3). Once the model has been completely generated it is exported as input files for the Finite Element software KRATOS [4]. An initial model without a tunnel is stored additionally in order to determine the initial stress state in the ground. This stress state is transferred to the actual simulation model afterwards. During the simulation, the mesh is constantly being adapted to follow the current location of the machine. This procedure makes sure that the excavation process is modelled

correctly, since the elements to be excavated are at the correct position at any step of the simulation.

### 3 IMPLEMENTATION DETAILS

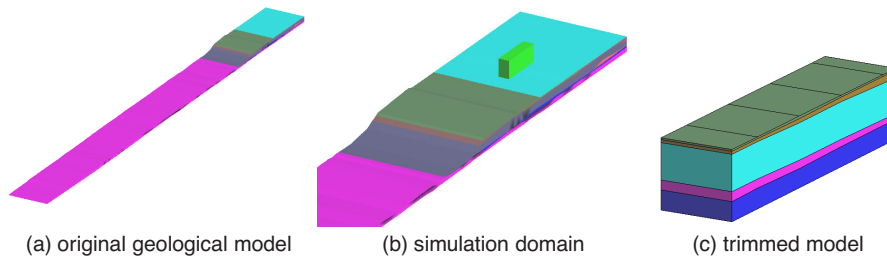


Figure 2: Trimming of the simulation domain

#### 3.1 User-defined trim function

The geological model consists of a set of volumes representing geotechnically distinct layers of the ground. These volumes are imported to GiD as a set of ACIS files. In addition to that, the domain to be simulated is imported. In Figure 2a, the complete geological model is shown. Figure 2b depicts the simulation domain to be selected from the complete model. A TCL function integrated to the problemtype is then used to intersect all available geotechnical domains with the actual simulation domain. Afterwards, the geological representation of the simulation domain (see Figure 2c) can be used for the generation of the simulation model.

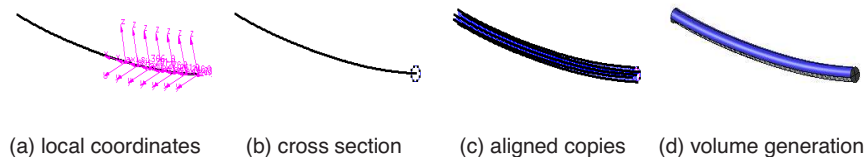


Figure 3: Generation of the tunnel geometry by means of the `align` function

#### 3.2 Generation of tunnel geometry

The geometry of the tunnel is characterised by its alignment and its diameter. The different steps that are performed in order to create the tunnel geometry are illustrated in Figure 3. The generation starts with a set of local coordinate systems that are created along the tunnel alignment (see Figure 3a). Afterwards, a circle of the same diameter as the tunnel is generated in the first station of the alignment (see Figure 3b). This circle is, in the third step, copied along the

set of local coordinate systems using the `align` function of GiD (see Figure 3c). Finally, the complete geometry is created as a volume (see Figure 3d).

### 3.3 User-defined surface selection

The surface selection tool implemented into GiD allows for the automatic determination of boundary conditions. In order to guarantee a support of the model boundaries that is free of restraints, all boundary surfaces have to be supported orthogonally to their orientation. Since the GUI component is switched off during the generation of the model, an algorithm was needed that automatically detects the bottom, side and top surfaces. This is being done by evaluating the number of higher entities that are connected to each surface. If there is only one higher entity defined (i.e. one Volume that owns the respective surface), it has to be a free surface. Subsequently, the position of the surface is compared to a global bounding box that is calculated for the complete model. Once the centre point of the surface touches the bottom or one of the sides of the bounding box, the respective property is assigned to the surface. The remaining free surfaces consequently form the top surface of the model. The latter is needed in order to calculate the depth of each point in the model which is employed to predict the virgin stress state.

## 4 CONCLUDING REMARKS

The overall work flow and selected implementation details that are used to perform a batch-controlled pre-processing for the numerical simulation of shield tunnelling problems have been presented. It has been shown that GiD, once it is enriched with tailored customisations, is able to automatically perform pre-processing for complex models without any user interaction. However, this requires a good quality of the input data, since the user will not be able to manually fix problems (e.g. in the definition of geometries) during the pre-processing.

## 5 ACKNOWLEDGEMENTS

This work has been supported by the European Commission within the Integrated Project TUNCONSTRUCT (IP011817-2). Co-funding to the first author was also provided by the Ruhr-University Research School funded by the DFG in the framework of the Excellence Initiative. This support is gratefully acknowledged.

## REFERENCES

- [1] F. Nagel, J. Stascheit and G. Meschke: "Three-phase modelling and numerical simulation of shield tunnelling in partially saturated soils", *CD-ROM Proceedings of the ECCOMAS Thematic Conference on Computational Methods in Tunnelling (EURO:TUN 2007)* Eds.: J. Eberhardsteiner et al. (2007)
- [2] J. Stascheit, F. Nagel, G. Meschke, M. Stavropoulou and G. Exadaktylos: "An automatic modeller for Finite Element simulation of shield tunnelling", *CD-ROM Proceedings of the ECCOMAS Thematic Conference on Computational Methods in Tunnelling (EURO:TUN 2007)* Eds.: J. Eberhardsteiner et al. (2007)
- [3] European Integrated Project IP011817-2 TUNCONSTRUCT, <http://www.tunconstruct.org>
- [4] P. Dadvand et al.: "KRATOS: An Object-Oriented Environment for Development of Multi-Physics Analysis Software.", *WCCM V, Fifth World Congress on Computational Mechanics* Eds.: H.A. Mang, et al. (2002)

## Author Index



C. Almeida Bueno e Silva .....	23
M. Abedi.....	103
L. Alvarez.....	55
A. Andrade-Campos.....	121
M. L. Arganis .....	75
J. L. Batoz.....	59
F. Bilteryst .....	59
E. Bladé .....	43, 75
J. Blasco .....	83
M. Bordone .....	27
R. B. J. Brinkgreve .....	11
M. A. Celigueta .....	31
Jan Cervenka .....	39
M. Chiumentì .....	27
P. Chobsilprakob.....	91
G. Corestein .....	43
C. Corte.....	47
J. A. Cruz.....	75
P. Dadvand .....	51
H. Delingette.....	17
F. De Luna.....	75
D. Di Capua .....	55
J. Dib .....	59
E. Escolano.....	83, 95, 99
M. Espino .....	83
S. Farnoush.....	103
R. Fatehi .....	103
M. Fayyaz Bakhsh.....	103
M. Fernández .....	17
A. Ferriz Canals.....	63, 69, 111
R. Flores .....	99
O. Frutos .....	63, 69, 111
O. A. Fuentes.....	75
L. E. García-Castillo.....	79
D. García-Doñoro.....	79
B. Garitte.....	125
A. German .....	83
I. Gómez-Revuelto .....	79
S. González Horcas .....	87
M. Kaltenbacher .....	107
G. Keryer .....	117
Ki-Du Kim .....	91
C. Labra.....	95
H. Landes .....	107
A. Larese .....	31
S. Latorre.....	31
I. Lewon .....	59
R. Lopez .....	99
A. Loussert .....	117

---

M. Maidana .....	83
M. T. Manzari .....	103
A. Maymó Molina .....	63, 69
M. Meiler .....	107
R. Mendez .....	111
J. E. Mendoza .....	75
G. Meschke .....	151
H. Mestouri .....	117
H. Naderan .....	103
J. Niewald .....	39
A. Nikolic .....	143
P. Norachan .....	91
J. A. Oliveira .....	121
S. Olivella .....	125
E. Oñate .....	27, 95, 99, 147
M. Pasenau .....	83
J. Pennecot .....	135
M. R. Peyrau Rubio .....	139
J. Pinho-da-Cruz .....	121
N. Pinyol .....	125
A. R. Pulino Filho .....	23
D. Rakic .....	143
R. Ribó Rodríguez .....	139
M. Sanchez .....	75
R. Slavkovic .....	143
E. Soudah .....	27
J. Stascheit .....	147, 151
S. Suthasupradit .....	91
W. Swolfs .....	11
F. Teixeira-Dias .....	121
J. Vaunat .....	125
M. Zivkovic .....	143